# A Comparative Investigation on the Tribology and Microstructure of MWCNT Reinforced h-AMMC Sintered by Conventional and Microwave Heating Route

*A Dissertation Submitted*

In partial fulfillment of requirements

for the degree of

**Master of Engineering**

in

**Production Engineering**

By

Rajat Kumar

(801785008)

Under the supervision of

**Dr. Hiralal Bhowmick** (Associate Professor)

**Dr. Dheeraj Gupta** (Associate Professor)

THAPAR INSTITUTE
OF ENGINEERING & TECHNOLOGY
(Deemed to be University)

**MECHANICAL ENGINEERING DEPARTMENT**

**THAPAR INSTITUTE OF ENGINEERING & TECHNOLOGY, PATIALA**

**August, 2019**

# CERTIFACATE

I hereby declare that the thesis entitled "**A Comparative Investigation on the Tribology and Microstructure of MWCNT Reinforced h-AMMC Sintered by Conventional and Microwave Heating Route** " is an authentic record of my work carried out as requirement for the award of degree of **Master of Engineering** in **Production Engineering** at **Thapar Institute of Engineering & Technology, Patiala** under the supervision of Dr. Hiralal Bhowmick, Associate Professor and Dr. Dheeraj Gupta, Associate Professor, Mechanical Engineering Department, Thapar Institute of Engineering & Technology, Patiala during July 2017 to August 2019. The matter embodied in this report has not been submitted to any other Institute or University for the award of any degree.

Rajat

Date:- 10/9/2019

Rajat Kumar

It is certified that the above statement made by the student is correct to the best of my knowledge and belief.

**Dr. Hiralal Bhowmick**
(Associate Professor)
Mechanical Enigineering Department
Thapar Institute of Engineering &
Technology, Patiala - 147004

10/09/19

**Dr. Dheeraj Gupta**
(Associate Professor)
Mechanical Enigineering Department
Thapar Institute of Engineering &
Technology, Patiala - 147004

# Acknowledgement

I take the opportunity to express my heartfelt gratitude to my supervisors **Dr. Hiralal Bhowmick** and **Dr. Dheeraj Gupta** for their unreserved guidance, constructive suggestion and encouraging me at important junctures in this research work. I am thankful for the positive suggestions, and meticulous guidance that helped me to improve my scientific writing and carry out the new research. I felt really motivated and honored to work under their guidance throughout my entire thesis work.

I am thankful to **Dr. T.P Singh**, Head of Mechanical Engineering Department, Thapar Institute of Engineering and Technology for providing necessary help to carry out this thesis work. I am thankful to the office staff of the ME department, TIET for their help and cooperation throughout my study. I would like to express my gratitude towards **Dr. Puneet Sharma** and **Dr. S.S Mallick** who allowed me to access the facilities of Physics and Material Department laboratories and Laboratory of Bulk Solids and particle technology in Mechanical Engineering Department, respectively.

I would like to express my gratitude towards Mr. Sandeep Bansal (PhD Research Scholar), Mr. Harpreet Singh (PhD Research Scholar) and Mr. Sandeep Sharma (PhD Research Scholar), for their technical support and who also took interest in my work. A gratitude towards my friends Jonty Mago, Pratya Bhardwaj and Ebin Mathew who motivated me, provided technical supports and essential valuable advices during my work. I am also thankful to the other members of **Surface Engineering and Tribology Research Lab** as well as Mr. Narinder Singh and Mr. Sarabjeet for assisting and guiding me in the laboratory works. Last but not least, I am thankful to my family and relatives.

Rajat Kumar

# Abstract

In the current work Al-alloy, AMMC and MWCNT-reinforced hybrid AMMCs have been fabricated successfully with the help of Microwave Hybrid Heating as well following conventional route of powder metallurgy. This was followed by a detailed investigation on the microstructural, physical, mechanical and functional behavior of the fabricated materials. Different metallurgical and mechanical characterization techniques such as optical microscopy, scanning electron microscopy (SEM), field emission scanning electron microscopy (FESEM), Vickers's micro hardness and porosity measurements have been used. EDS point and area mapping, XRD and Raman spectroscopy has been carried out for the compositional analysis. The tribological characteristics i.e. wear and friction, of fabricated Al, AMMC and h-AMMC has been studied by using a Pin on Disc sliding wear Tribometer. Graphical analysis of coefficient of friction of h-AMMC has been analysed using Windcom software for both conventional as well as microwave technique.

The results reveal the viability and significance of microwave material processing over conventional methods for the fabrication of AMMC. h-composite exhibits higher hardness than Al matrix and Al+SiC composite. The results of compositional analysis indicated that the intensity of formation of different oxide phases such as $Al_2O_3$, $Cr_2O_3$, $MnO_2$ and CuO in conventional sintering process is significantly higher as compared to microwave sintering process. From wear study, it has been found that wear and friction properties of h-composite are better than Al matrix and Al+ SiC composite. However, the nature of distribution as well as % of MWCNT is found to have significant effect on the tribological characteristics. Further, it has been found that h-composite with a composition (Al+15%SiC+1%MWCNT) significantly enhances the tribological performance in different operating conditions.

**Keywords:** h-AMMC, MWCNT, Porosity, Sinter, Microwave, Tribology.

# Table of Content

# List of Figures

# List of Tables

# Nomenclature

**AMMC-** Aluminium metal matrix composite

**h-AMMC –** Hybrid aluminium metal matrix composite

**SiC-** Silicon Carbide

**CNT-** Carbon nanotubes

**MWCNT –** Multiwall carbon nanotubes

**$B_4C$-** Boron Carbide

**$MnO_2$-** Manganese oxide

**CuO - Copper** oxide

**$Al_2O_3$ -** Aluminium Oxide

**Al -** Aluminium

**MMCs-** Metal matrix composites

**HP-** Hot pressing

**SPS-** Spark plasma sintering

**MHH-** Microwave Hybrid Heating

**XRD –** X- ray Diffraction

**SEM -** Scanning Electron Microscope

**FESEM -** Field Emission Scanning Electron Microscope

**Si -** Silicon

**Cu -** Cupper

**EDS –** Energy- dispersive X-ray spectroscopy

# Chapter 1

# Introduction

## 1.1 Background and Origin of the Research Proposal

In the real-world applications, tribological contacts affect almost each and every sector of industry like automobile, aerospace, mining, food industry, wood product industry, textile industry, and etc. Tribological application consumes approximately 23% of energy from world's total energy consumption [1]. On the other hand, 28% of total energy is consumed by automobile sector [2]. The breakup of global energy consumption is shown in Figure 1.

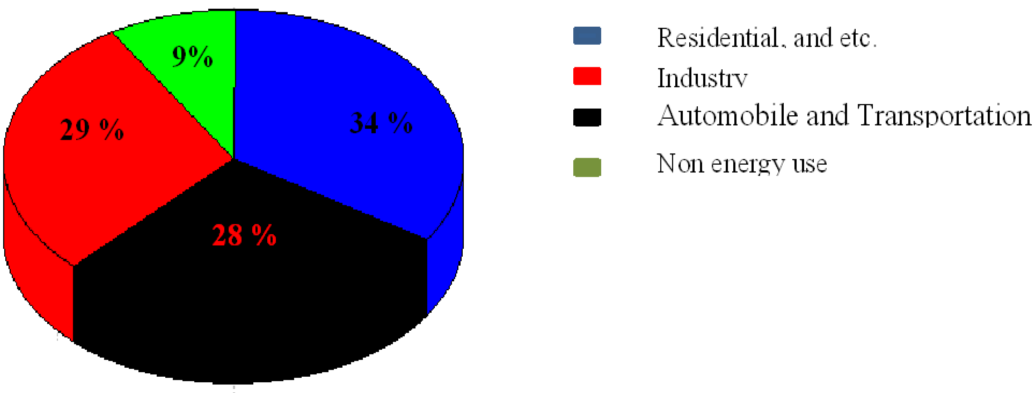


Figure 1 Breakup of Global energy usage [1]

There are four major economic sectors where friction loss and wear affect the most. However, cost incurred due to wear loss is more as compared to friction loss. This comparison is shown in Table 1, which show that wear loss is a big problem faced by the industries world-wide.

Table 1 Comparison of cost incurred due to wear loss over friction loss [1]

| Sector | Predominance of economic loss over that of friction loss |
|---|---|
| Automobiles Industry | 22 % |
| Mining Industry | 35 % |
| Energy Industry | 53 % |
| Residential | 35 % |

In automobile industry, the many applications where tribological properties play an important role includes component like engine, brakes, bearings, clutches, washer, and etc. [3]. Piston is one of the critical tribopair in IC engine because it works under high temperature, high pressure, corrosive and multi-regime wear conditions. In an IC engine the piston's primary responsibility is to take thermal energy created by fuel-air combustion and transform it into linear motion. In automobile engine the piston and piston rings rub against the cylinder walls. This cause high amount of energy losses due to friction loss, mechanical loss, wears loss. The friction and wear losses again depend upon the piston and cylinder arrangement [4]. Although, there is the existence of other losses, however, approximately 48% of losses are covered by friction [5]. The distribution of friction and wear losses [6] by different components of an IC engine is shown in Figure **2**. According to several studies it was found that in India, due to incorrect lubrication and severe wear, the destruction of equipment is around 50-60 % of total failure and in turn it results in high price of maintenance [7]. In India, BHEL is the first organization who made a department of tribology for examining the journal bearing [8].

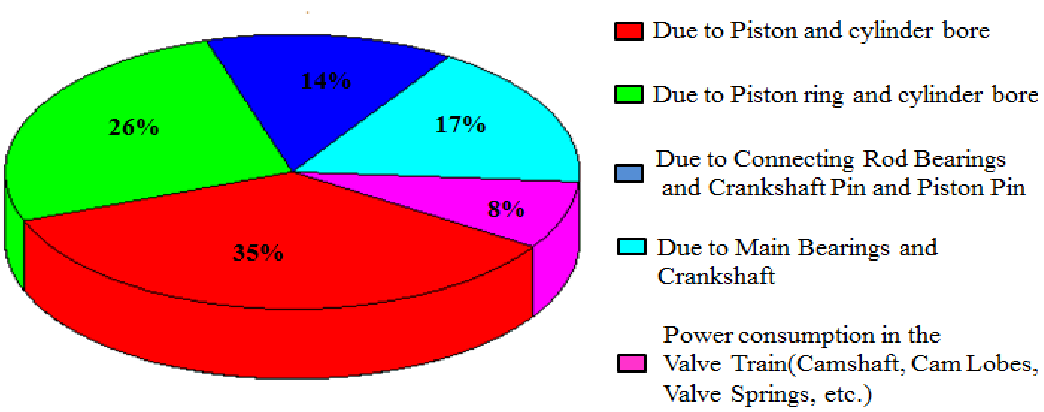


Figure 2 Losses in engine due to different component [6]

To overcome the above mentioned losses, we need to improve the tribological conditions in engine. The decision of material selection adopting suitable tribological solutions for the various engine components of the automotive industry is highly complex and ever challenging due to the utmost concern related to the fuel economy, improved safety, global warming and energy usage. Aluminium castings have been traditionally used for almost

100% of pistons in petrol and diesel engines. However, one of the most significant drawbacks of aluminium alloys is that they demonstrate low wear resistance. Despite of its widespread use in automotive applications, Aluminium alloys perform poorly at high temperature applications. To overcome some of the limitations associated with the alloys, development of metal matrix composites are getting growing interest amongst the researchers. However, limitations associated with the manufacturing costs as well as the inherent casting defects of such composite piston hindered the future research on the development of AMMC based piston materials.

Benefits of improving the tribological condition in engine includes increment in output power, reduction in fuel consumption, increased engine life and durability, decrement in maintenance time and increase service interval, and decrease harmful exhaust emission [8], [9]. Modern pistons for internal combustion engines require highly specialized and cost effectively developed materials which should be characterized by low density, suitable thermal expansion and conductivity, resistance to thermal shock, good tribological properties, enhanced mechanical properties including fatigue strength, hardness and capability for vibration damping [10]. The subsequent sections in this chapter provide a brief overview of the fundamental concepts of the prerequisite knowledge that will be useful and necessary for accurate interpretation of the works presented in the subsequent chapters.

## 1.2 Fundamental concept of Wear

Wear is defined as the unwanted removal of material from the surface when it comes with the contact of mating surface. Figure **3** shows a flow diagram depicting the different types of wear modes resulted from the different types of contacts materials and operational conditions [11]. Wear affect the life of machine, reliability, durability, increase maintenance cost, and etc. There are main three ways of wear which is physical separation, melting and chemical dissolution [12].

In physical separation, material is removed due to fracture. Fracture may cause by the brittleness of material, fatigue of material, and also due to ductility of material. Melting of material due to frictional heating is also responsible of material removal, is an another form of wear. In case of chemical dissolution wear takes place by the oxidization and diffusion of material surface [13].

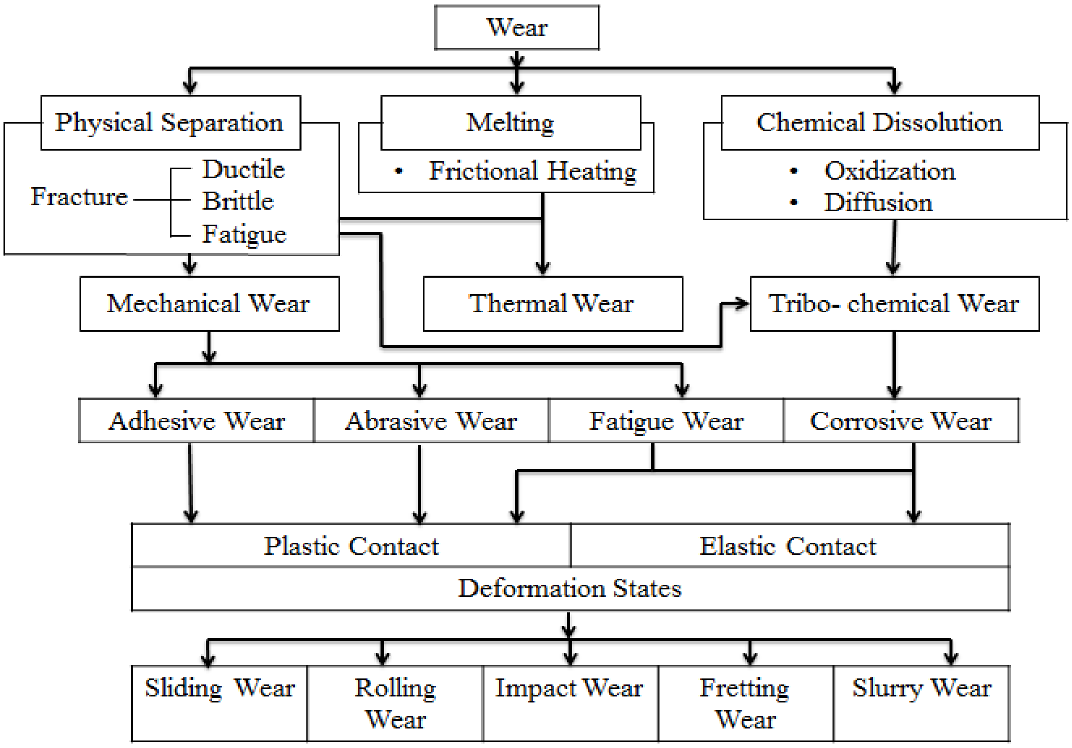


Figure 3 Flow diagram of wear [11]

Further, there are three sub-categories of wear viz. mechanical wear, thermal wear and tribo-chemical wear. Mechanical wear is mainly divided into four categories such as adhesive, abrasive, fatigue and corrosive wear.

Adhesive wear (Figure 4) occurs when two surfaces contact with each other and forms junction at localized asperity contacts or cold-welds between them. During sliding, the adhesion junction breaks down under the action of compression force and shearing and subsequently, a new junction is formed which also breakdown during successive sliding actions. In this way, there is a continuous formation and rupture takes place in this mode of wear of the moving contacts. During this process, material is transferred or loss takes from either or both surface. This type of wear can be minimized with the help lubricant or hard coating, provided the coefficient of friction of the contact is reduced [14]–[16].

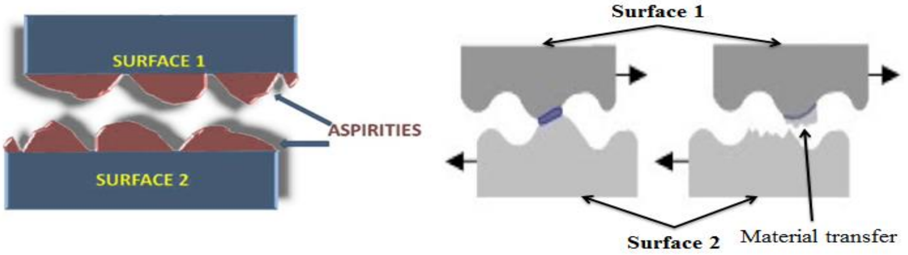


Figure 4 Adhesive Wear [15]

Abrasive wear takes place when material removal of one surface occurs by another hard material, accomplished by the interlocking and plowing action of hard asperities. In case of abrasive wear, grooves with various depths are formed on the weaker surface due to the removal of material. The abrasive wear is shown in Figure **5** [17]-[18].

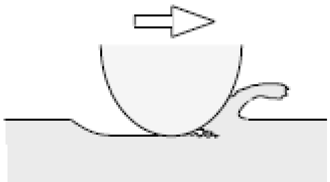

Figure 5 Abrasive Wear [15]

The concept of fatigue wear is different from the above two wear modes. Both adhesive and abrasive wear does not need repeated cycle operation. If wear is happened due to repeated cycle of rotation or sliding under cyclic loading than that form of wear is known as fatigue wear [19]. On the other hand, in case of corrosive wear the tribopairs operate under corrosive environment. There are two type of corrosive wear i.e. wet and dry. The corrosive medium may be water, acid, seawater, etc. or it may be dry gases such as natural gas, nitrogen, etc. [20]. In this mode of wear, a reaction layer is formed due to tribo-chemical reaction, however, it is removed by the sliding friction and hence, wear of material starts with due course.

## 1.3 Fundamental concept of Friction

Whenever there is a relative motion between two bodies, a resistive force will act on them in the direction opposite to the motion of the body. This resistive force is known as Friction. It is believed that there are two major causes of friction mechanism i.e. adhesion and material displacement. Further, friction is classified into two types i.e. static friction and kinetic friction [21].

Coefficient of friction (CoF) is defined as the ratio of friction force to the applied load. CoF is a system property, not a material property. The mathematical equation of cof is given below:

$$\boldsymbol{F = \mu N}$$

Where, F= Friction Force (Newton)

N= Applied or Normal Load (Newton)

μ= Coefficient of friction

The above equation of friction force shows that friction force is directly proportional to applied load [22], however, independent of apparent area. Surface roughness between two bodies affects the coefficient of friction. Higher the surface roughness, higher will be the CoF. Else, various parameters such as type of lubrication, contact stress, temperature, environmental condition and contact geometry also affect the coefficient of friction. By doing some modification between the contact conditions of two sliding bodies, wear and friction can be minimized. Applying lubrication or controlling the surface properties both friction and wear can be minimized.

## 1.4 Composite materials

The material which contains two or more elements (micro, nano and macro), with different physical and chemical properties as compared to base material and which retain their individual identity but enhances the overall properties, is known as composite materials. Hence, composite is different from alloy as alloys are homogeneous in nature but composites are always heterogeneous in nature. Generally composite have one base matrix element and one or two reinforced element in base matrix [23]. The reasons of developing composite material are that it is stronger, lighter, high creep resistance, high wear resistance, improve corrosion resistance, less expensive and long fatigue life than the traditional materials.

### 1.4.1 Matrix

The matrix is the primary phase in composite which remains in bulk form. Generally, matrix holds the secondary phase which is imbedded in matrix, due to more ductile in nature. There are some examples of light weight matrix like aluminium, magnesium, titanium, and etc. [24]. There are mainly four types of matrixes which are given below and shown in Figure **6**. Accordingly, these are called polymer matrix composite (PMC), metal matrix composite (MMC), ceramics matrix composite (CMC) and carbon-carbon matrix composite (CCMC).

In this thesis, aluminium has been used as the matrix material to fabricate the suitable hybrid aluminum metal matrix composites (h-AMMC) to address the issues related to the tribological and manufacturing aspects and fulfill the proposed research objectives. Aluminium has unique properties like light weight, low density, corrosive resistance, soft in nature, high strength and weight ratio. The various applications AMMCs are used include various industries such as automobile, marine tribology, aerospace, and etc.

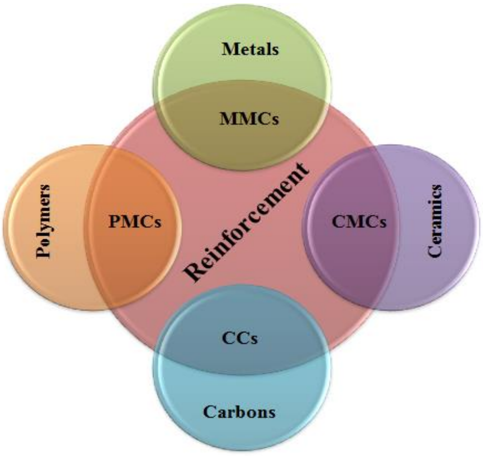


Figure 6 Different types of matrixes

### 1.4.2 Reinforcements

The reinforcement is the secondary constituent of the composite which is added into the base material or matrix to enhance the property of base matrix. The reinforcement can be ceramic, fibers, flakes, etc. The selection of reinforcements in the composite depends upon what properties are required from the developed composite [25]. For example, in piston cylinder arrangement the most concerned properties are wear resistance, friction strength and hence for such applications ceramics reinforcement like SiC, $Al_2O_3$, etc are used. The different types of reinforcement which can be used in making or fabricating a composite are shown in Figure **7**.

In the study presented in this report, two types of reinforcements are used for the reasons which will be explained in the subsequent chapters. One is used as the hard reinforcement to enhance some specific mechanical properties. The hard reinforcements may include carbides, oxides, nitride and silicates. In the present research work SiC is used as the hard reinforcement. The second reinforcing agent is used for the enhancement of functional properties which may include graphite, $MoS_2$, MWCNT, etc. For the some obvious reasons which will be detailed in the later chapters it will be seen that MWCNT is used as the second reinforcing agent for the fabrication of hybrid composite and carry out the further research works. So, there is a need of providing a brief fundamental background of CNTs and hence, a brief introductory discussion on CNTs is made below.

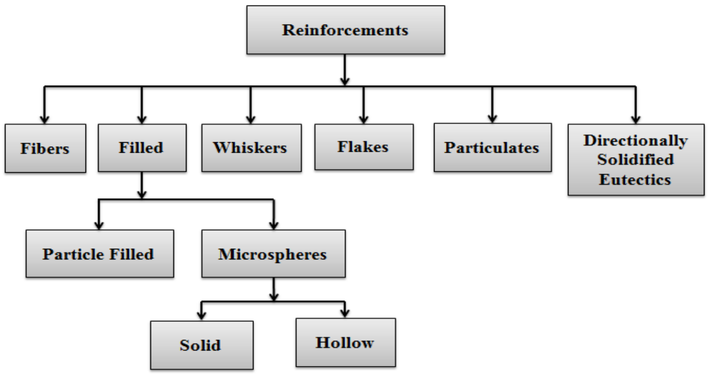


Figure 7 Different types of reinforcements [11]

## 1.5 Carbon Nanotubes (CNTs)

The carbon nanotubes are formed by the rolling of carbon atoms sheet. If the diameter of CNTs is 1-2 nm than the nanotubes comprise of single-walled and hence, called single-walled carbon nanotubes (SWCNT). Diameter of multi-walled carbon nanotubes (MWCNT) ranges from 4 to 100 nm or even more than that (Figure **8**). CNT has extremely superior physical and mechanical properties, in addition to its self-lubricating nature. Addition of CNTs in metal matrix can help in intensifying the properties of MMC in terms of strength, stiffness, essential stability at high temperature, improving the electrical and thermal conductivity, which in turn enhance the performance of industrials components.

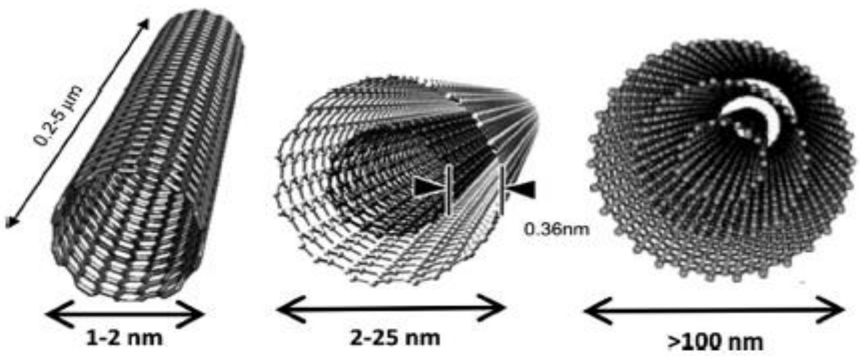


Figure 8 Single and multi-walled CNTs [26]

Numerous methods are developed by researchers to calculate the elastic modulus and strength of CNTs. One of the most suitable methods is based on the amplitudes of thermal vibration of nanotubes. Using this method, the average value of elastic modulus was found to be 1.8 TPa whereas from an alternative study by Brenner, it was found to be approximately 1060 GPa [27]. The stiffness value of SWCNT was found in the order of 1 TPa, which was predicted using a Molecular Dynamic (MD) simulation [28]. Using an alike technique called laser ablation, the modulus of MWNTs was found to be 1.25 TPa [26].

Despite its superior mechanical properties, SWNTs are not extensively used as reinforcement because of high producing and purified cost. MWNTs are easier to create. However, use of MWNTs inherits one drawback associated with the pulling out of the outer tube from inner tubes under tensile stresses. This phenomenon is generally termed as “telescopic extension of multiwall carbon nanotubes” or “telescoping effect” [29].

The presence of CNT can be illustrated by the Raman shifting. There are basically two main graphite bands of MWCNT shown by Raman spectrum, as shown in Figure **9**. The range of G band ranges from 1550 $cm^{-1}$ to 1610 $cm^{-1}$. The D band or defective band is found between 1340 $cm^{-1}$ to 1360 $cm^{-1}$ due to the presence of disorder in carbon systems [30]. From an another study, the D-peak of CNT was found at 1354 $cm^{-1}$ which indicated the defects related to the CNT formation and G-peak of CNT was found at 1566 $cm^{-1}$ which shows that CNT nature is as graphitic [31].

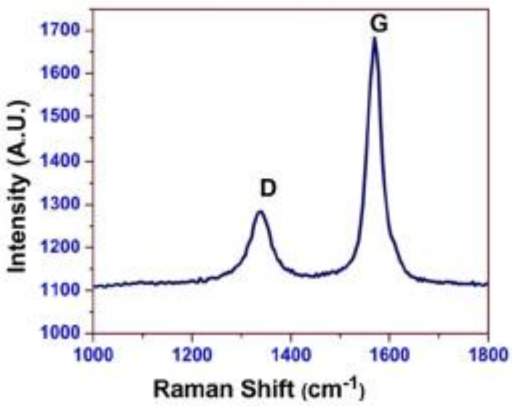


Figure 9 Raman spectroscopy of MWCNT [30]

## 1.6 Conventional Sintering

There are some requirements of sintering process which should be fulfilled by any process which are shown in Figure **10**.

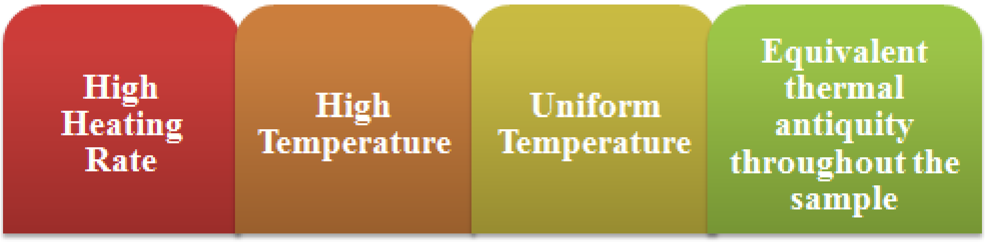


Figure 10 Basic requirement of sintering

The sintering process can be done by fossil fuel furnace, induction furnace or electrical resistance furnace but they consume high energy and time. For extensive time and high temperature expensive heating element is used to maintain this condition [32]. This type of sintering is known as conventional sintering. In conventional sintering the material is heated in electric resistance furnace, induction furnace or fossil fuel.

## 1.7 Fabrication Techniques of composite material

There are many fabrication techniques by which aluminium metal matrix composites are fabricated. The most common and economical production route for composite fabrication is Powder Metallurgy (PM) and Casting. As compared to the conventional casting, better dimensional and geometrical precision and good mechanical properties can be obtained by PM. Below are most commonly used processing techniques that are being traditionally used for composite fabrication.

### 1.7.1 Stir Casting

Stir casting is a low cost process. In this process, aluminium bar is melted in a furnace (Figure **11**). When solid aluminium becomes red hot liquid then clean sample of reinforcement powder is added to the melt. After the addition of reinforcement, the mixture is mixed with the help of stir. After a certain period of time, the mixture is poured into a die for solidification.  Ultrasound energy also can be used for continuously stir the melt and particles [33].

Stir casting route of composite fabrication is accompanied with many limitations such as high manufacturing defects, large volume of materials, high porosity and relatively slower process. In this process reinforcement phase or distribution of reinforcement is not uniform all over the matrix phase. The non-uniformity comes into existence due to irregular flow of melted mixture at the time of pouring into the mould. Besides, at the time of solidification, stir of molten metal is not possible [34].

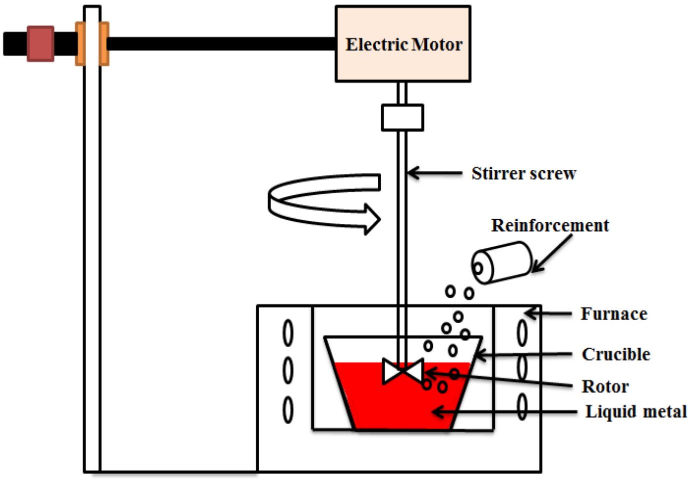


Figure 11 Systematic diagram of stir casting

### 1.7.2 Powder Metallurgy

Powder metallurgy (PM) is one of the most economical and common method for the fabrication of composite materials. By the help of PM good dimensional and geometrical precision can be achieved alongwith the superior mechanical properties. Using this process, composites with enhanced properties like hardness, mechanical durability, wear resistance, thermal durability, and thermal conductivity with decreased porosity can be obtained. Many real world applications where the demand of high quality and low cost material are required such as in automotive and aerospace applications [35]-[36], PM route can be an ideal choice . Depending upon the type of pressure and heat application, PM's route can be sub divided into four different methods as shown in Figure **12**.

Prior to sintering, the material powder is compacted by the UTM or hydraulic press at certain load. During compaction process, powder is put between the die plunger arrangement and a predefined load is applied and hold for a certain period of time. Following this, the powder sample is converted into green compact and ready for performing sintering on it. However, conventional sintering process has the following limitations:

- It is time consuming process.

- Evenif the porosity of the fabricate is less than that of the casting process, however, as compared to some of the other available techniques it lags behind.
- Produces defects due to non-uniform heating. The structure of micro or nano composites may be destroyed after sintering.
- Lastly, it involves more energy and relatively costlier process.

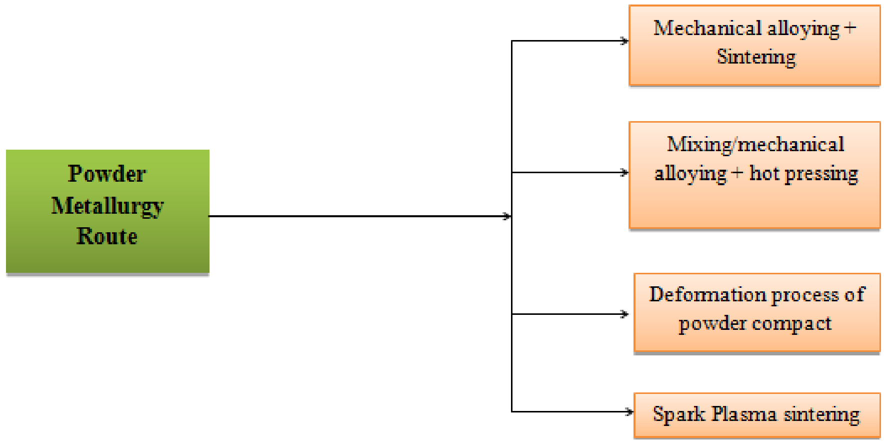


Figure 12 Powder metallurgy

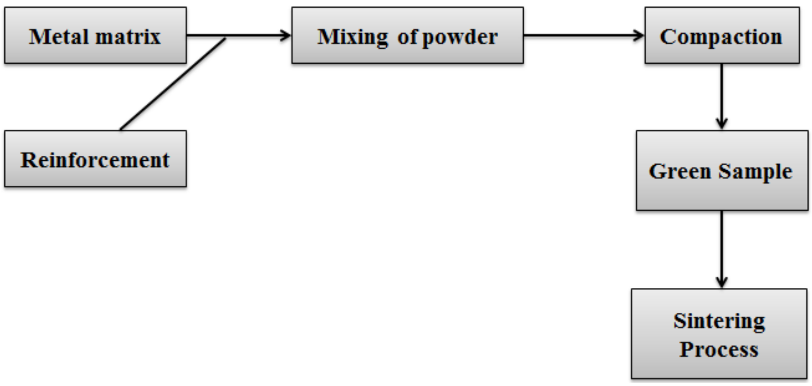


Figure 13 Conventional sintering process by PM route

### 1.7.3 Hot extrusion process:

The hot extrusion is the process in which material is extruded at hot working condition which means that the processing of material is done above recrystallization temperature. Hot extrusion protects the material from work hardening and help in pushing the materials through the die. For aluminium, the hot extrusion process is done at a temperature range of

350-500 $^{0}$C. Mostly, hot extrusion perform horizontally by the help of hydraulic press [37]. The systematic diagram is shown in Figure **14**. However, it has some inherent limitations such as product uniformity is the big issues by this process, high set up cost and only same type of product can formed at a time.

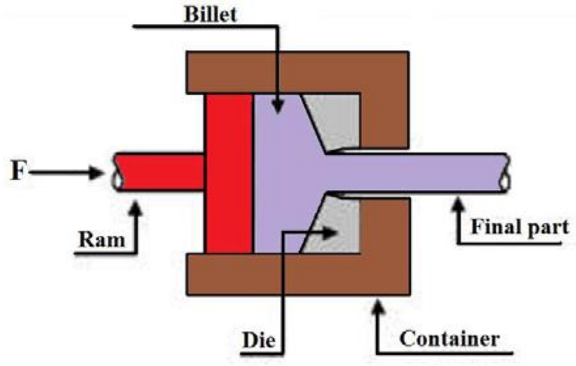


Figure 14 Hot extrusion process [38]

### 1.7.4 Spark plasma Sintering:

The SPS (spark plasma sintering) is a technique in which material is fabricated at low atmospheric pressure. Arc discharge is generated with the help of pulsed direct electric current in a die wherein the green compact sample is placed. The punch and die is made of graphite (Figure **15**). With this technique, a heating rate of 100-1000$^{0}$C min$^{-1}$ can be achieved [38]. Its major limitation includes high set up cost, only simple shape sample are prepared and the cost of pulsed DC generator is very expansive.

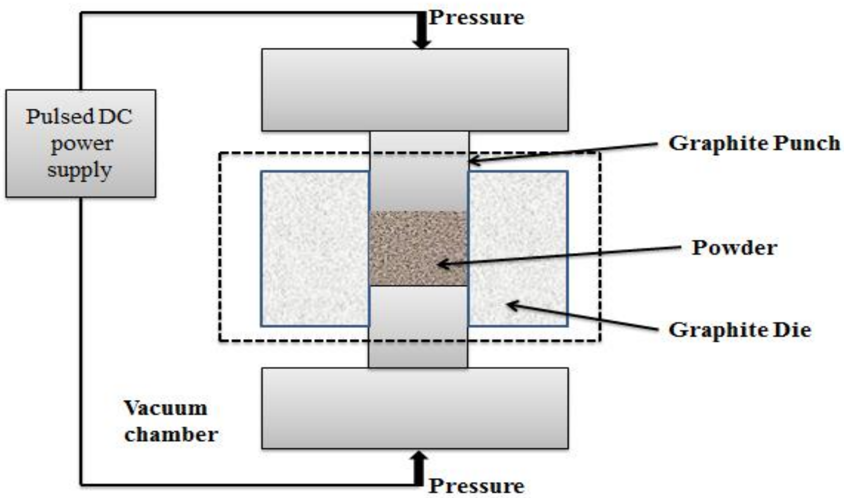


Figure 15 Systematic diagram of SPS [39]

### 1.7.5 Spread dispersion Process:

In this process (Figure **16**), sheets of material are placed in layered fashion, then pressed and after that rolled them to creating single or one layer material. This procedure expands the rigidity of material or composite. Researchers declared that the 66% of original rigidity can be expanded and grain structure can be refined to 20 nm. This process is usually used for the fabrication of nano composite. In a study it was shown for Al-CNT composite there is remarkably uniform dispersion of CNTs is obtained by this method and CNT was credited to with no porosity without bunches or CNTS free zones, and improved holding between Al/CNT and maintenance of graphite properties [40].

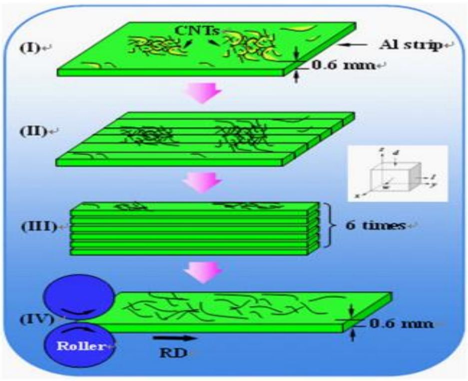


Figure 16 Spread dispersion method [40]

### 1.7.6 Hot Press Consolidation Process:

Hot squeezing is powder metallurgy method in which high pressure; low strain rate is utilized for the powder compact at that high temperature in which enlistment of sintering and creep procedure is conceivable. Some researcher utilized hot press combination process as opposed to doing sintering of AMMC with CNT and other reinforcement [41]. However, this method is accompanied by some limitations such as non-uniform heating rate, time to heat the surface, high temperature differences between the surface and core that can destroy the mold, etc.

## 1.8 Microwave Heating process

To overcome some of the limitations associated with the conventional sintering recently microwave sintering is being used. But for microwave sintering, the selection of material powder is the challenging task due to the reflection of microwaves from metallic surface [42]. There are three ways by which microwave interact with material which are named as transparent interaction, opaque interaction and absorber interaction. And all three are shown in Figure **17.**

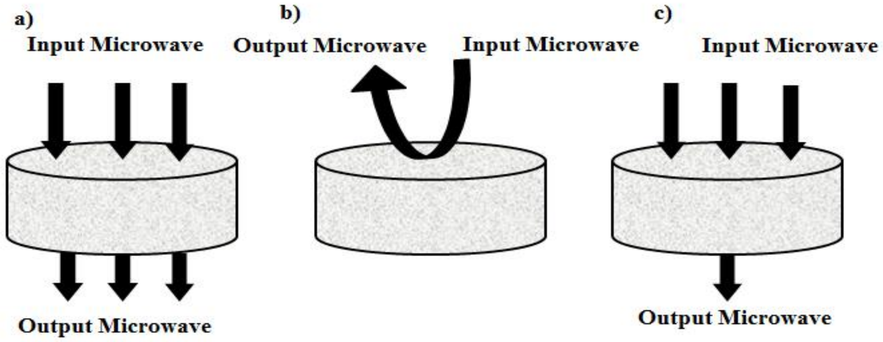


Figure 17 Microwave interaction with materials a) Transparent b) Opaque c) Absorber [43].

In the case of transparent materials all the microwaves pass through the material without any loss. These materials have low dielectric properties. In opaque materials, microwave cannot penetrate the surface and are reflected back. In third condition, almost all microwaves are absorbs by material due to the property of high dielectric losses. The value of dielectric loss factor decided the absorption of microwave by material [44]. Further, there is one more way of interaction of materials is called mixed absorption. This interaction of material is observed in the case of multi-phase material or composite materials in which one of the materials is having the property of low dielectric loss and another having high dielectric loss. Selective heating play a significant factor in the case of mixed absorbs interaction [45]. So it is observed that the microwave interaction with materials is totally depending upon dielectric properties of material. Processing of metallic material through conventional microwave heating route is quite a challenging task. Hence, there need to be hybridization of this heating technique.

### 1.8.1 Microwave Hybrid Heating

The hybrid microwave heating process is the two directional heating mechanism in which heating is done by direct microwave heating as well as by susceptor which has the property of absorbing microwave with high dielectric loss at low temperature [46]. The temperature movement of both conventional sintering as well as microwave sintering is shown in Figure **18**.

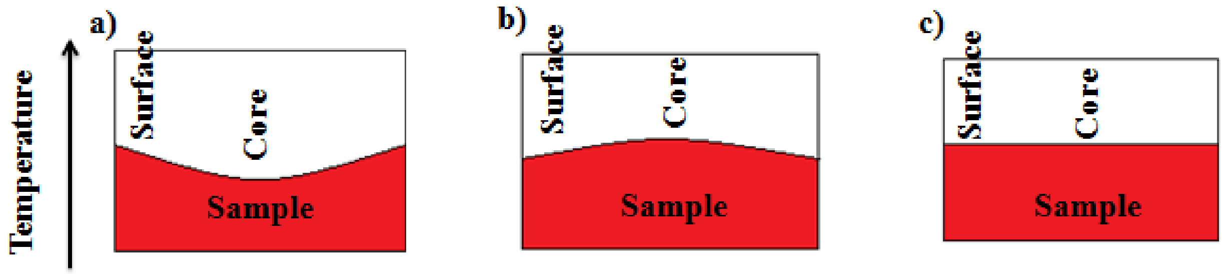


Figure 18 Movement of temperature during sintering: a) Conventional, b) Microwave, c) Hybrid Microwave [32]

The combination of microwave and susceptor which coupled with microwave and work as external heat source can be used as the rapid cladding, sintering, joining and other heating process. In this work hybrid microwave heating is used for sintering process. There are many advantages of hybrid microwave process over conventional techniques which are detailed below [47]-[48] and in Figure **19**:

- Time and energy saving
- Provide volumetric heating of sample which helps in providing the uniform heating of sample.
- Selective heating of sample which help in lowering the defect in sample.
- Cost saving process which make it economical process.
- It involves less pollution which make it environment friendly process.
- It also provides the variety of processing different material.

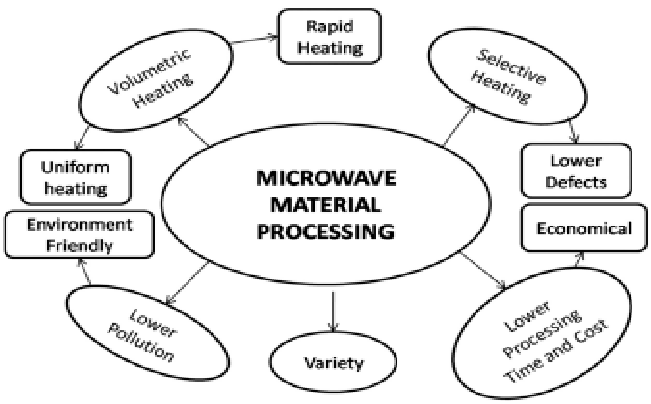


Figure 19 Advantages of Hybrid microwave heating process [49]

In this thesis, sintering of AMMCs is done by hybrid microwave heating process.

## 1.9 Summary

In this chapter, an introductory discussion is presented on the various topics which will be very useful to grasp and interpretation of the work presented in the later chapters. For example, a brief background on the role of tribology in various industries, fundamental so friction and wear, composites and their fabrication techniques, potential use of novel reinforcements for hybrid metal matrix composite such as CNT. A novel and emerging technique for the fabrication of composite i.e microwave hybrid heating is also discussed in brief.

# Chapter 2

# Literature Review

## 2.1 Research on the Development of AMMC for potential automotive applications

From the last few decades, a great deal of works has been carried out internationally in the field of AMMC to explore its potential automotive applications. A glimpse of such works can be found in some of the notable review articles of Allison et al., and Chowla et al. [50]-[51]. Donomoto et al. [52] developed a CF reinforced AMMC piston for diesel engine. From their study, it was reported that the designed material performed well at elevated temperatures in terms of mechanical, thermal and tribological point of view. They recommended the use of AMMC for the strengthening and modification in the area of top land and top ring groove of piston to avoid the sacrificing of manufacturing cost and productivity.

Hunt et al. [53] provided a comprehensive review on the potential automotive applications AMMCs and illustrated the limitations which result from the materials and design of existing AMMC for pistons and other engine components to improvement of engine operation features. Dolata et al. [54] for their investigation developed composite pistons of Al/SiC and SiC/C by mould casting and found that there is a heterophase reinforcement from utilization the technology of mould casting. Goni et al. [55] suggested a new low cost metal matrix composite for pistons, clutch discs, and train brake discs.

The research on the AMMC for automobile material development in India is very limited and incomprehensive. Most of the Indian authors, presented some of the well-structured and concised review of the relevant researches that are being carried out worldwide on the prospect of AMMC in automotive applications [56]–[59]. A very few researchers focused their works on the development and performance analysis of the AMMC piston materials. Krishnan et al. [60] fabricated Al-Si-graphite particle composite alloy pistons by casting. From their preliminary finding it was concluded that Al-G composite can be a highly potential material for automotive piston material. Karthe et al. [61] made an attempt to develop the AMMC piston materials by adding the glass fiber to aluminium piston and found an improvement in the thermal and mechanical property of the piston. Additionally, a few preliminary and more simplified studies on the design and analysis of AMMC pistons were also carried out by some researchers [62], [63].

Al alloys used for the above studies mostly involved Al6061, 6063, 7075, A390, A356 as matrix material and $Al_2O_3$, SiC, $ZrO_2$ as hard reinforcements. Now-a-days, carbon nanotubes reinforced MMCs (CNT-MMC) are being explored for automotive applications. CNTs have proven ultrahigh strength and modulus [27], [64].

## 2.2 Investigations on the Mechanical Properties of CNT-reinforced AMMC

In a study, Al-0.5 wt. % CNT composite strip was fabricated with help of conventional sintering [65]. Remarkable improvement in the mechanical properties of AMMC was observed by the addition of CNT. Kuzumaki et al. [66] fabricated the Al/CNT composite using 5 vol. % and 10 vol. % CNT. They had mixed the aluminum powders and carbon nanotubes by ultra-sonication which was then followed by hot pressing and extrusion. It was reported that, there is no enhancement in tensile strength by the addition of 5 vol. % and 10 vol. % of CNTs in aluminium matrix. This happened due to the cluster formation of CNTs and dispersion of CNTs was found poor which was attributed to the no increment in tensile strength of AMMC as compared with pure aluminium.

A.M.K. Esawi et al. [67] fabricated the Al/CNTs composites with different wt % of CNTs. They showed that by the addition of CNTs in aliminium there is an increase the tensile strength as compared to pure aluminium. They observed that addition of 2% wt. CNTs shows the most significant strengthening effect. However, further addition of CNTs did not show any significant positive result in terms of tensile strength enhancement.

Danilo Marini et al. [68], in their work investigated the young modulus of Al and Al-MWCNT composites with four different percentage of MWCNT fillers. They conducted four point bending tests for all the samples at different temperatures to estimate the flexural strength. Mansoor et al. [69], successfully fabricated the Al/CNTs composite by using induction melting. In his study, no evidence was found on the segregation of CNTs as confirmed by SEM and TEM studies. Due to adequate dispersion of CNTs there was an increase in strength, hardness and ductility.

Liao et al. [70], fabricated the Al-CNT composite with help of ball milling followed by vacuum sintering. Then they extruded it at $500^0$C with an extrusion ratio of 9:1. Extrusion process redistributed the reinforcement homogeneously due to a large deformation. Compression stress was generated in the presence of CNTs during powder mixing. However, they found thermal mismatch during sintering, due to the consolidation and shrinkage effect. Hiroki Kurita et al. [71], fabricated the AMMC with MWCNT by different methods like Spark Plasma Sintering, CHAM, and Hot Extrusion. For SPS and hot extrusion, powder ultra-sonication was done in the presence of ethanol as well as MWCNT had acid treatment using the hetero-agglomeration principle. It was found that the there is an improvement in tensile strength by 40% and an ductility was enhanced by 27.3% as compared to the cast Al.

In the SPS process, they found that the nano scale surface defects of MWCNTs were penetrated by temporarily formed liquid Al and an $Al_4C_3$-free interface was formed between Al matrix and MWCNTs. In case of hot extrusion, they found that MWCNTs was aligned straight and dynamically recovered and found crack free Al matrix without any interfacial $Al_4C_3$. This implied that the improvement in tensile strength was directly created from an effective load transfer at the MWCNT/Al interface.

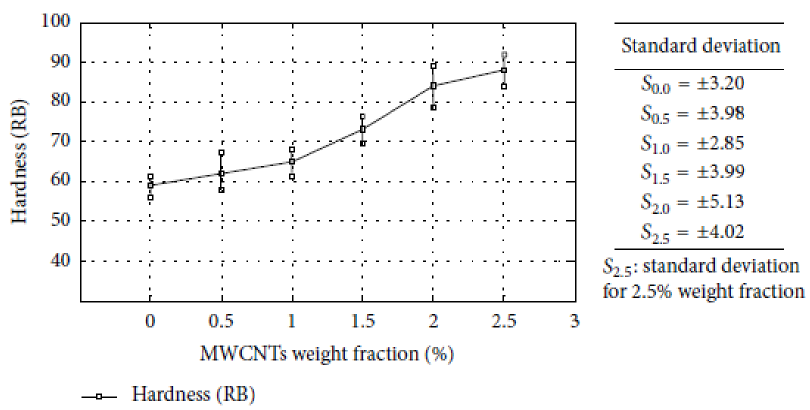


Figure 20 Variation of hardness of Al-MWCNT composite with fraction of MWCNT [72]

Elshalakany et al [72], fabricated Al/MWCNTs by combination of Rheocasting and Squeeze Casting techniques. The powder (Al/MWCNTs) was mixed by the help of ball milling process using stainless steel balls for 8hr at 200rpm. The ball to powder volume ratio was 8: 1. The hardness of composite was increased by increasing wt.% of MWCNT as shown in Figure **20**. It is found that ultimate tensile and yield strength properties increases by increasing the % of MWCNT and shows the optimum value at 1.5%MWCNT. Further increment of

MWCNT lower the ultimate tensile and yield strength due to difficulty in the entrapment of hydrogen during the reinforcement addition.

Majid et al [73], fabricated Al-MWCNT composites with 0 wt.%, 1.0 wt.%, and 5.0 wt.% MWCNTs by hot extrusion technique. The mixture was prepared by ball-milling process. The ball milling process for composite was done for different time off period but the significant result of hardness was found at 4h of ball milling process followed by extrusion at 500 °C. Due to the excessive strain hardening in the presence of MWCNTs in Al they found that there is an increase in yield strength upto 500% as compared to pure aluminium.

*M. Jagannatham et al*. [74], fabricated Al/CNT composites with different wt.% of CNT reinforcement (0.5wt.%, 1.0wt.%, 1.5wt.%, 2.0 wt. %) which were added after mixing for 1 h. In this study, the authors sintered the composite by two methods i.e. conventional sintering and hot extrusion sintering using UTM with extrusion ratio of 1:16. Before the extrusion of Al/CNTs composite the samples were heated up to $450^0$C and after that samples were kept for 90-min soaking time. The author reported that only up to 1wt. % of CNTs in aluminium matrix an effective improvement in hardness and tensile strength can be achievable. They believed that further increase in CNT content gives reserve effect which in turn reduces the hardness and tensile strength after the addition of 1wt. % of CNTs. Formation of $Al_4C_3$ in Al-CNT composite is shown in Figure **21**.

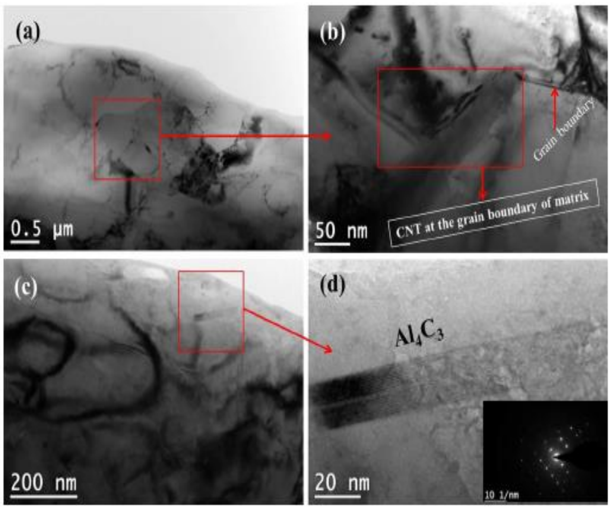


Figure 21 TEM images of Al-CNT composites; (a) 1 wt. % CNT, (c) 2 wt. % CNT, (b and d) magnified image of a and c showing the pattern of $Al_4C_3$

## 2.3 Research and Development on the Tribological Behavior of CNT-reinforced AMMC

The superior properties of CNTs such as electrical, optical, mechanical properties and self-lubricating properties make it potential novel nanomaterial for its application in tribological components. The important role of CNT as reinforcement in metal matrix can be in the form of reduction in coefficient of friction and improvement of wear resistance of nano composite. Besides, due to its light density it has potential to play a brilliant role in lightweight industrial applications. Investigations [75], [76] exhibit that self-lubricating nature of CNT helps in reducing the wear rate and the coefficient of friction of MMC with the reinforced CNT composite because CNTs generate a film which acts as lubricant between contacts surfaces during sliding. The MWCNT have van der waals forces which are weak in nature. When MWCNT is reinforced in matrix, during sliding MWCNT walls have a tendency to slide due to weak van der walls. Wear resistance also increase with adding of CNT in metal matrix due to the CNTs play as a spacers that avoid a protection that there is no straight contact of metal/CNT composite with rough surface [77]. For the significant tribological enhancement various associated factors are also important such as size of CNT, amount and spreading of CNTs in metal matrix.

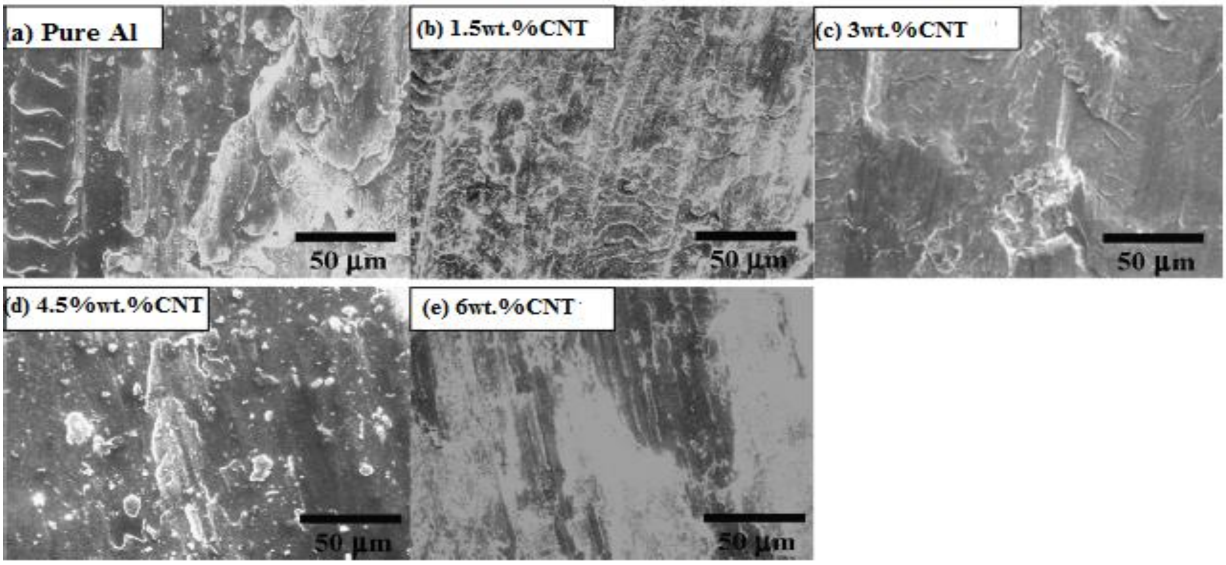


**Figure 22 SEM images of wear tracks for (a) pure aluminum and composites containing MWCNTs of (b) 1.5 %, (c) 3%, (d) 4.5%, and (e) 6.%, respectively.**[78]

*H.J. Choi et al.* [78], investigated the wear and friction properties of Al-MWCNT composite with the different percentage of reinforced MWCNT (1.5%, 3%, 4.5% and 6%) and found that addition of 4.5 vol% of MWCNT give significant improvement in wear resistance as well as yield strength. It also offered lower coefficient of friction which they attributed to low hardening effect and predominance in self-lubricating effect of WCNT. The Cof and wear loss (at 0.12m/sec sliding speed and 30KN load) as observed by them is shown in Figure 22.

*Al-Qutub et.al.* [79], shown that the coefficient of friction of monolithic alloy has more fluctuation than Al6061-CNT composite and have low coefficient of friction. In this study, it was observed that with the increase in load there is an increase of the coefficient of friction for both monolithic alloy and composite. Following the worn surface analysis of composites it was found that at higher load the adhesion in composite was excessive which results in sub-surface fracturing and delamination. However, it was found that upto a certain load, CNT is tribologically beneficial, after which it shows negative impact.

Manjunatha et.al. [80], studied wear behavior of Al6061-CNT with 0.1 wt. %,0.2 wt.%,0.3 wt.%, 0.4 wt.%, 0.5wt.% CNT, sliding against EN25 disc. In their study, 0.5 wt% showed best result in terms wear behavior, which they attributed to the interfacial bonding of CNT with aluminum matrix. They also found increased wear with sliding distance which they believed to be due to work hardening of the surface leading to abrasion. Pe´rez-Bustamante et.al. [81], for their study fabricated Al2024+CNT composites with different wt. % of CNT (1%wt, 3wt% and 5%wt). They found upto 37% and 21% enhancement of wear resistance.

Bastwros et.at. [82] have shown that as load increases, the CoF decreases but wear rate increases, as shown in Figure **23**. It was also reported that the fluctuation in coefficient of friction is higher at higher load. The authors believed that under lower load CNT are wearing off gradually rather than crushed which cause smooth friction behavior.

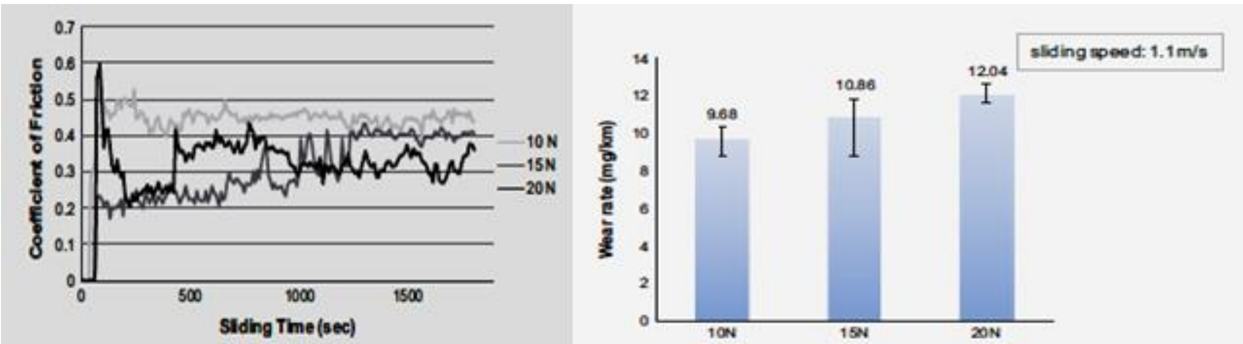


Figure 23 Plot of coefficient of friction vs. sliding time and wear rate vs. applied load [82]

## 2.4 Research and Development on the Tribological Behavior of CNT-reinforced Hybrid AMMC

K.R.Padmavathi et al. [83] studied the tribological behaviour of CNT reinforced hybrid AMMC composites (Al+15%SiC+0.5%CNT and Al+15%SiC+1%CNT) and shows that by increasing the CNT % in hybrid composite there is a decrease in the CoF as well as wear loss. Carvalho et al. [84] worked with AlSi-CNT-SiCp composites and found that CNT have two impact on tribological behaviour of composite. Firstly, its self-lubricating effect and secondly its strengthening effect. Authors compared the wear behaviour and friction resistance of hybrid composite with that of AlSi composite and found that the addition of CNT improves the wear behaviour and COF. Hekner et.al. [85], investigated the effect of friction and wear behaviour of Al-SiC(n)-CNT at $450^0$C and compared with the performance of Al-SiC and found that CoF in case of hybrid composite is slightly higher than that of Al-SiC composite.

Kiran Raj et al. [86], investigated the wear properties of Al-CNT-Eglass hybrid composites (A7075+(0.5wt.% ,1%wt.%,1.5wt. % & 2wt.%CNT)+(1wt. % & 5wt.%) E glass) and found that composites with (0.5% and 1%) CNT and (1% and 5%) E glass decrease the wear resistance. However, on increasing the CNT content to 1.5% and 2% wear rate increases significantly. Zakaulla et al. [87] also investigated the tribological properties of Al2024+10%$B_4$C+(0-2)%MWCNTs. Their findings showed that Al2024+10%$B_4$C+2%MWCNT exhibits lower wear and coefficient of friction as compared to Al2024+10%B4C+1%MWCNT and Al2024+10%B4C. They attributed it to the less void, pit and grooves in case of 2%MWCNT which in turn offers the sample high modulus and thermal stability.

*Ali Alizadeh et al.*[88] fabricated hybrid composites (Al5083+5vol. %CNT+ (5vol. %&10vol. %) B4C) by powder metallurgy. Powder was made ready by ball milling for 5 hr at rotational speed of 250 rpm, the ball to powder ratio was 10.1. The segregation of CNT in the aluminum matrix after milling is shown in Figure **24** & Figure **25.** It found that the addition of CNT in Al5083 reduce the wear resistance due the agglomeration of CNT. Highest wear resistance was found by the addition 10% of B4C in Al-CNT composite.

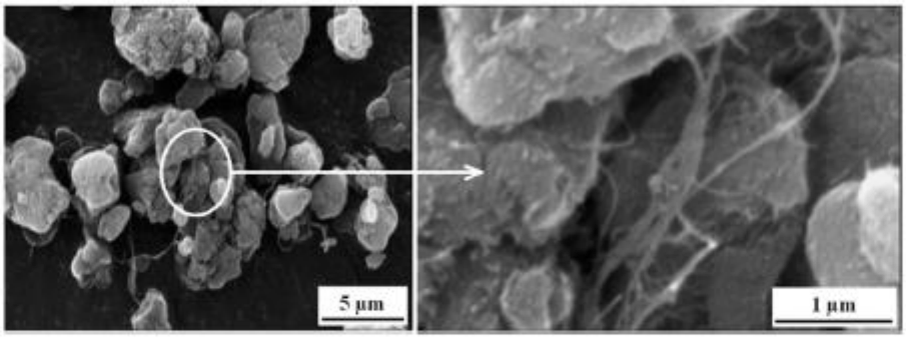

Figure 24 Carbon nanotubes segregation on the surface of aluminum particles after milling [88]

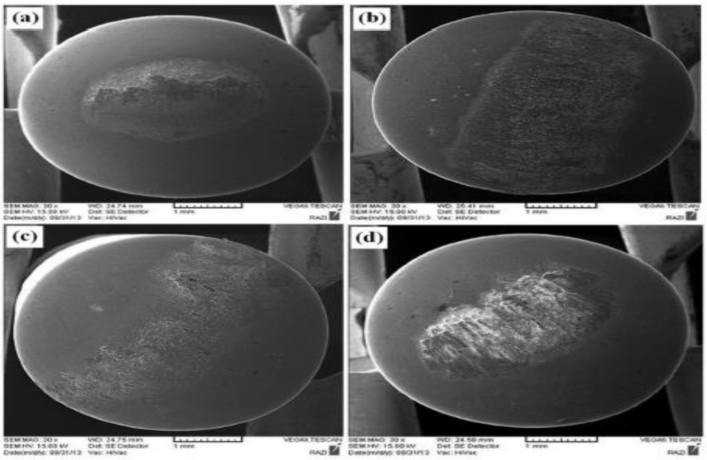

Figure 25 SEM image of (a) Al 5083; (b) Al-5 vol.%CNT; (c) Al-5 vol.%CNT- 5 vol.%B4C and (d) Al-5 vol.%CNT- 10 vol.%B4C after wear test.[88]

Hekner et al. [89] fabricated a hybrid aluminium composite with 1%wt CNT and performed tribological testing at room temperature. In their study, the authors compared the mass loss and coefficient of friction of Al-SiC composite with Al-SiC-CNT composite. The composites were fabricated by hot pressing technique. However, there was no scientific rationale was provided for the wear mechanism.

## 2.5 Research and Development on the Tribological and Metallurgical Characterization of AMMCs Fabricated by Microwave Heating route

Most of the works reported till last few years fabricated AMMC for their investigation using more conventional casting route, which has its inherent drawbacks. The currently used processes for the fabrication of the AMMCs are stir casting, powder metallurgy, conventional laser sintering, and spark plasma sintering (SPS). But these mentioned processes have a lot of limitations which affects the efficiency and use of MMCs. The problems associated with the different processes include porosity in powder metallurgy due to slow heating rate, thermal distortion of the material due to intense laser beam in laser sintering, only simple and symmetrical shapes can be manufactured with SPS. Besides, some disadvantageous associated with piston material development using traditional casting route includes ceramic particles' sedimentation, floatation or agglomeration (results in poor castability), poor solidification and crystallization, inferior mechanical properties, including reduced corrosion resistance of a composite. Hence, there is a need of an alternative manufacturing technique.

Microwave material processing route has been extensively explored by some of the Indian researchers, especially for cladding and sintering [47], [90]–[92]. For AMMC, the sintering temperature is near $600^0$C which can be achieved by conventional microwave sintering in 30 min with an increment cycle of 250C/min [49],[93]. Ghasali et al. [94], fabricate the Al/CNT composite with microwave sintering. The author also fabricated the hybrid AMMC with CNT and graphene. By using microwave sintering the author found that there is an enhancement in density and micro hardness of composite as compare to conventional sintering. More recently in 2019, Madhan at al. [95] has carried out a study to compare the microstructural and mechanical characteristics of $Al_2O_3$-SiC composites fabricated by conventional and microwave sintering.

However, in case of conventional microwave sintering most metals reflect the microwave irradiation at room temperature [96]-[97]. These problems can be overcome by using the newly introduced MMC fabrication process i.e. sintering by microwave hybrid heating (MHH), which uses the concept of hybrid or two directional heating [49]. The prospect of MHH technique for such metallic materials has been reviewed by Gupta et al. [91]. In 2016, Maitli et al. [98] has reported the characterization of AMMCs fabricated by microwave rapid sintering. However, as per the author's knowledge there are very limited works reported which include the mechanical, metallurgical and functional characterizations of hybrid AMMC that has been processed through MHH route.

## 2.6 Research Gaps

Following observations are made and research gaps are found based on the extensive literature survey that has been carried out in this chapter.

- CNT-MMCs are emerging out as a new class of material for lightweight applications. However, despite of its potential benefits in tribological applications adequate attention is not given in this direction of research, which is still in the infancy stage.

- Most of the study associated with CNT-MMCs till now is focused on the fabrication and mechanical characterizations.
- Besides, adequate attention is not given for developing and performing functional characterization of CNT reinforced h-AMMCs. The prospect of CNT reinforced hybrid MMCs for tribological environment is yet to explore.
- Recently, microwave material processing route is gaining interest due to its cost and energy effectiveness as well as capability of yielding processed material with superior properties. However, processing of metallic materials through this approach is quite challenging. Powder metallurgical route in combination with hybrid microwave material processing can be one such option which can be helpful in optimizing the processing time and be made environment friendly process to fabricate the MMCs.
- Finally, development and characterization of CNT-reinforced hybrid AMMC using the suggested material processing technique will open up a new dimension for further research in the development of lightweight AMMCs for the potential applications such as piston material development.

## 2.7 Thesis Objectives

The proposed research work is aimed at to achieve the following objectives:

- Development of CNT-reinforced h-AMMC via powder metallurgy route in combination with microwave hybrid heating sintering process.
- Influence of processing parameters on the mechanical and physical properties of microwave sintered CNT-reinforced h-AMMCs.
- Metallurgical characterizations of CNT-reinforced h-AMMC fabricated by both conventional sintering and microwave sintering.
- Friction and wear behavior of the composites fabricated by conventional and MHH route.
- Statistical analysis of tribological behavior of microwave sintered h-AMMC.

# Chapter 3

# Materials, Methodology and Experimental Procedure

## 3.1 Introduction

In the previous chapter an extensive literature has been carried out, potential research gaps are identified followed by the formulating of research objectives. This will help us in the material selection process and experimental setup for pilot study. In this chapter, detailed workplan is presented alongwith the material selection and experimental procedure. The details of various tools and techniques used for fabrication of hybrid composites, their characterization and functional studies are also detailed in this chapter. Designs of experiment and input and response parameter are also discussed.

## 3.2 Workplan followed to achieve the objectives

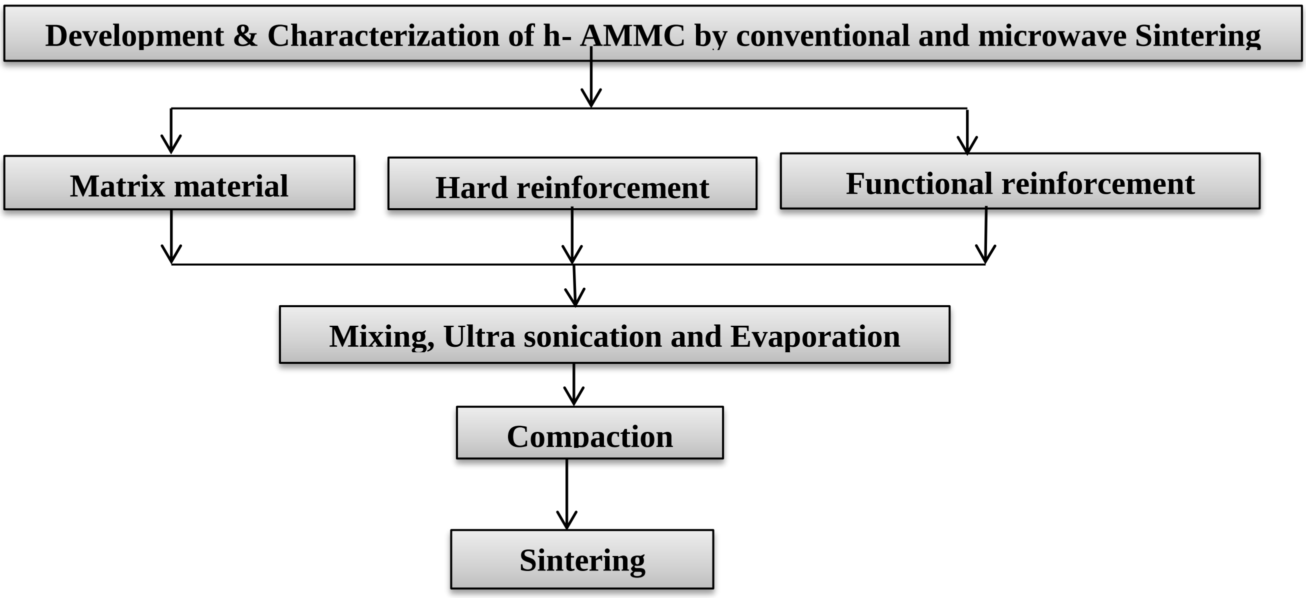

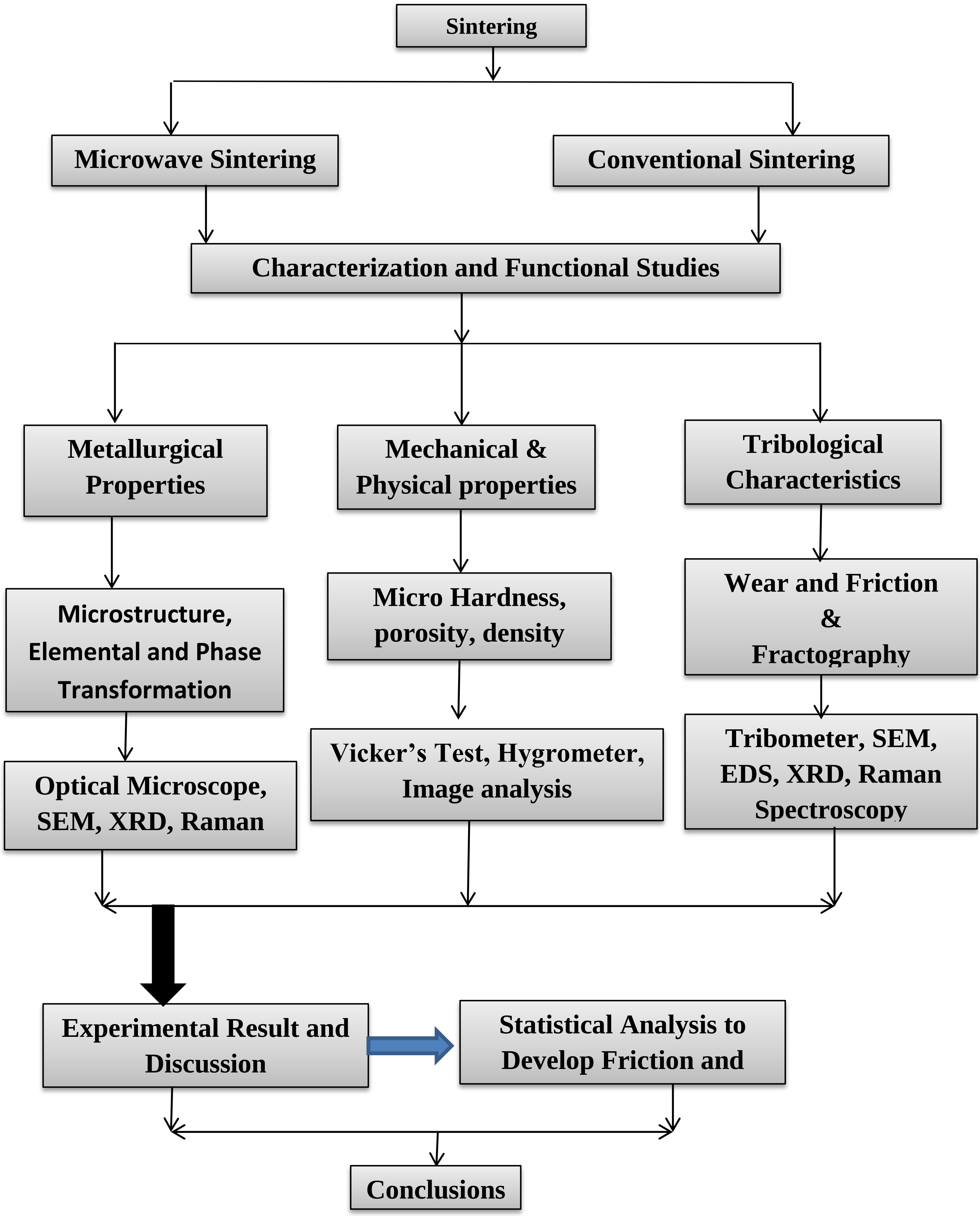


Figure 26 Detailed work plan

## 3.3 Material Selection

### 3.3.1 Metal Matrix

The selection of base material is done on the basis of abundance, low cost, light weight, high strength to weight ratio, high wear and friction resistance, high thermal conductivity, low coefficient of thermal expansion and high toughness and corrosion resistance. All the above mentioned properties make us an obvious choice to go with aluminium metal matrix. So aluminium is used as the base material. In this study, A390, a grade of piston material, is used as matrix material for AMMC.

Table 2 Chemical Composition of A390 used (wt. %)

| O | Al | Si | Ti | Cr | Mn | Fe | Ni | Cu | Zn | Sn | Sb |
|---|---|---|---|---|---|---|---|---|---|---|---|
| 1.75 | 77.5 | 15.96 | 0.14 | 0.12 | 0.33 | 0.92 | 0.51 | 1.31 | 0.94 | 0.11 | 0.41 |

### 3.3.2 Reinforcements

Reinforcement plays an important role in composite materials. Different reinforcement gives different properties in composite materials. The selection of reinforcement for making composite should depend upon the desired properties like thermal stability, low density, increase strengthening in metal matrix, as well as how these reinforcements interact and form interfacial bonding with metal matrix. In hybrid composite two or dual reinforcements are used i.e one hard reinforcement and another soft or functional reinforcement. Hard reinforcements may be $B_4C$, SiC, $Al_2O_3$, TiC, and $TiB_2$, whereas functional reinforcements may be MWCNT, Graphite, Molybdenum, etc.

#### *3.3.2.1 Hard Reinforcement*

In this study, SiC used is as the hard reinforcement. Prior to the selection, a detailed comparision of the properties for a few alternative hard reinforcing agents were made, as shown in

Table **3**. The key properties of SiC such as low density, high hardness, low thermal expansion, high thermal conductivity, high strength, high elastic modulus helps in improve the properties of metal matrix when added to them. As per literature survey, it has been proven that SiC helps in improving hardness, wear resistance when added in the AMMC. Some additional properties of SiC is also listed in Table 4.

Table 3 Selection of hard reinforcement

| **S.No** | **Name** | **Density ($g/cm^3$)** | **Thermal Expansion ($10^{-6}$/K)** | **Melting Point ($^0C$)** | **Microwave Interaction** | **Tribological Properties** |
|---|---|---|---|---|---|---|
| **1.** | Boron nitride | 3.45 | 1.2 | 2,973 | - | Good as Lubricant |
| **2.** | Boron Carbide | 2.52 | 9.4 | 2,763 | Less /optimum at 5% | Good wear and friction |
| **3.** | Aluminium oxide | 3.987 | 8.1 | 2,072 | _ | Not much effective |
| **4.** | Titanium carbide | 4.93 | 7 | 3,160 | No | Good |
| **5.** | Titanium diboride | 4.52 | 8 | 3,230 | _ | Good wear and friction as well as Corrosion |
| **6.** | Zirconium dioxide | 5.68 | 12.2 | 2,715 | _ | Good |
| **7.** | Aluminium nitride | 3.260 | 4.5 | 2,200 | _ | Good |
| **8.** | Silicon Carbide | 3.2 | 11 | 2,830 | Yes Approx. 30% [18] | Proven Excellent for AMMC |

Table 4 Additional properties of SiC

| | |
|---|---|
| Density | 3.21 $g/cm^3$ |
| Hardness | 2800 $Kg/mm^2$ |
| Elastic modulus | 410 GPa |

| | |
|---|---|
| Melting Temperature | $2730^0$C |
| Thermal Conductivity | 120W/m$^0$K |

*3.3.2.2 Functional Reinforcement*

In this study, CNT is used as functional reinforcement for the fabrication of hybrid composite. As already mentioned in Chapter 1, CNT has superior mechanical and physical properties in addition to its lubricant nature. The addition of CNTs in metal matrix helps in enhancing the properties of composite in terms of high strength and stiffness, essential stability at high temperature, excellent electrical and thermal conductivity and of course might be tribological characteristics, which need further investigation. The details of CNT used for this work is shown in Table **5**.

Table 5 Detail of Soft Reinforcement (CNT)

| | |
|---|---|
| Diameter of carbon nano tubes | 10-20 nm |
| Length of carbon nano tubes | 1μm |
| Density | 2.6 g/cm$^3$ |

The morphologies and composition of the powders used for making h-composite is shown by the SEM micrographs and EDS spectra in

Figure 27.

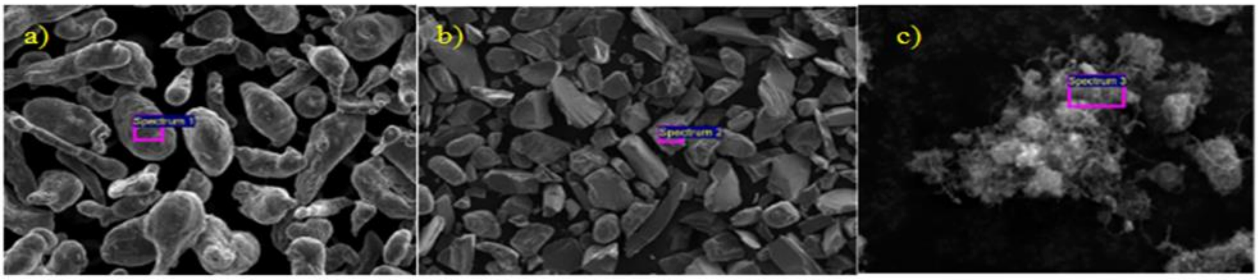

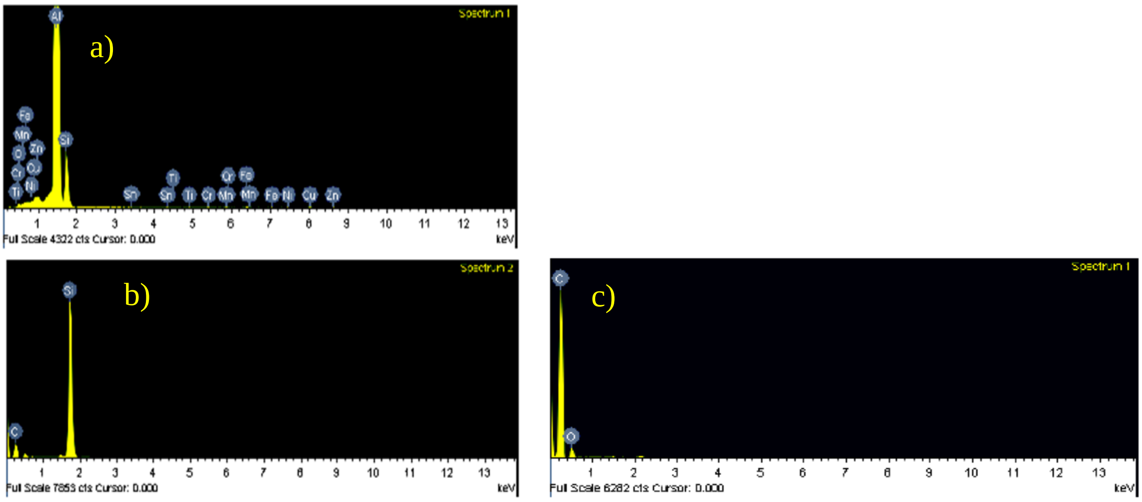


Figure 27 SEM and EDS of a) A390, b) SiC, c) MWCNT

## 3.4 Fabrication of Composites

### 3.4.1 Mixing of Powders

For the current study, the powdered ingredients of h-composite is initially prepared by crushing, followed by the dispersion using ultra-sonication technique. Zhong et. al, [99], reported in his work that for the good dispersion of MWCNT in aluminium powder, atleast 30 min of ultrasonication of  this mix in alcohol is required. The size of aluminum powder used in their work was 50 nm. Rael et. al, [100] used same technique for the dispersion of MWCNT in aluminum powder of 45 µm in the presence of isopropyl. For their study they reported that 1h of ultra-sonication of Al+MWCNT mixture is inadequate for the good dispersion of MWCNT in aluminum powder and to overcome the Van der Waal forces, as the wt. % of MWCNT increased.

The size of aluminum powder used in this study is 35µm. For the adequate dispersion of MWCNT, ultra-sonication is done under the presence of isopropyl for 90 min. It is found that after ultra-sonication of Al/SiC powder with MWCNT for 60 min with 10 sec pulse ON and 2 sec pulse OFF time is inadequate, since some amount of cluster were visible. So, the time is increased to 90 min. For ultrasonication an Oscar ultrasonicator was used, which is situated in bulk solid laboratory of the Mechanical Department. A schematic diagram of ultrasonication process is shown in Figure **28**. After ultra-sonication the powder mix is put in atmospheric condition for evaporation of isopropanol.  Figure **29** shows a SEM micrograph of loose powder mix obtained after ultrasonication process.

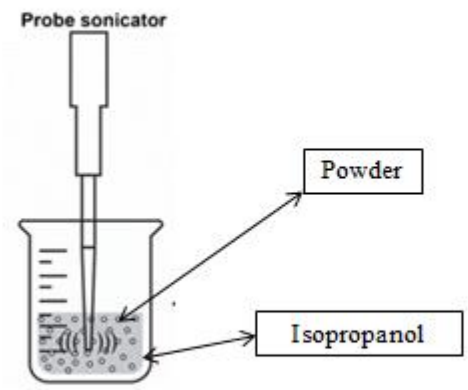


Figure 28 A schematic diagram of ultra-sonication

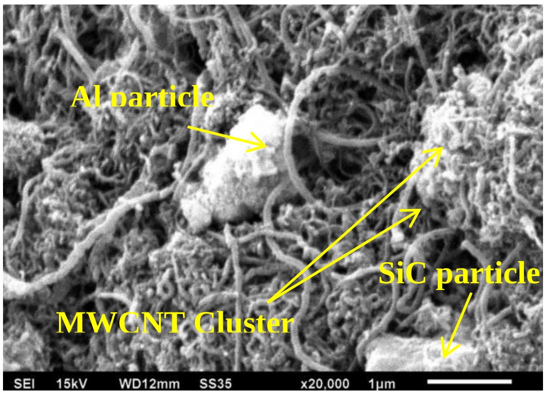


Figure 29 SEM images of loose powder mix after ultra-sonication

### 3.4.2 Compaction of Powders

Once powder mix is ready after ultrasonication they are processed for compaction to make green pallet of h-AMMC by the help of hydraulic press. The plunger and die arrangement which was designed for this purpose is shown in Figure **30**. The details of die and plunger are given in Table **6**.

Figure 30 Plunger and die arrangement

Table 6 Details of material and dimensions of Die & Punch

| Components | Material | Measurements (mm) |
|---|---|---|
| Overall diameter/ Outer diameter | EN31 steel | 50mm |
| Hole size | Tungsten Carbide | 8mm |
| Overall height | | 50mm |
| Plunger | HSS | 7.92mm(diameter),54mm (height) |
| Anvil | EN31 steel | 7.92(diameter), 4 (height) |
| Base Plate | EN31 steel | 24.95(diameter), 5 (height) |
| Pallet size | AMMC | 8mm(diameter), 12mm (height) |

To make the pallets, compaction of material was done by a hydraulic press (Figure **31**) under the working load of 8 Ton to 9 Ton with a holding time of approximately 1 to 1.5 min. Prior to this, the die was cleaned properly with help of acetone and then applied silicon spray in the inner surface of hole and plunger. The reason for applying silicon spray was that the plunger can't jam in hole of die after the making of pallet.

Figure 31 Hydraulic Press

Figure **32** shows some of the pallets which were made using this approach. The green pallets are now ready for sintering process.

Figure 32 AMMC pallets before sintering

### 3.4.3 Conventional Sintering

For conventional sintering, a muffle furnace is used, as shown in Figure **33**. The pallet is covered with alumina paint before putting a sample in muffle furnace. Thickness of alumina paint coating was in the range of 1μm. The purpose of using alumina paint coating was to avoid the oxidation of powders at the time of sintering. The h-AMMC is sintered at a temperature of 600 $^0$C for 2h in the muffle furnace.

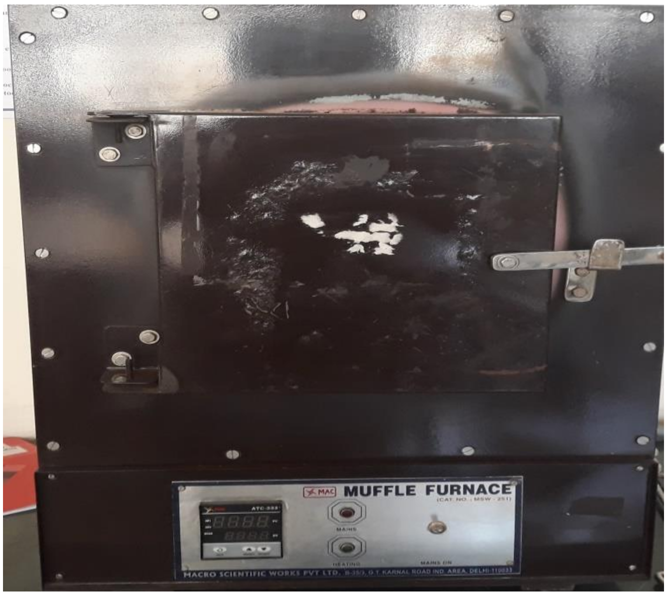


Figure 33 Muffle Furnace

### 3.4.4 Microwave Hybrid Sintering (MHS)

It is well known fact that the microwave doesn't interact with metals at room temperature. It is completely reflected by the metals and cause sparking. So the process of hybrid heating has been utilized for current work. In this process, a susceptor is used which have good microwave absorbing capacity or can say high tangent loss factor. For the current study, a domestic microwave oven (900W and 2.45 GHz) was used to carry out the sintering process at approximately 600 $^0$C. In microwave, sample was sintered by hybrid heating. Hybrid heating was designed with the help of alumina separator in the form of alumina tube wrapped around the pallets and charcoal as the susceptor medium. For sintering, the green pallet is placed inside the alumina tube and the top end of the alumina tube is being closed by using alumina sheet to prevent any contamination by the charcoal powders. Alumina has properties to transmit microwaves completely and has a large skin depth. Charcoal powder is sprinkled over the alumina sheet and tube for hybrid heating. This initially absorbs the all microwave irradiation and elevates its temperature and transfer the heat to the metal. Which helps to increase the temperature of the metal and then metal start absorbing microwaves directly. Then the whole setup is placed inside the microwave oven. The systematic diagram for the microwave hybrid sintering process using the domestic microwave is shown in Figure **34**.

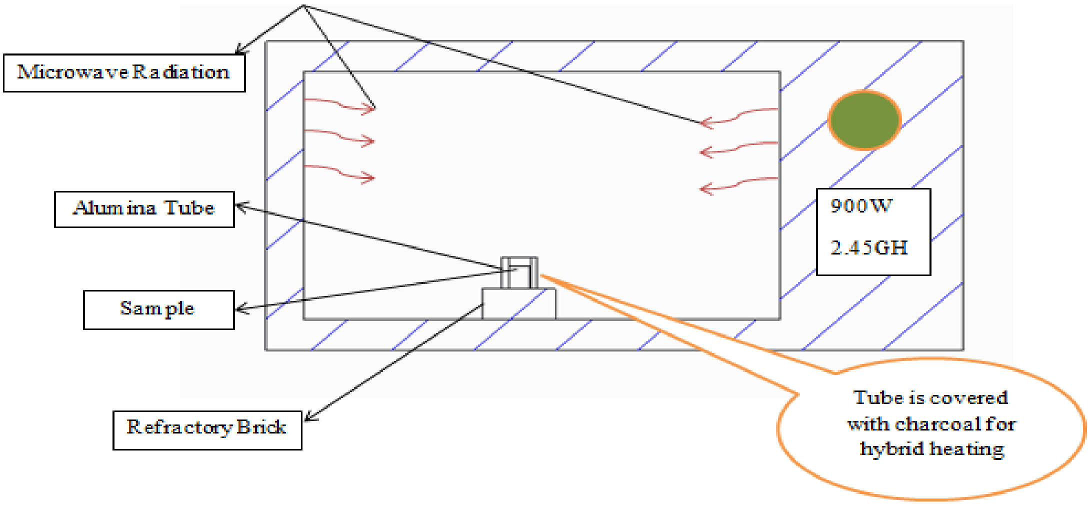


Figure 34 Systematic Diagram of Microwave Sintering

Prior to finalize the processing time under microwave sintering process, a few pilot experiments were carried out to optimize the processing time. Since microwave hybrid heating for MMC sintering is a novel technique, so a very less amount of literature is available on the mechanism and sintering time of h-AMMC. Some authors have reported that the composites sintered at optimized time perform better [101]-[102]. So based on literature, a number of pilot runs have been performed to optimize the sintering time for the fabrication of h-AMMC required for the present work.

Figure **35** shows some of the sintered aluminium and composites fabricated during the preliminary trials by varying the exposure time. It can be seen clearly from the Figure **35** that under the over exposure or under exposure the composite can be burnt or under sintered. Based on this pilot study, it was found that the time for microwave sintering lies in the range of 6 min-10 min, depending upon the composition.


Figure 35 Pilot runs to optimize the microwave sintering time (a) aluminium, (b) h-AMMC

## 3.5 Characterization of fabricated composites

Following the sintering process, the prepared samples are sectioned along its cross section by using a low-speed diamond cutter for the purpose of characterization study. Then the cross section of the sample is polished by the emery papers of various grades. Finally, polishing of the samples is accomplished by using diamond polishing paste on disk polishing machine. The polished samples are then characterized with the help of various characterization techniques.

### 3.5.1 Optical Microscope

Optical microscope (40x, 100x and 400x magnification) is used for the qualitative and quantitative investigation on the morphology and microstructure of h-AMMC. Shape, size and manner of dispersion of hard particles (SiC) was easily detectable with the help of optical microscope. The sample was well polished and etched before the examination of microstructure. For etching Keller solution is used and sample immersed in the solution for 15to 30sec. By the help of an image analyzer attached to the optical microscope, porosity analysis also performed following the ASTM standard B-276. The optical microscope used in this work shown in Figure **36**.

Figure 36 Metallurgical Microscope

### 3.5.2 Scanning Electron Microscope (SEM)

In SEM high energy electron focus beam used for generate different variety signals to get information about sample morphology, chemical composition, and crystalline structure. The SEM used for this study is a highly accurate and precise instrument (Make: JSM-6510LV, JEOL Ltd, Tokyo, Japan) for fast characterization and imaging of fine structures and has a magnification range from 5–300,000 X (printed as a 128 mm x 96 mm micrograph). It was used to study the worn surfaces and investigate the wear mechanism. This facility (Figure **37**) is available at SAI Labs, Thapar Technology Campus, Patiala.


Figure 37 Scanning Electron Microscope

(Photo Courtesy: SAI LABS Thapar Institute of Engineering & technology)

### 3.5.3 Field Emission Scanning Electron Microscope (FESEM)

The FESEM is used for the topology of very small particle size of material which is in the order of nm. In FESEM field emission work as source of electron. In this study to see the topology of MWCNT, micro structure and to see how MWCNT is bonded with aluminium matrix, FESEM is used. For the present work this facility (Figure **38**) was accessed at Central University of Punjab, Bathinda.

Figure 38 Field Emission Scanning Electron Microscope

(Photo Courtesy: Central University, Bhatinda)

### 3.5.4 X-ray Diffraction (XRD)

X-ray Diffraction is used to detect the phase formation as well as for the crystal structure, grain orientation in the materials. The XRD works on the principle of Bragg's law. Bragg's law is used to describe the interference pattern which is scattered by crystals. The systematic diagram of XRD's working principle shown in Figure **39**.

Figure 39 Principle of X- ray Diffraction

(Photo Courtesy: SAI LABS Thapar Institute of Engineering & technology)

### 3.5.5 Raman Spectroscopy

Generally, Raman spectroscopy is used to find out the intramolecular bond or chemical bonding distinguished by different wavelength at which vibrational and rotational motion occurs for a matter. In this study, the Raman spectroscopy is used to observe the bonding of MWCNT with aluminium matrix. This spectroscopy work on the principle of Raman shift which is used for converting the spectral wavelength and wavenumber into the spectrum from shift. There is formula for all this which is given below:

$$\Delta_{\bar{V}} = (\frac{1}{\lambda_0} - \frac{1}{\lambda_1})$$

**Where:** $\Delta_{\bar{v}} =$ Raman shift expressed in wavenumber

$\lambda_0$= excitation wavelength

$\lambda_1$= Raman spectrum wavelength

For MWCNT excitation wavelength 532 nm, scan range 500 $cm^{-1}$/nm to 2000 $cm^{-1}$/nm with grating of 600 grooves/mm for 532 nm and 1800 grooves/mm for 325nm at 10mW or 100% power. This facility is available in IIT Mandi, Himachal Pradesh.

Figure 40 Raman spectrometer (Photo courtesy - IIT Mandi)

### 3.5.6 Vickers Hardness Tester

For micro hardness measurement of AMMC the Vickers hardness tester is used which is situated at the manufacturing and instrumentation lab, in TIET. Micro hardness test gives the information about the mechanical hardness of AMMC. A diamond indenter is with indent load which ranges from 10 gm to 1000 gm. The indent on the surface of material was then process trough software to evaluate the micro hardness in HV. The measurements of hardness were repeated at various locations of the same cross-section as well as at various cross-sections along the length of the specimen. The Vickers hardness tester used for this study is shown in Figure **41**.

Figure 41 Vickers Hardness Tester

### 3.5.7 Pin on Disc Sliding Wear Tribometer

To characterize the dry sliding wear and friction characteristics of the fabricated composites a pin-on-disc sliding wear tribometer (Make: Ducom Pvt Ltd) is used. The wear study has been carried out with the pins made of Al alloy, AMMC and hybrid AMMC, sliding against CI disc for 30 minutes various sliding velocities, load and sliding distances.

Coefficient of friction of material was calculated using the following relation.

$$F = \mu N$$

Where: F = Friction Force in Newton

μ = Coefficient of Friction

N = Applied load in Newton

The wear loss was calculated by the weight loss method for this study. The relations are given below:

$$Volume\ loss\ (mm^3) = \frac{mass\ loss\ (g)}{density\ (g/cm^3)} \times 1000$$

$$Wear\ rate\left(\frac{mm^3}{m}\right) = \frac{Volume\ loss\ (mm^3)}{Sliding\ Distance\ (m)}$$

$$Specific\ wear\ rate(mm^3/Nm) = \frac{wear\ rate(mm^3/m)}{load\ (N)}$$

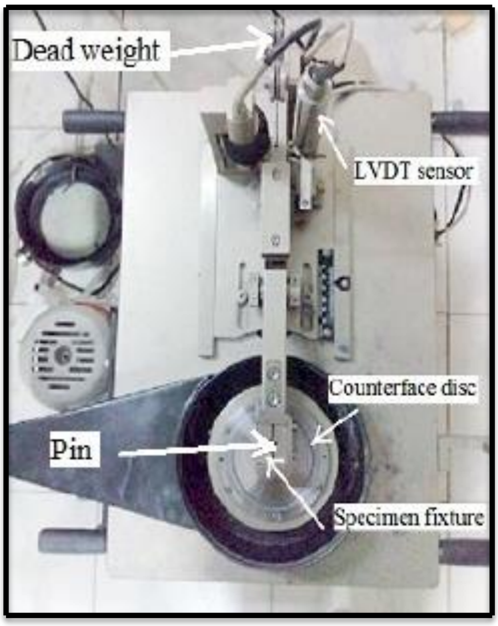


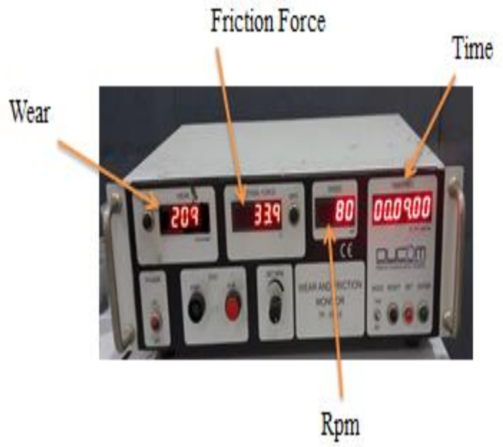


Figure 42 Parts of pin on disc sliding wear tribometer

Since the present work will deal with the various operating parameters so for the discussions of experimental results a detailed tribological investigation is performed using constant load and speed, for various compositions. This will be followed by the comparison of tribological performance under different load loads and sliding distance. for the present work a design of experiments has been made with the various influential parameters that may affect the tribological performance. The Table 7 shows the operating parameters of the tribological testings whose results are discussed in chapter 5. Chapter 6 will then present a detailed statistical analysis on the tribological performance of h-AMMC.

Table 7 Details of operating parameters and compositions for tribological testings

| **Operating Parameters** | **Compositions** | | | | | |
|---|---|---|---|---|---|---|
| Load=10 N, Speed=1 m/sec, Sliding distance= 2000 m | Al | Al+ SiC | Al+SiC +0.5% MWCNT | Al+SiC +1% MWCNT | Al+SiC+ 1.5% MWCNT | Al+SiC+ 2% MWCNT |

# Chapter 4

## Results and Discussion: Mechanical, Microstructural and Phase Analysis of Sintered Alloys and Composites

### 4.1 Microstructure and Phase Analysis

The microstructure is an essentinal root map to define many of the mechanical and metallugrical properties. In light of this microstructural analysis of aluminium and AMMCs has been carried out with help of metrallurical microscope (Make: Reyteck) and SEM.

#### 4.1.1 Microstructure and Phase Analysis of Aluminium

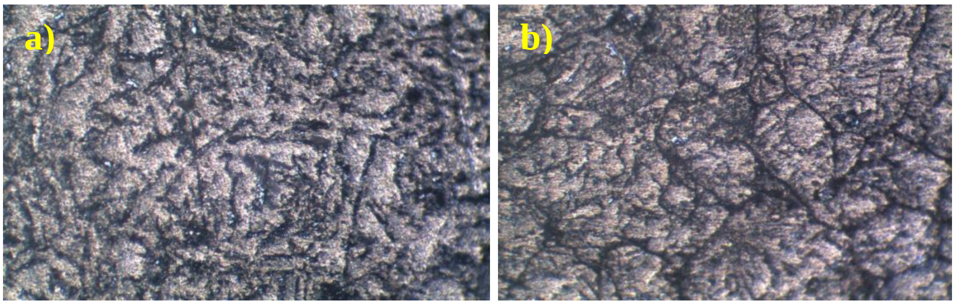


Figure 43 Optical Microscope image of Aluminium matrix a) Conventional sintering b) Microwave Sintering

The Figure **43** show the optical microscope images of sintered AMMC through conventional and microwave route, respectively. It has been clearly shown in the images that microwave sintered AMMC has better densification than conventional sintered AMMC. The fine grain structure can also be seen in microwave sintered AMMC which proves it better than the competitive technique (conventional sintering).

The formation of oxide is serious concern in sintering process which directly effect the mechanical properties of AMMC. The formation of oxide is directly influenced by processing time. With less processing time the chance of less oxide sintering during the process. Accordingly, when EDS analysis has been carried out on the sintered surfaces, less amount of oxygen has been detected in case of microwave sintered samples. This in turn validates the viability of process and aviod the formation of some brittle intermetallic phases. The EDS of alumnium metal matrix is shown in Figure **44**. All these above facts from the prelimanry investigtions associated with aluminium confirms that microwave sintering is favourable sintering process with less grain growth, refined microstructure and more densification of powders over conventional sintering.

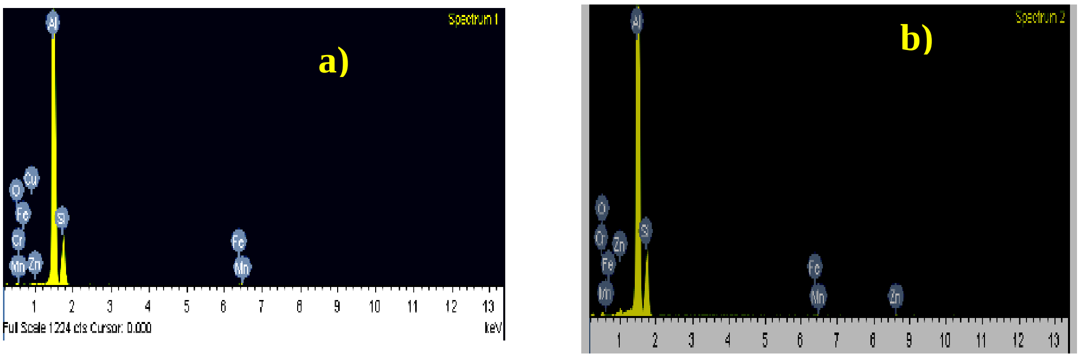


Figure 44 EDS of Aluminium matrix a) Conventional sintering b) Microwave sintering

The XRD spectra of both conventional as well as microwave sintered Al metal matrix is shown in Figure **45** and Figure **46**, respectively. The analysis of XRD spectra shows the viability of microwave sintering process as the rapid and volumetric heating approach which reduces the possibility of formation of oxides due to very less processing time (360 secs) as compared to conventional sintering process (2 hours). The intensities of different oxide phases such as $Al_2O_3$, $Cr_2O_3$, $MnO_2$ and CuO in conventional sintering process is significantly higher as compared to microwave sintering process.

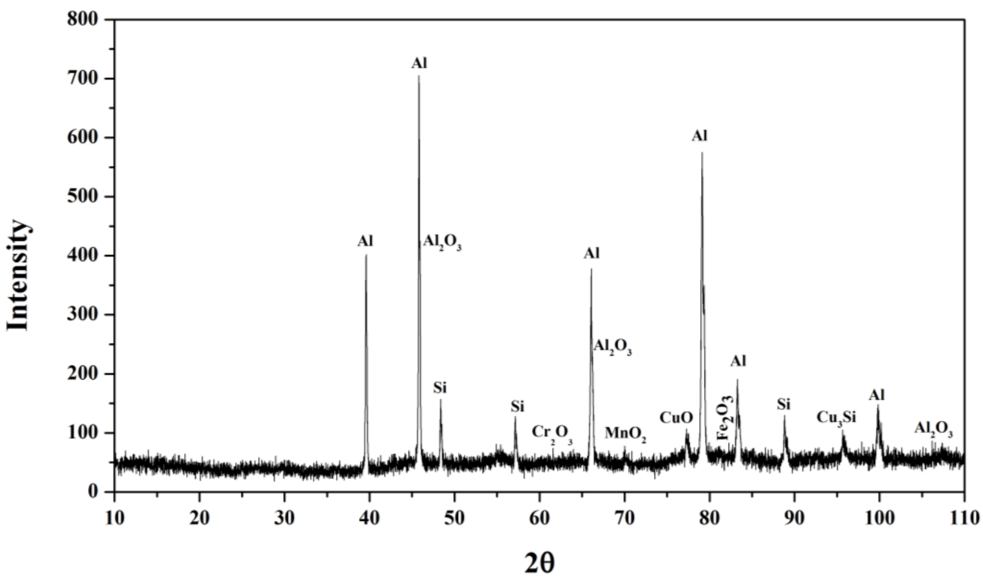


Figure 45 XRD image of Aluminium matrix by Conventional Sintering process

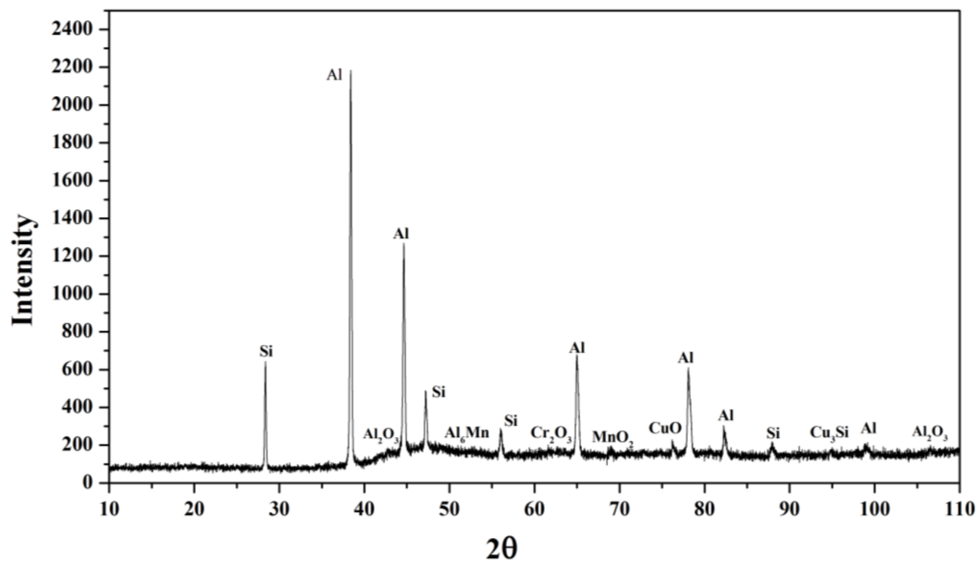


Figure 46 XRD image of Aluminium matrix by Microwave Sintering process

The α-Al phase is observed in both the conventional and microwave sintering alongwith $Cu_3Si$ phase. The peak of Si, Al and other phase have less intensity and sharpness in the XRD of microwave sintered aluminium as compared to conventional sintering. This implies that the grain coarsening of aluminium is less in microwave sintering as compared to conventional sintering [103]

### 4.1.2 Microstucture and Phase Analysis of Al+SiC Comosite

The preliminary investigation on the microstructure of Al+SiC composite is observed under the metallurgical microscope which is shown in Figure **47**. The utrasonication of aluminium and SiC powders helped in achieving the uniformity in distribution of SiC powder in metal matrix. For better analysis of microstructure of Al+ SiC composite fabricated by both conventional and microwave sintered composite, micrographs are captured at higher magnification with the help of SEM. The SEM images of microstructure are shown in Figure **48**.

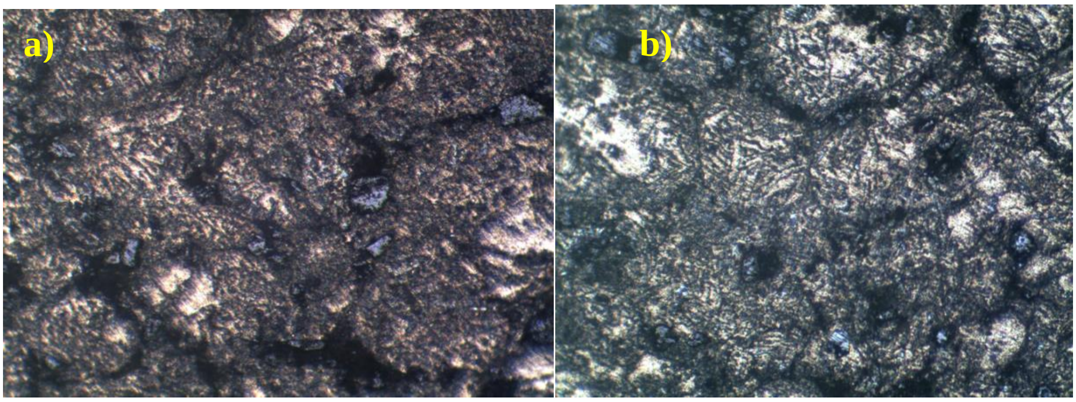


Figure 47 Optical Microscope image of Al composite with SiC a) Conventinal sintering b) Microwave sintering

In the SEM micrographs, at some locations the agglomeration of SiC is found in the aluminium matrix which is happened during mixing caused by the difference in density and particle size and tends to fill the interstitial space between the Al particles. Otherwise, the distribution of SiC is found reasonably uniform throughout the matrix. It has been found that there is more crack in case of conventional sintered composite as compared to microwave sintered composites.

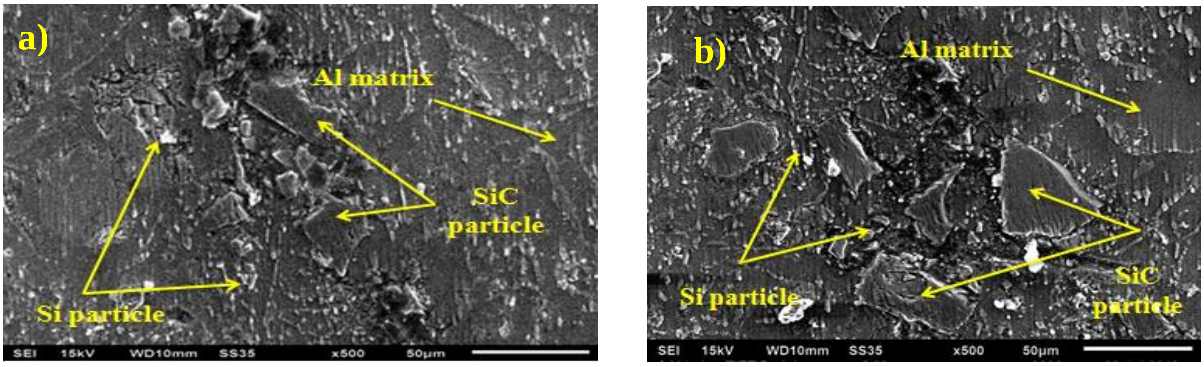


Figure 48 SEM image of Al composite with SiC a) Conventinal sintering b) Microwave sintering

The EDS of both the conventional and microwave sintered composite are shown in Figure **49**. From the EDS, the presence in rich state of aluminium and silicon with carbon has been confirmed.

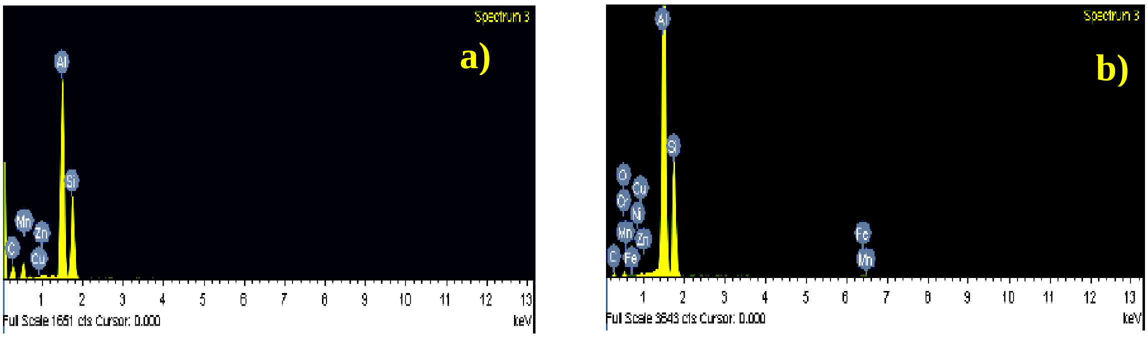


Figure 49 EDS of Al composite with SiC a) Conventional sintering b) Microwave sintering

Figure **50** shows the XRD pattern of Al+SiC composite. The XRD study reveals the different phases such as $Al_2O_3$, $MnO_2$, CuO and $Cu_3Si$, in addition to the primary phase Al and SiC. The oxide phases are detected due to the reaction of the elements of base metal with oxygen at high temperature during sintering. The phase $Cu_3Si$ is intermetallic which might be formed due to the dilution of Cu present in base matrix with Si present in reinforcement. However, possibility of formation of such intermetallics at low temperature is quite low.

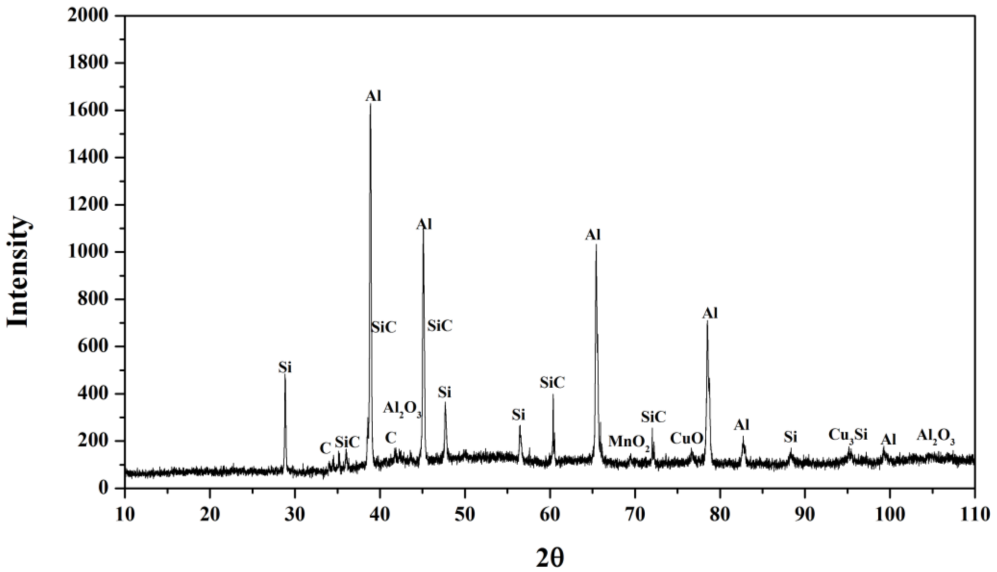


Figure 50 XRD analysis of Al+ SiC

### 4.1.3 Microstructure of MWCNT reinforced h-AMMC composites

The microstructure of MWCNT reinforced h-composites are captured with help of FE-SEM and shown in Figure **51** and Figure **52**. It is clearly observed that the dispersion of MWCNT through aluminum matrix is uniform with help of ultra-sonication technique. At few local areas, the agglomeration of MWCNT is found due to the nano sized property of MWCNT which tends to fill interstitial space between the aluminium matrix at the time of compaction and sintering [104].

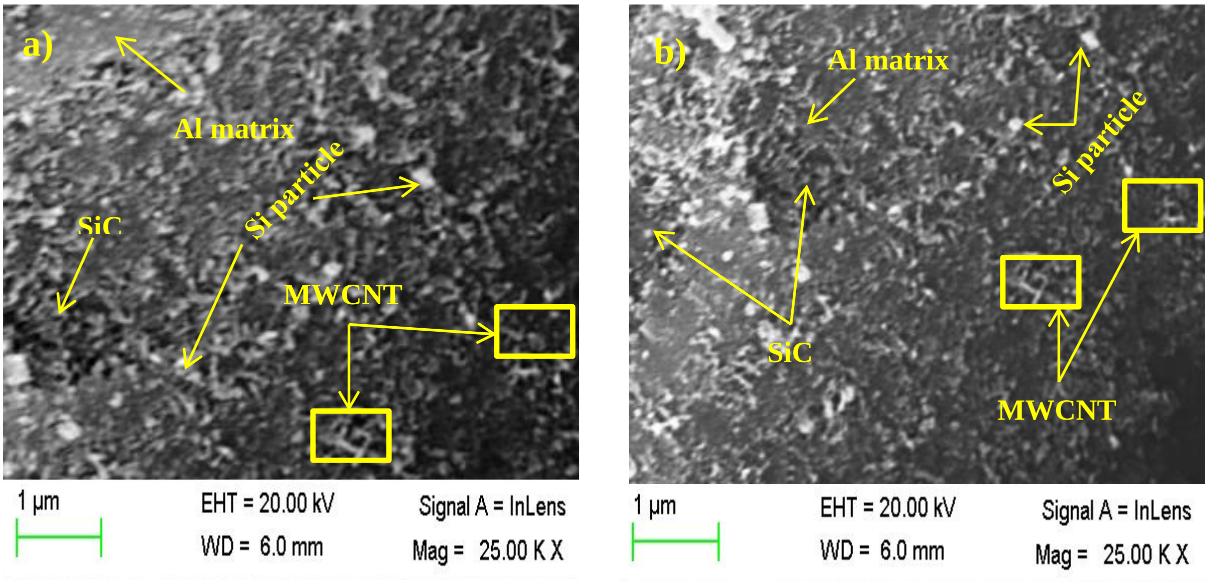


Figure 51 FE-SEM image of h-AMMC with MWCNT a) Conventional Sintering b) Microwave Sintering

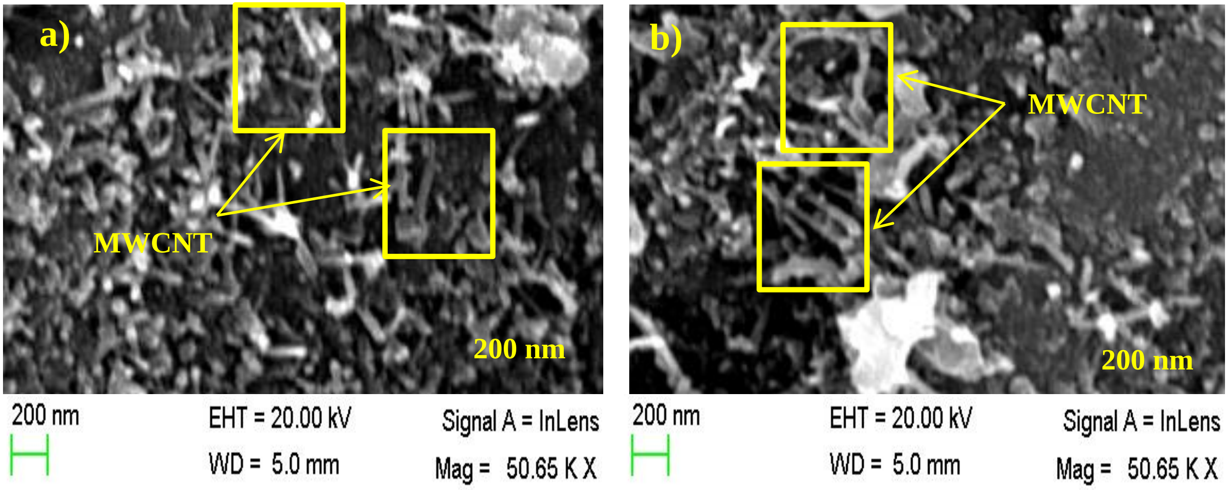


Figure 52 Magnified image of h-Composite with MWCNT a) conventional sintering b) microwave sintering

The presence of MWCNT is confirmed by the EDS area mapping of h-composite and magnified image of MWCNT which is shown in Figure 53. The distribution of MWCNT in h-composite is shown through red color intensity where the carbon distributions rise from MWCNT as well as carbon particle of SiC. A uniform distribution of C is shown in area mapping which implies that a uniform distribution of MWCNT. The green color show the Al particle and blue color show Si particle and orange color show cu particle distribution respectively. The white color shows the oxygen in h-composite which might possibly came from environmental and oxidation condition. It is evident from the carbon and Si distribution that besides the carbon of SiC, it contains significant distribution of additional carbon which is attributed from the MWCNT.

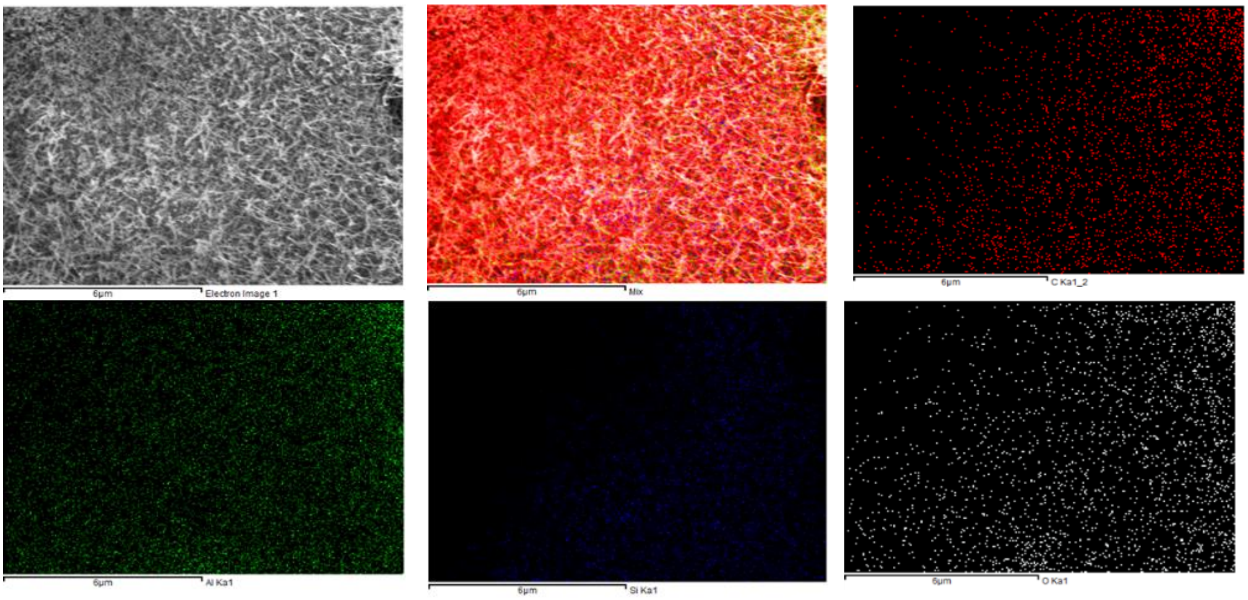


Figure 53 Area mapping of h-composite

The FE-SEM of 1% MWCNT shows the better dispersion and bonding with Al matrix which is also confirmed later by the analysis of XRD. The Figure **54** and Figure **55** shows the XRD patterns of h-composites with 1%MWCNT and 2% MWCNT, respectively. The XRD study revealed the different phases such as $Al_4C_3$, $MnO_2$, CuO, $Al_2O_3$, C, Si, Al and SiC. The presence of oxide phases such as $Al_2O_3$, $MnO_2$ and CuO might be due to the oxidation of matrix material at high temperature during sintering. The graphite phase was found in both 1%MWCNT and 2%MWCNT. XRD peak at $26.8125^0$ confirms the presence of elemental carbon phase which is coming from MWCNT [105]. The C-peak found at $28.3456^0$ is saturated carbon peak for h-composite with 1%MWCNT and in case of h-AMMC with 2%MWCNT it was found at $27.9854^0$. The phase $Al_4C_3$ confirms the interfacial reaction between MWCNT and Al matrix at low temperature during the time of microwave sintering. The phase $Cu_3Si$ confirmed the dilution of Cu present in base matrix with Si present in reinforcement as at low temperature the possibility of reaction of intermetallic is less.

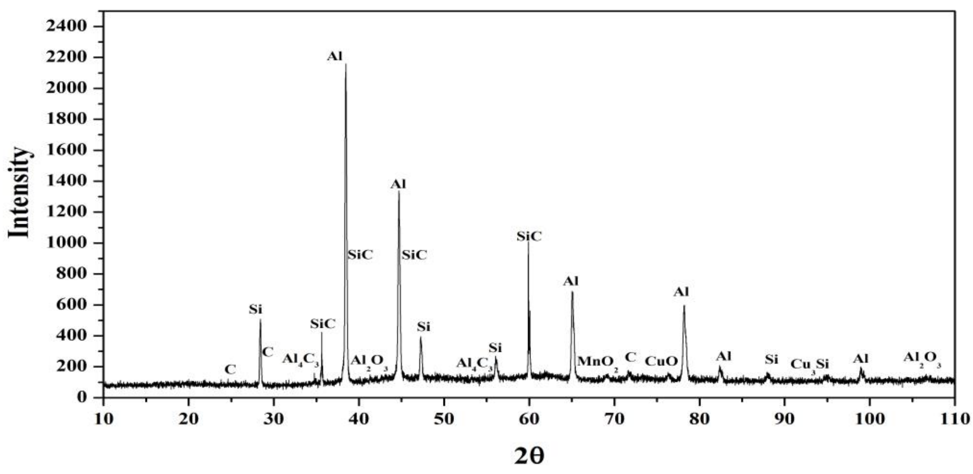


Figure 54 XRD analysis of h-composite with 1% MWCNT

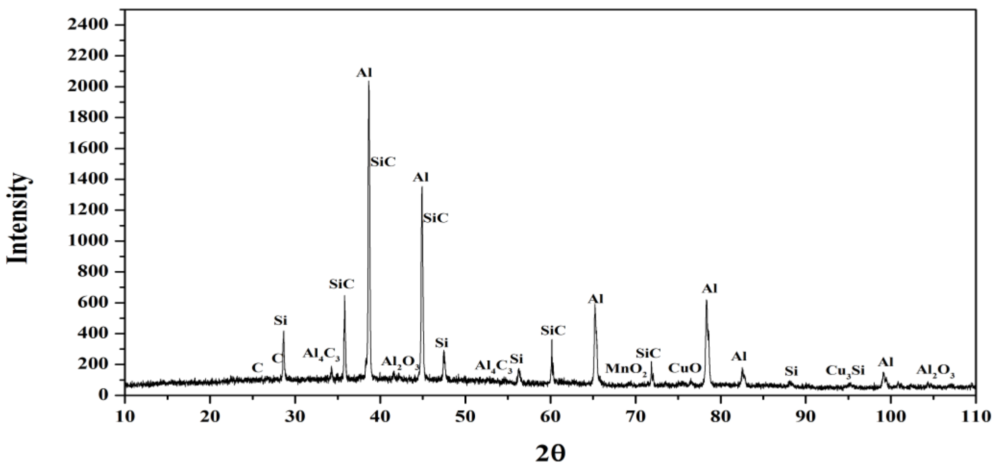


Figure 55 XRD analysis of h-composite with 2% MWCNT

Further, the presence of MWCNT phase and structure in the microwave sintered h-AMMC composites is confirmed and illustrated through Raman spectroscopy (Figure **56** and Figure **57**). There are basically two main graphite bands of MWCNT shown by Raman spectrum in Figure **56**. The range of G band is from 1550 $cm^{-1}$ to 1610 $cm^{-1}$. MWCNT band can be found between this range. Due to the in-plane vibration of the C–C bond is found in this range. The D band, defective band is found between 1340 $cm^{-1}$ to 1390 $cm^{-1}$ due to the presence of disorder in carbon systems [106].

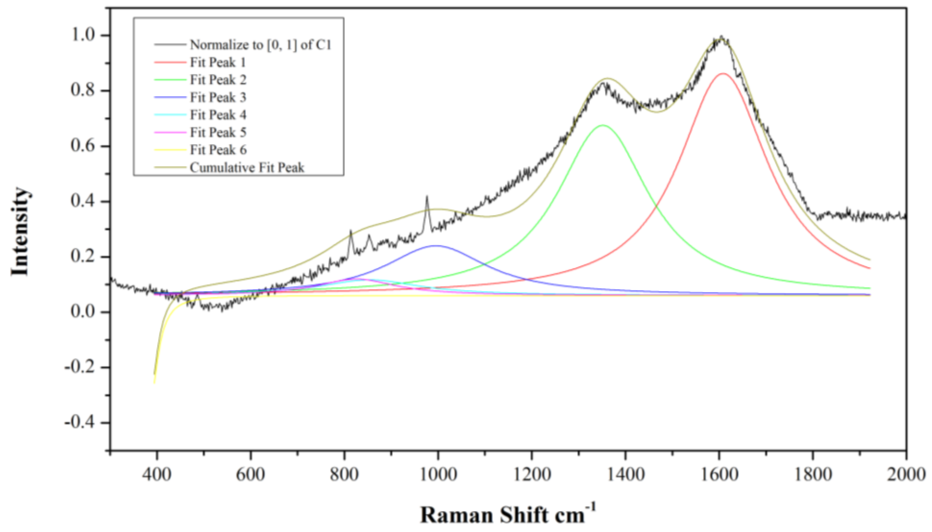


Figure 56 Analysis of Raman Spectroscopy of h-composite with help of origin 8.5.

The Figure 57 shows the Raman spectroscopy of h-composite with different % variation of MWCNT. The D-peak of MWCNT is found at 1384 $cm^{-1}$ which indicates that the defects related to the CNT formation and the graphitic G-peak of CNT is found at 1604 $cm^{-1}$.

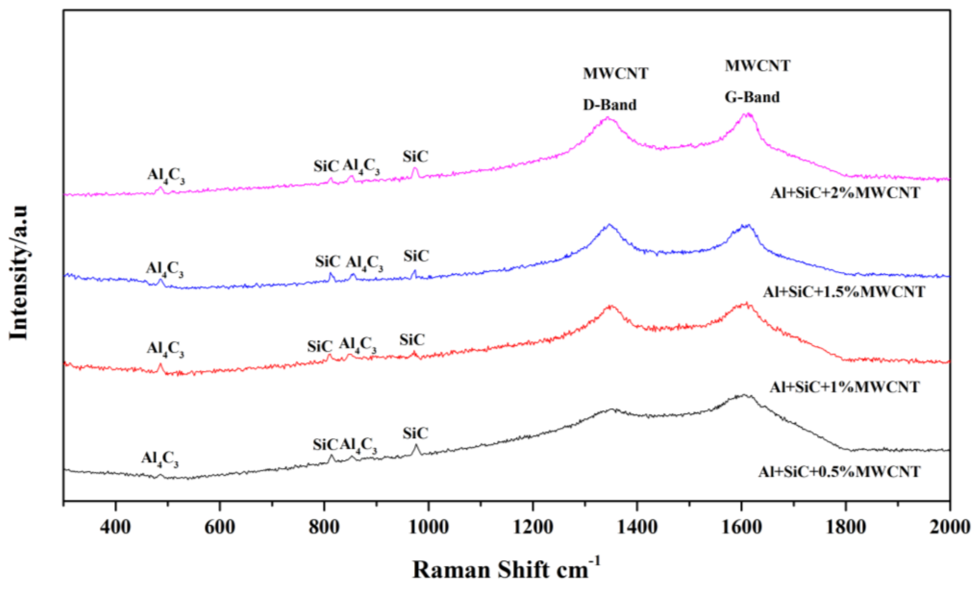


Figure 57 Raman Spectroscopy of h-composite with % variation of MWCNT

The $Al_4C_3$ peak observed at 481$cm^{-1}$ and 852 $cm^{-1}$ which also confirm the Al and MWCNT interfacial bond during the time of sintering. The SiC phases are observed at 813 $cm^{-1}$ and 982 $cm^{-1}$ [107], [108]. A Lorentz function is used to fitting the peak of $Al_4C_3$, SiC and MWCNT with help of origin 8.5. The $R^2$ value of function is 0.94562, which is close to 1 and suggests a strong relation of function. The fitting curve is shown in Figure **56**.

## 4.2 Porosity Analysis

The porosity analysis of aluminium matrix has been done with help of image analyzer software. The porosity analysis has been carried out using ASTM standard B-276. The optical and SEM image of conventional and microwave sintered alumnium is shown in Figure **58** and Figure 59, which shows the presence of pores in conventional sintering and in microwave sintered samples. Porosities are highlighted by red coloured dots in the Figure **58**.

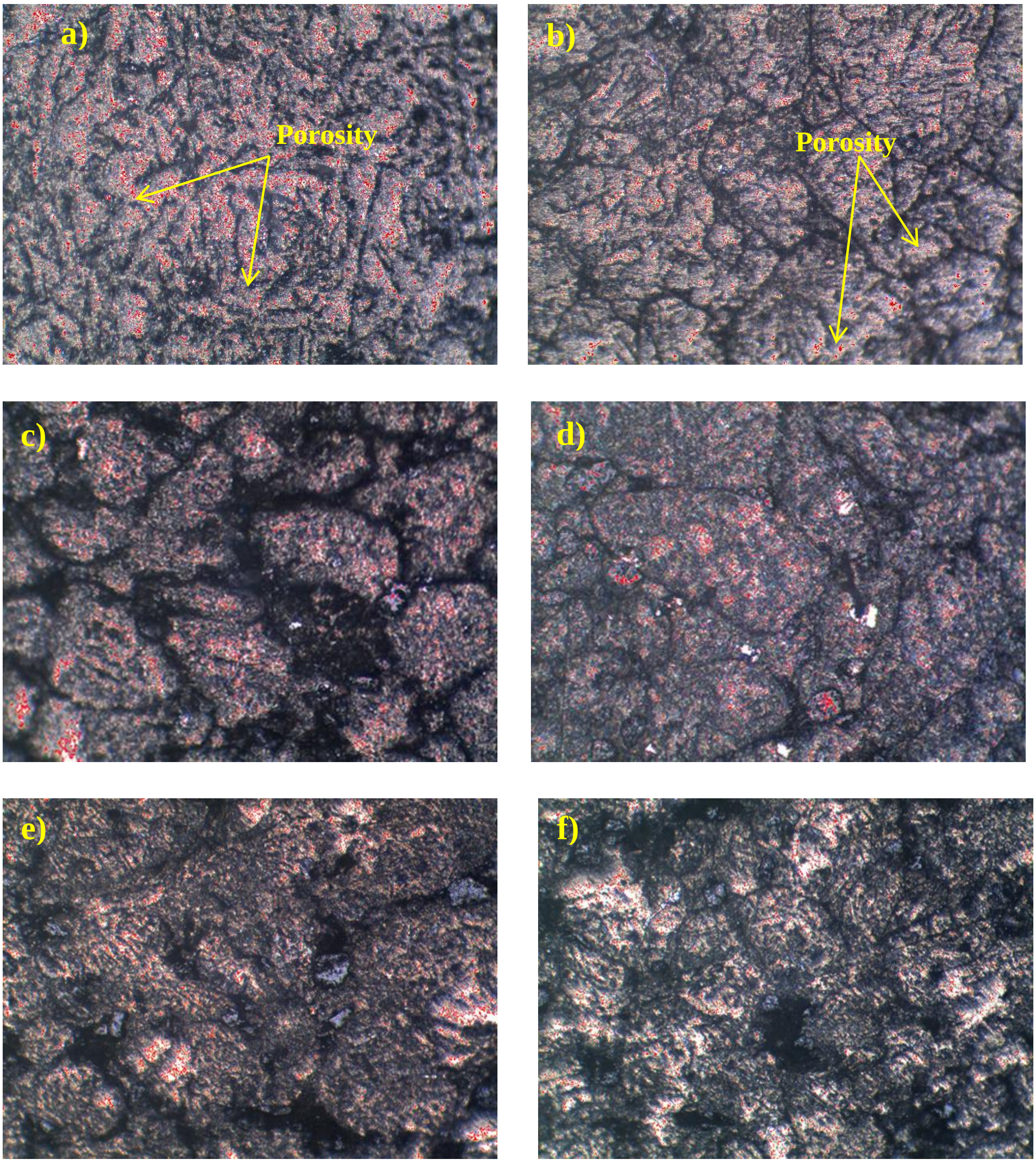

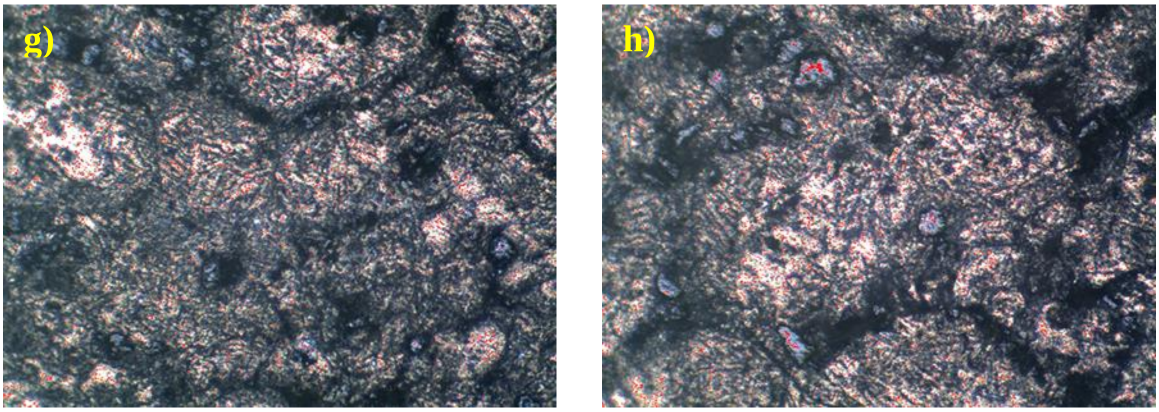


Figure 58 Optical Images after Porosity Analysis of conventional sintered (a) & (b) Alumnium, (c&d) Al+SiC, (e&f) Al+SiC+1%MWCNT, (g&h) Al+SiC+2%MWCNT

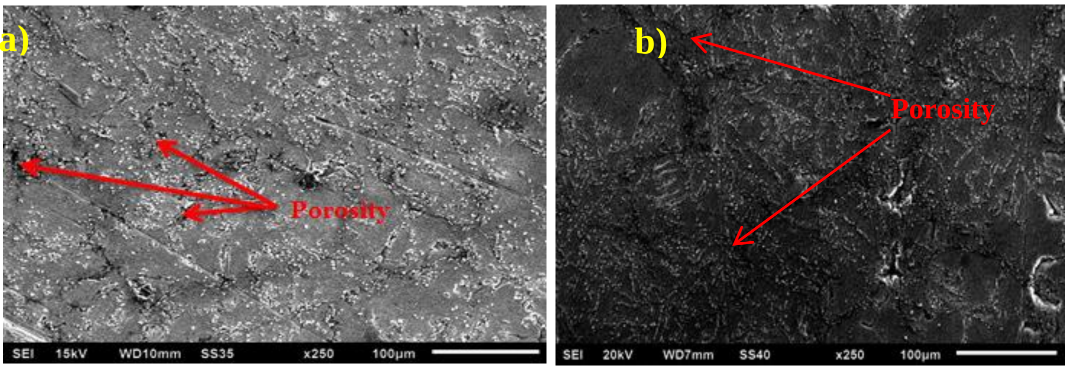


Figure 59 SEM image of sintered aluminium matrix a) Conventional, b) Microwave sintering

The details porosity analysis report is shown in Table **8**. From above porosity analysis it was confirm that in microwave sintering there is less % of pore as compared to conventional sintering. The porosity found in case of conventional sintered and microwave sintered samples are in the range of 1.37% and 0.94%, respectively. The extent of porosity found to be significantly less as compared to the earlier developed processes. Reduction in porosity is beneficial for enhancing the hardness, tensile strength and wear resistance of the fabricated materials.

The analysis of pororsity of fabricated composites reveals that the porosity has been incresaed when reinforcment SiC added in alumnium matrix this happened due to the difference in melting temperature of alumnium and SiC which produce thermal mismatch. Further, addition of MWCNT also decrease the porosity of h-composite. The nano size of MWCNT helps in reducing the porosity to some extent as voids has been filled by these nano sized particles of MWCNT and ultimately reduces porosity. The same trend has been followed in both microwave as well as conventional sintered composites. Although, microwave sintered composite posses less porosity as comared to the conventional sintering due to the fact that the unique characteristics of microwave rapid and uniform heating.

Table 8 Detailed Porosity Analysis Report

| **Sample** | **Total object** | **Pore %** | **Max. Perimeter (Micron)** | **Min. Perimeter (Micron)** | **Max. Area (Micron Sqr)** |
|---|---|---|---|---|---|
| **Conventional Sintered Al** | 8187 | 1.37% | 207.243 | 1.4094 | 125.0189 |
| **Microwave Sintered Al** | 8167 | 0.94% | 201.625 | 1.4094 | 121.9626 |
| **Conventional Sintered Al+SiC** | 5201 | 1.55% | 269.7851 | 1.4094 | 300.9391 |
| **Microwave Sintered Al+SiC** | 6823 | 1.12% | 176.8251 | 1.4094 | 184.6108 |
| **Conventional Sintered Al+SiC+ 1%MWCNT** | 17639 | 1.35% | 183.7872 | 1.4094 | 154.5907 |
| **Microwave Sintered Al+SiC+ 1%MWCNT** | 13086 | 1.04% | 67.1373 | 1.4094 | 41.5902 |
| **Conventional Sintered Al+SiC+ 2%MWCNT** | 15372 | 1.45% | 195.2337 | 1.4094 | 144.9571 |
| **Microwave Sintered Al+SiC+ 2%MWCNT** | 12753 | 1.07% | 53.4464 | 1.4094 | 10.3044 |

The less amount of porosity in microwave sintered AMMC clearly revealed the significe of microwave sintering over conventional sintering. There is an increase in the amount of porosity due to slow heating rate and long soaking time during the fabrication of AMMC through conventional sitnering. But microwave sintering, due to its inherent fast heating and uniform heating and cooling rate help in reducing the formation of less amount of porosity.

## 4.3 Density of Fabricated Al-alloy, AMMC and h-AMMC

The density of A390 (Al-Si matrix) is 2.72 g/cm$^3$, density of SiC is 3.21 g/cm$^3$ and that of MWCNT is 2.6 g/cm$^3$. Thus, theoretically, with the addition of SiC in Al matrix density of composite should increase, however, addition of MWCNT in Al slightly decreases the overall density of composite. Since SiC is the primary reinforcement, so initially the density of hybrid composite is more as compared the base matrix. However, further increase in the % of MWCNT, the overall density of h-composite starts to reduce.

The theoretical density of both conventional and microwave sintered h-composite can be found by given equation:

$$\boldsymbol{\rho_c = \{(\rho_a * \%of\ A) + (\rho_b * \%of\ B) + (\rho_c * \%of\ C)\}/100}$$

The experimental density of both conventional and microwave sintered h-composite is measure by Archimedes principle. The term relative density is more popular as it tells how denser the material is as compared to the reference material. The term relative density may be defined as ratio of experimental density of the material to the theoretical density of reference material.

The relative density of both conventional as well as microwave sintered h- composite shown in Figure **60**. From the figure it is observed that the addition of SiC in aluminum matrix increases the densification of composite in both the fabrication technique due to the uniform distribution of SiC. Also, it is evident that the microwave sintered composite are more compact than conventional sintered composite which is due to the more porosity, micro defect due conventional heating process.

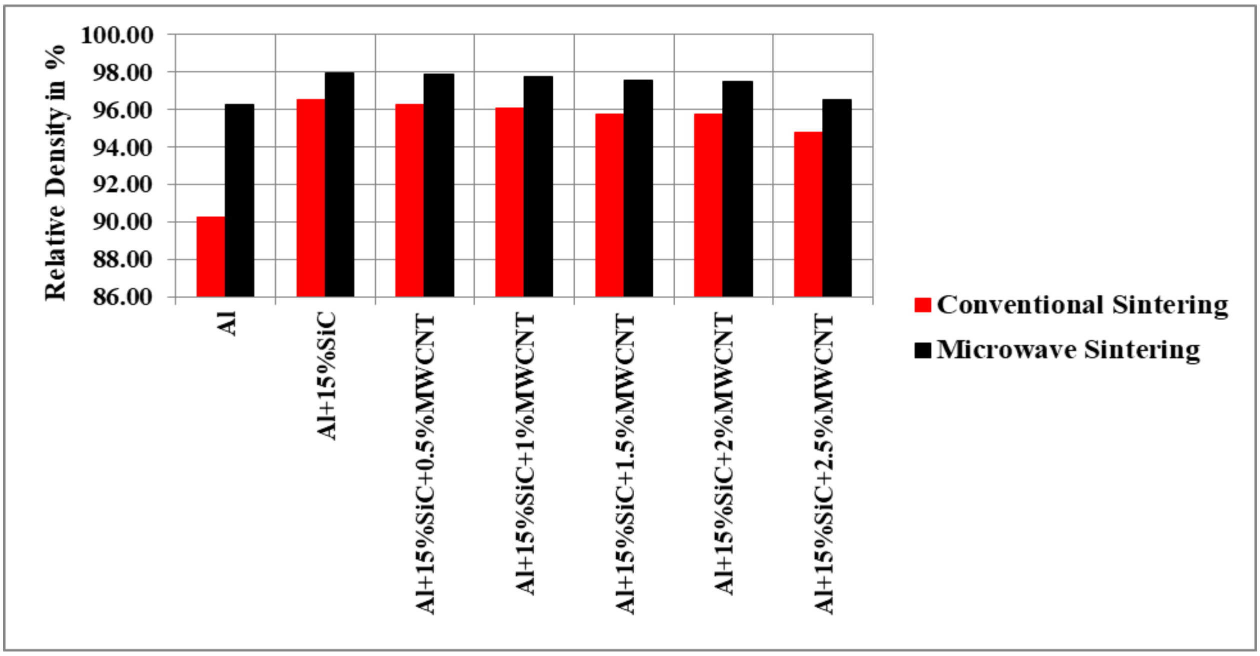


Figure 60 Comparison of relative densities of samples sintered by conventional and microwave route.

The relative density of h-composite reinforced with 1%MWCNT is found to be 0.955 and 0.977 in case of conventional and microwave sintering, respectively. Relative density of h-composite with 2% MWCNT is found to be 0.951 and 0.975 in case of conventional and microwave sintering, respectively. It is shown that in all the cases of microwave sintering has more relative density as compared to that of conventional sintering. Thus, it is concluded that microwave sintering can be deemed as a favorable method for enhancing the densification of ceramics reinforced AMMC, which is in agreement with the literature [95].

## 4.4 Vickers Hardness of Fabricated Al-alloy, AMMC and h-AMMC

The micro hardness of h-AMMC was measured by the help of Vickers Hardness tester. The load applied for testing is 300 gm with a 20 sec dwell time. It is found that the micro hardness of h-AMMC increases with the increasing % of MWCNT. The microhardnesses of the various samples fabricated by both the method is shown in Figure **61** and Table **9**. The standard deviation associated with the experimental results for different compositions are also included in the table. It is seen that the average micro hardness of conventionally sintered Al is 59.3 ± 2.17 HV, whereas average micro hardness of microwave sintered Al is incremented by 15% (66.72 ± 2.22 HV). It is observed that the addition of 15% SiC in aluminium matrix increase the hardness of composite by 35.4 % for conventional sintered and by 36.21 % for microwave sintered composite. Hardness generally depends upon grin size and presence of defects. It was observed earlier that the microwave sintered samples have less porosity, fine grain sized structures and presences of cracks were negligible [109].

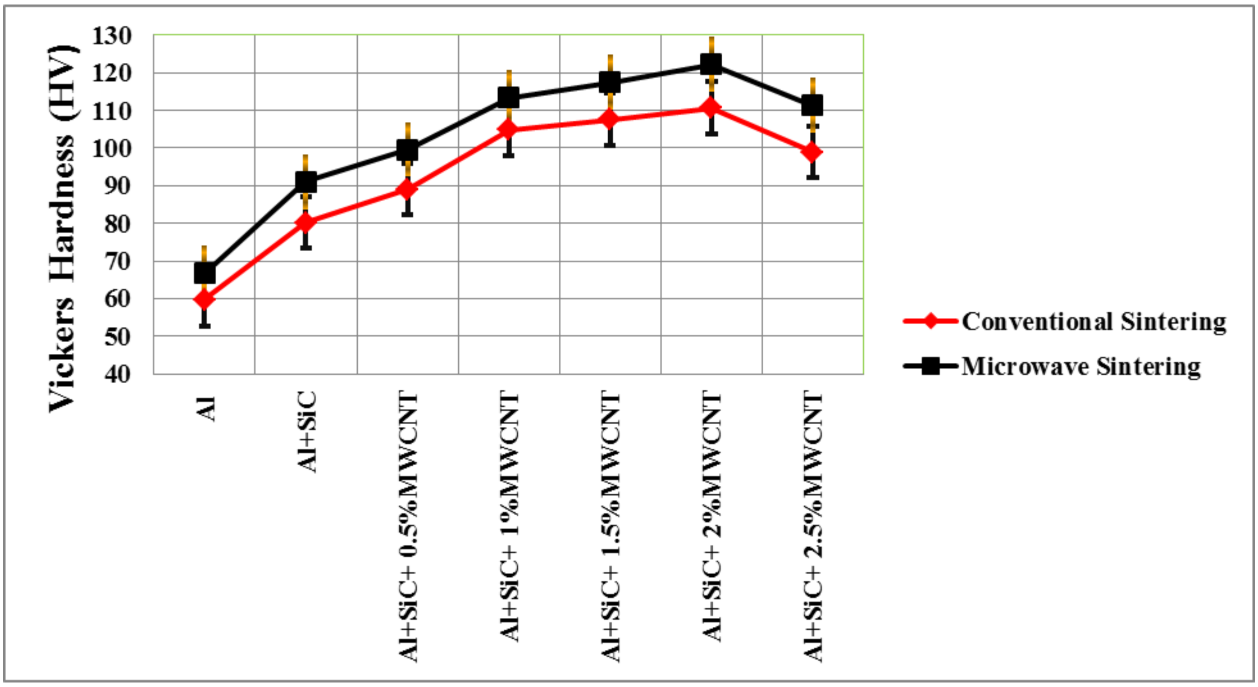

Figure 61 Micro hardness of AMMC with variation % of MWCNT from conventional and microwave sintering

Table 9 Microhardness of conventional and microwave sintered samples

| S.No | Composition | Microhardness (conventional sintering) | Microhardness (microwave sintering) |
|---|---|---|---|
| 1 | Al | $59.64 \pm 2.17$ | $66.72 \pm 2.22$ |
| 2 | Al+ SiC | $80.21 \pm 5.52$ | $91.01 \pm 5.31$ |
| 3 | Al +SiC+ 0.5% MWCNT | $89.02 \pm 6.50$ | $99.64 \pm 4.54$ |
| 4 | Al +SiC+ 1% MWCNT | $104.91 \pm 5.32$ | $113.36 \pm 6.02$ |
| 5 | Al +SiC+ 1.5% MWCNT | $107.61 \pm 5.02$ | $117.86 \pm 4.77$ |
| 6 | Al +SiC+ 2% MWCNT | $110.65 \pm 5.13$ | $122.02 \pm 4.62$ |
| 7 | Al +SiC+ 2.5% MWCNT | $98.26 \pm 2.94$ | $111.45 \pm 3.12$ |

The addition of 1% MWCNT in Al-SiC composite increases the hardness by 29.75% in case of conventional sintering and 24.5 % in case of microwave sintering. There is another reason for the lower hardness in case of conventional sintered composites which is due to the thermal expansion mismatch between the Al, SiC and MWCNT which in turn generate the residual internal stresses produced during the conventional sintering.

The enhancement of hardness by the addition of MWCNT in h-composite is caused due to the fact that MWCNTs increase the dislocation density of matrix during the time of cooling at room temperature which helps in improving the strengthening and hardening of matrix [72]. This happens due to the difference in coefficient of thermal expansion between the aluminium matrix and MWCNT. The increment in hardness due to uniform dispersion of CNTs was due to the filling of voids of metal matrix by CNTs.  However, this phenomena is prevalent and more effective upto a certain CNT volume % or wt.%. After exceeding that particular amount of CNTs % will gives reverse result due to the cluster formation of CNT which  does not able to fill the micro voids.

For example, in the present situation after 1% MWCNT when, further addition of MWCNT was investigated an increase of micro hardness of h- AMMC for both the sintering methods were observed, but the rate of increase is insignificant. Finally, with the addition of 2 wt% of MWCNT a decrease in the hardness is distinctly visible. This occurs due to the localized agglomeration or poor dispersion of MWCNT in the aluminium matrix, which leads to the weak interface strength or weak bond between the MWCNT and aluminium matrix. In this type of situation, CNTs will be agglomerated with the aluminum particles. So these agglomerated CNTs create a problem in complete sintering of AMMC which leads to the formation of defects. This effect increases the porosity in the final composite, due to the lack of strong bond or misalignements and entanglement of MWCNT at the grain boundaries. Thus, it results in the reduction of hardness [72] at higher concentration of CNTs.

# Chapter 5

# Results and Discussion: Functional Behavior of Al-Alloy, AMMC & CNT reinforced h-AMMC

## 5.1 Introduction

In this chapter, the results of a comparative investigtion on the tribological characteristics of Al-alloy, AMMC and h-AMMC fabricated by both the sintering route will be presented and discussed. The comprative study is done in the context of wear rate, weight loss and coefficent of friction for the samples sintered by both conventional and microwave heting.

## 5.2 Wear Study

### 5.2.1 Wear Behavior with varying compositions

In this work h- AMMC contain 15% SiC and five varation in the wt.% of MWCNT. The comparision of weight losses and wear rates for samples fabricated by both the sintering methods are shown in **Figure 62** and

Figure 63. From the graphs of weight loss and wear rate it is evident that the microwave sintered h-AMMC exhibits better performance in term of wear resistance as compared to the conventional sintering. By the help of microwave sintering, the wear resistance of h-AMMC is enhanced on an average of 22.7% as compared to the conventional sintering. This happened due to the higher hardness of microwave sintered h-AMMC, poor interfacial strength between Al-SiC or Al-CNT and higher porosity in h-AMMC in the case of conventional sintering. All these weight losses and wear rates are calculated for the dry sliding condition with a sliding speed of 1 m/sec and an applied load of 10N.

It is observed that by the addition of SiC and MWCNT in aluminium matrix there is a decrease in the wear loss as well as wear rate. It is observed that around 80% weight loss is decreased by the addition of 1% MWCNT in h-AMMC as compared to Al-alloy. The wear rate is decreased by the addition of 1% MWCNT by 81.5% (from $2.0596 \times 10^{-3}$ to $3.8021 \times 10^{-4}$), in the case of microwave sintering. Choi et al. [88], showed in his reseach that the addition CNT in aluminium matrix decrease the wear rate by the mechanism of CNT penetratation into aluminium grain. The reduction in weight weight loss and wear rate continues to 2% MWCNT for both the sintering method. Afterwards, the addition of MWCNT in h-AMMC gives reverese effect on the wear resistance property.

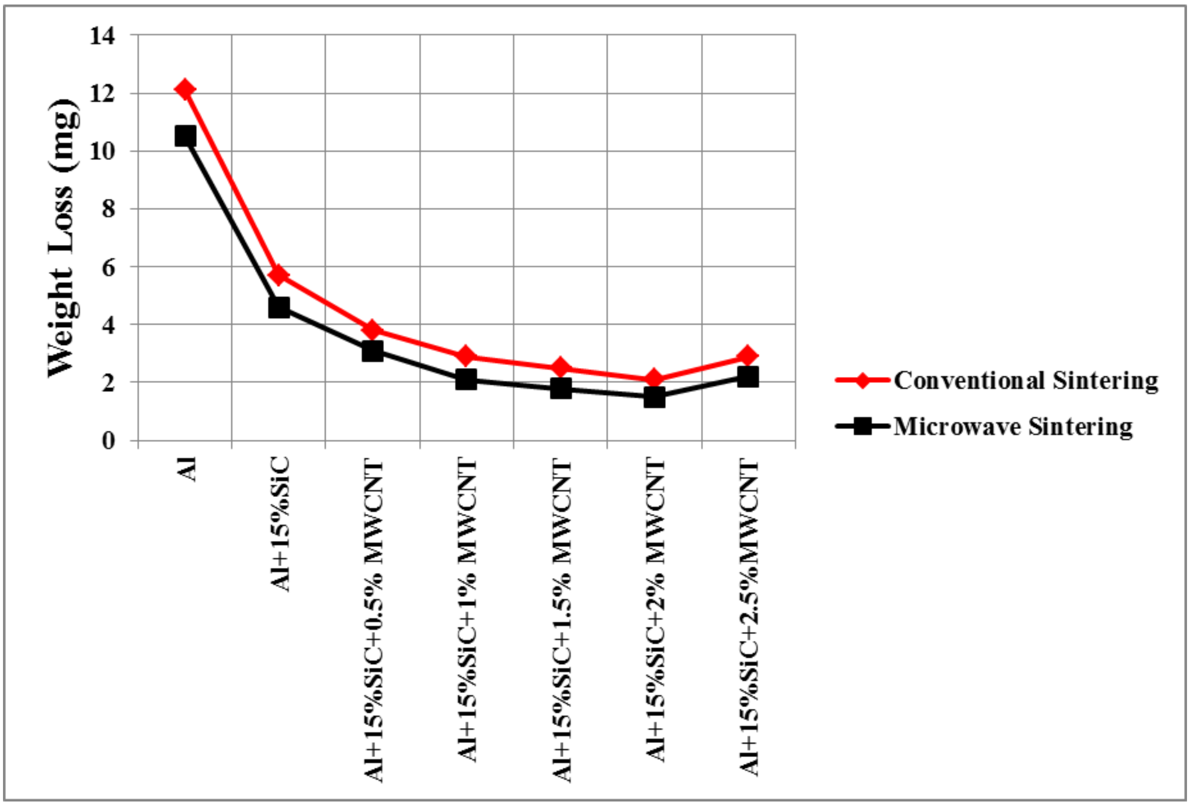


Figure 62 Weight loss for sintered samples with varying compositions

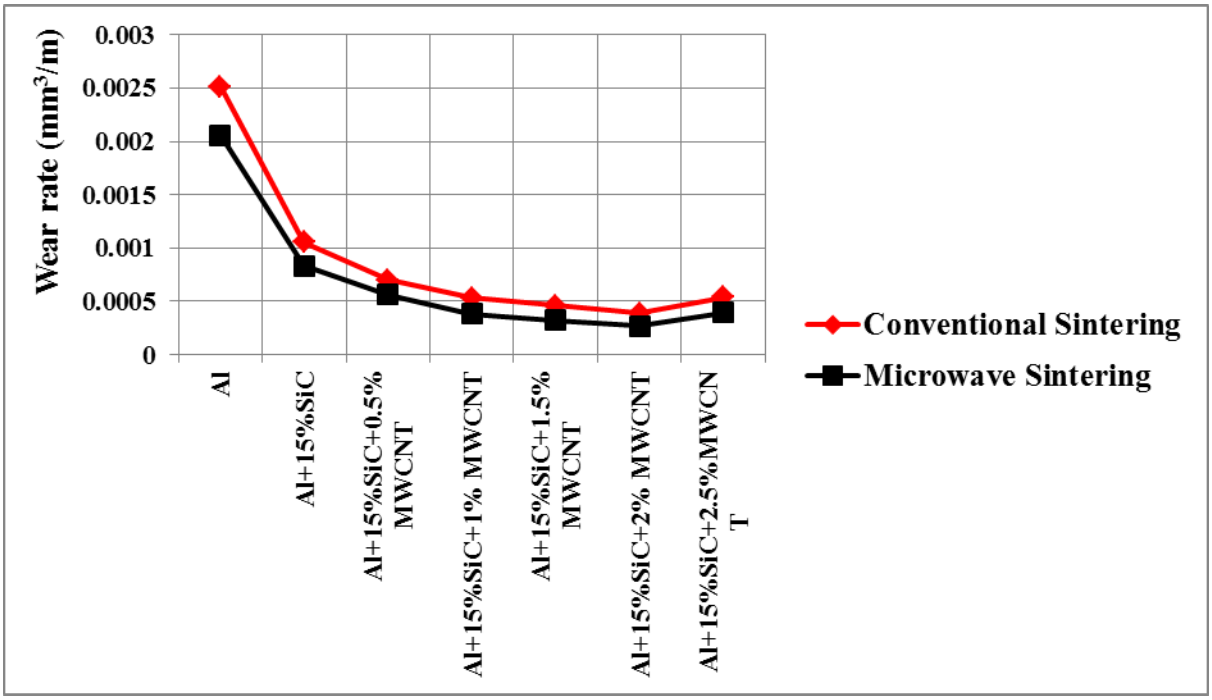


Figure 63 Wear rate for sintered samples with varying compositions

Wear rate increase rapidly after 2% wt. of MWCNT in h-composite. In case of microwave sintering, 2% MWCNT in h-AMMC improves the wear loss by 85.7%. and wear rate by 86.8% (from $2.0596 \times 10^{-3}$ to $2.7062 \times 10^{-4}$) as compared to base alloy. It is clearly seen that after addition of 1% MWCNT wear rate decreases by 5.32% only. This could be happen due to the starting of agglomation of MWCNT between the interstitial space between the aluminium matrix after 1%MWCNT in h-composite.

Beyond 2 wt% of MWCNT in h- AMMC, the wear loss and wear rate starts to increase again very rapidly for both the caseses of sintering. If CNT agglomate or segregrate at grain boundries or on the surface of particle which increase the wear rate of sample. This happen because during time of sintering full consolidation of sample does not happen due to that agglomation of CNT. So balling milling timing or ultasonication timing play an important role for the despersion of CNT. Like pluse time, amptitute, power in the case of ultrasonication and rotaional time, speed etc. in the case of balling milling. This research work mainly foucused on the ultrsonication technique for the dispersion of CNT in aluminium matrix.

This same trend of decreasing wear rate also observed in conventional sintered h-compoite. The decrease in wear rate by the addition of 1% MWCNT is in the range of 78.7% (from $2.5155 \times 10^{-3}$ to $5.3506 \times 10^{-4}$) and for 2% MWCNT this enhacement is about 84.5% (from $2.5155 \times 10^{-3}$ to $3.8803 \times 10^{-4}$). However, for the same composition the decreased wear rate observed for microwave sintered composite is equivalent to the 25% reduction of wear rate of the sample when compared with the same sample of conventional sintering.

### 5.2.2 Wear Behavior under varying loads

Figure **65** shows the comparison of wear rate of composite at low and medium load. The comparison of these composite was done at same process parameters except applied load. The applied load has been increased from 10N to 30N. The sliding speed was 1m/sec and sliding distance was 2000m. A steep decrease in wear rate can be seen as reinforcement has been added in Al metal matrix. This trend of decreasing wear rate continues to 2% MWCNT reinforced h-composites. It is clearly seen that in case of aluminum and Al+ SiC composite the wear rate increases approximately 70.2% whereas in the case of h-composite with 1% MWCNT the wear rate increases at lower rate (62.5%) at same applied load (30N). This could be happened due to the self-lubricating nature of MWCNT and the unique property of MWCNT which could provide thermal stability during sliding at medium or heavy load.

For composites with 2% MWCNT the wear rate increases at the same rate which has been shown in aluminum and Al+ SiC composite, approximately at 70% at 30N load. This might be possible due to the starting of agglomeration which has been discussed earlier. The dispersion of MWCNT in h-composite plays a prominent role un defining the wear mechanism.

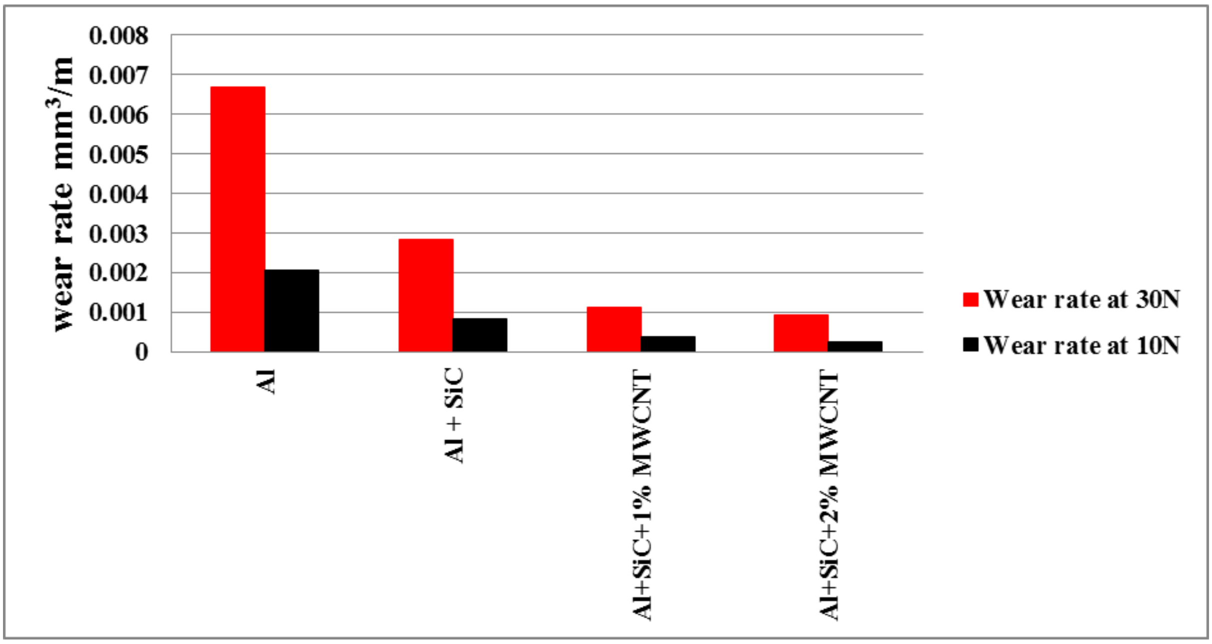


Figure 64 Comparison of wear rate of h-composite at 10N and 30N load with 1m/sec sliding speed

### 5.2.3 Worn Surface Analysis

To get insight of wear mechanism, the surface morphologies of worn out pins is done with help of SEM. For this purpose, specific cases of tribological testing are investigated in detail. The pins were sliding against cast iron disc at constant load of 10N, sliding speed of 1m/sec and for a sliding distance of 2000m. The Figure **65** shows the SEM micrographs of worn out tracks for aluminium matrix, Al+ SiC composite and h-composite with 1% and 2% MWCNT. A comparison of samples with these compositions fabricated by conventional sintered and microwave sintering is also shown in this figure. It is already found and discussed that wear is more in conventional sintered sample as compared to the microwave sintered sample. It was also discussed that by the addition of CNT upto a certain percentage in aluminum matrix a significant decrease in the wear was observed.

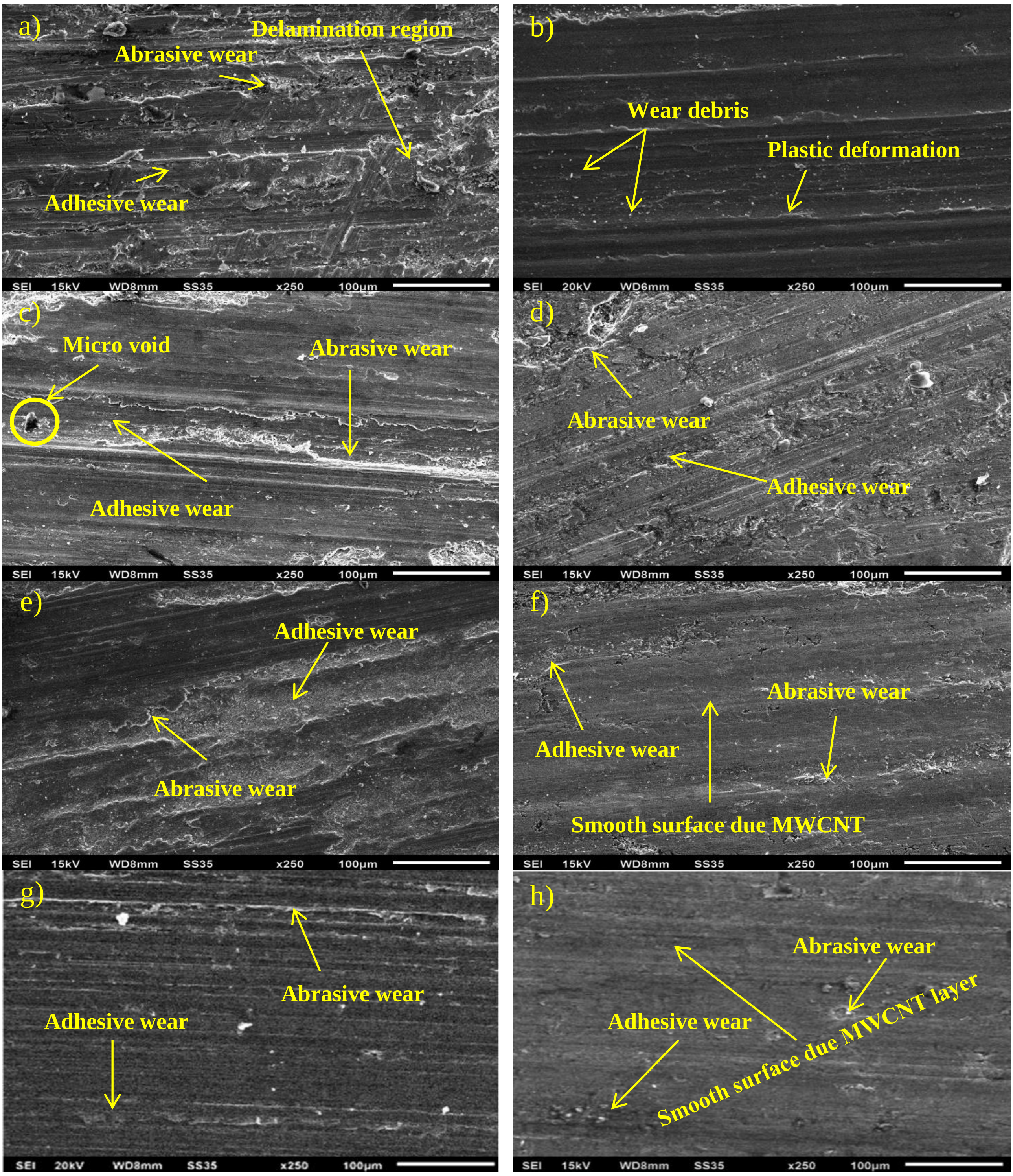


Figure 65 Wear track of Conventional sintered sample: a) Al, c) Al+ SiC, e) Al+SiC+1%MWCNT, g) Al+SiC+2%MWCNT, and Microwave sintered sample: b) Al, d) Al+ SiC, f) Al+SiC+1%MWCNT, h) Al+SiC+2% MWCNT (Sliding speed=1m/sec, Applied load=10 N).

The Figs 65(a) and (b) shows the worn out surfaces of aluminium matrix which is processed by conventional and microwave sintering, respectively. It is clearly seen that aluminum matrix exhibits the severe wear in case of conventional sintering characterized by abrasive, adhesive and delamination wears as compared to the microwave sintering. The worn surface of conventional sintered sample shows rough patches of delamination and deep ploughing strip implying severe adhesive wear. However, microwave sintered sample is characterized by uniform adhesive wear whereas abrasion is greatly reduced in this case. This is attributed to the uniform heating, refined grain size, less porosity and higher hardness.

Addition of SiC, hardens the composite matrix by the formation of hard phases as confirmed from the XRD analysis. The extent of adhesive and abrasive wear is greatly reduced for the both types of sintered composite samples (Figs.65 (c) and (d)).

The addition of MWCNT with SiC in aluminium matrix reduces the wear which is confirmed from the SEM images (Fig. 65 (e), (f), (g) and (h)). The possible reason behind this reduction in wear rate could be the self-lubricating property of MWCNT. This property reduces the friction which further reduces the adhesion between mating tribological parts and reduces the adhesion wear. The reduction in mass loss with the increase in % CNT content for both cases follow same trend. The Fig. 65 (e) and (f) show the wear mechanism of h-composite with 1%MWCNT. Due to the self-lubricating nature of MWCNT smoothened surface is observed in the wear tracks and less cracking surface even at region of severe wear. It could also be due to the better mechanical properties (hardness and strengthening) which are enhanced by MWCNT addition in Al+ SiC composite. The h-composite with 1%MWCNT shows less number of voids, pits and grooves as compared to alumninium and Al+ SiC composites. This trend also follows in case of microwave sintered composite. This could happen due to the presence of high modulus and thermally stable MWCNTs and Silicon carbide particles which increases hardness of h-composite and possibly increases the resistance to material flow during siding [79]. Microwave sintered hybrid composites show better resistance against wear as compared to conventional sintered composite in all cases.

Similarly, from the Fig. 65 (g) and (h) it can be seen clearly that the wear decreases considerably by addition of MWCNT in aluminium matrix. However, the wear rate decrease is reasonably less than that of 1% MWCNT, which could be due to a few local areas, the agglomeration of MWCNT is found, due to the Nano sized of MWCNT which lean towards to fill interstitial space between the aluminium matrix at time of compaction. Similar mechanism has been proposed and reported by some others also [104].

To further explore and validate the proposed mechanism additional wear tracks are also investigated. The detail information of morphologies of worn out microwave sintered composites is shown in Figure **66**. The pin was sliding against the cast iron at 1m/sec sliding speed, 30N load and for a sliding distance of 2000m.

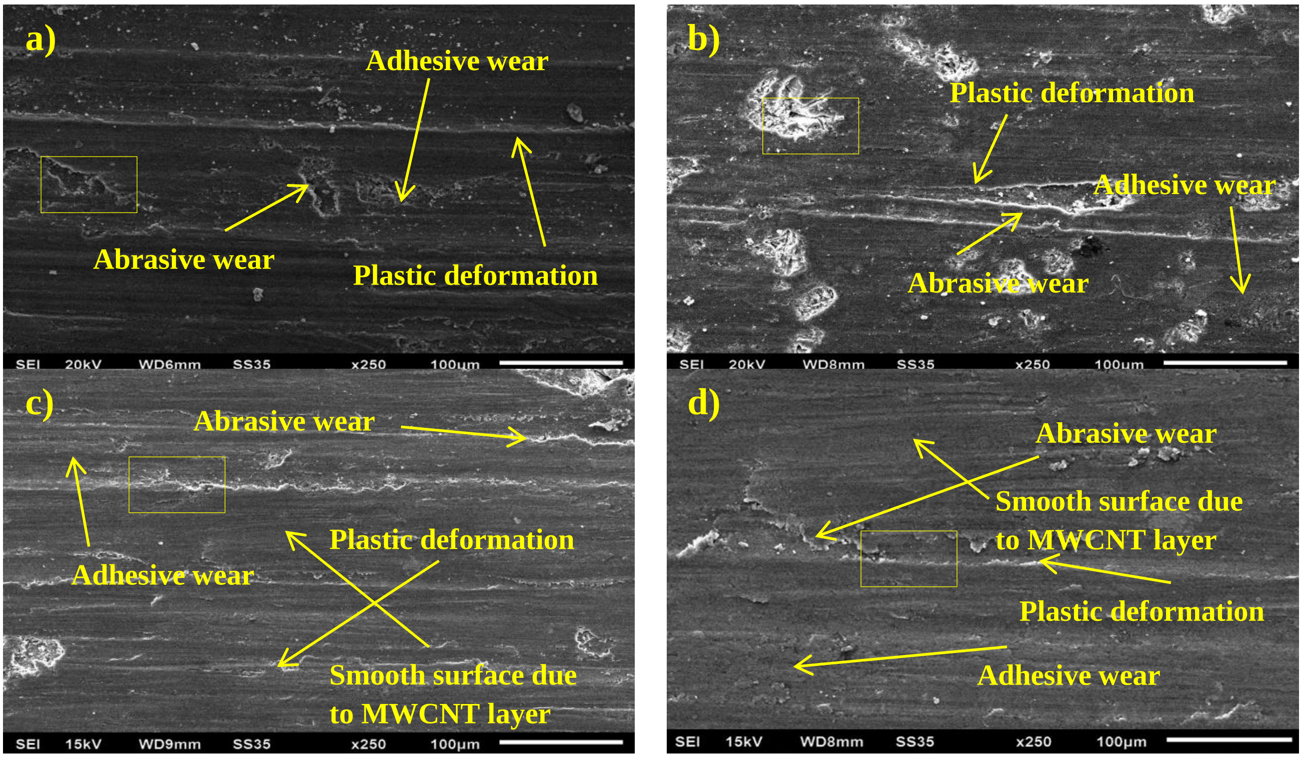


Figure 66 Wear track of Microwave sintered a) Al b) Al+ SiC c) Al+SiC+1%MWCNT d) Al+SiC+2%MWCNT at 1m/sec sliding speed with 30N load.

Figure **66** (a) shows the wear track of aluminum. In the case of aluminium, at low load condition more ploughing and declamation take place and more material flow during the sliding. At medium load more abrasive wear take place instead of adhesion wear and deep grooves also formed on the sliding surface of sample. The EDS analysis confirms that there is less adhesion wear in case of higher load which is indicated by the low intensity of Fe in the wear track, as shown in Figure **67** (a).

Figure **66** (b) shows the worn surface of Al+ SiC composite at higher load. It is clearly seen that there is more abrasive wear of SiC particle at mild wear condition. The addition of hard reinforcement in aluminum reduces the wear. It is also clearly seen that the wear less in Al +SiC composite than aluminum matrix. The abrasive wear of SiC particle was observed at 30N applied load. The EDS of worn out composite is also shown in Figure **67** (b).

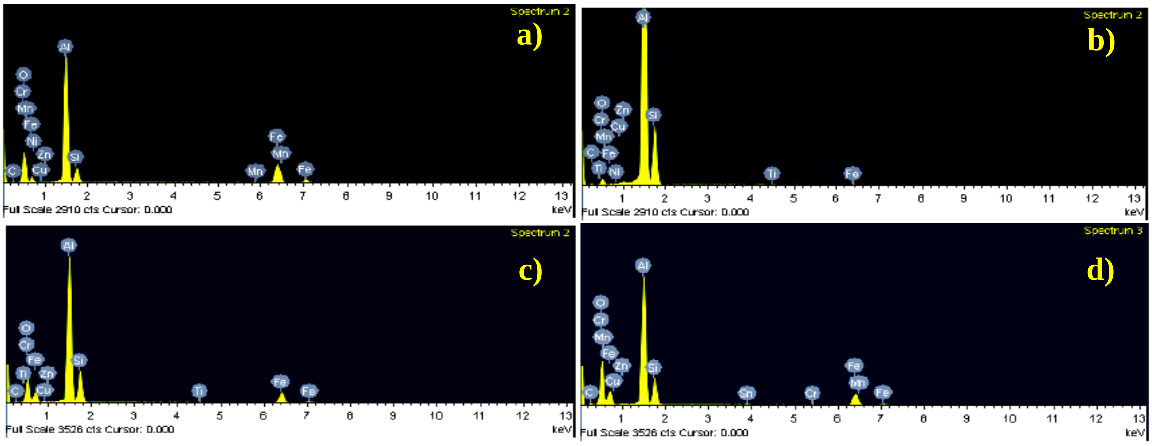


Figure 67 EDS of worn out Sample of a) aluminium matrix b) Al+ SiC c) Al+SiC+1% MWCNT d) Al+SiC+2% MWCNT

Figure **66** (c) and (d) shows the worn surface of h-composite with 1%MWCNT and 2%MWCNT, respectively at 30 N load. It is clearly shown that addition of MWCNT reduces the wear and exhibits smooth surface. This is due to the self-lubricating nature and strong bonding at the interface. Both adhesive and abrasive wear is less in h-composite as compared to aluminium and Al+ SiC. The EDS of both 1%MWCNT and 2%MWCNT h-composite is shown in a Figure **67** (c and d)).

## 5.3 Friction Study

The friction testing was also done against a rotating disc of cast iron disc at some applied loads. The friction study also done at 1m/sec sliding speed, 10N applied load and 2000 m sliding distance. The coefficient of friction could be calculated by formula which is given below:

$$\mu = F/N$$

Where:

F= Friction force which can be calculated by help of WINDCOM software.

N = Applied load in Newton

μ = Coefficient of friction

### 5.3.1 Friction Characteristics with varying compositions

The Figure **68** shows the coefficient of friction against different compositions for both conventional and microwave sintered samples. The microwave sintered composite shows the better result in term of coefficient of friction as compared to conventional sintered composite. This happen due to the better result of microwave sintered composite in term of hardness, better grain size, less porosity and high densification of composite. On an average 13.73% of coefficient of friction decreases is observed for composites fabricated by microwave heating over conventional heating.

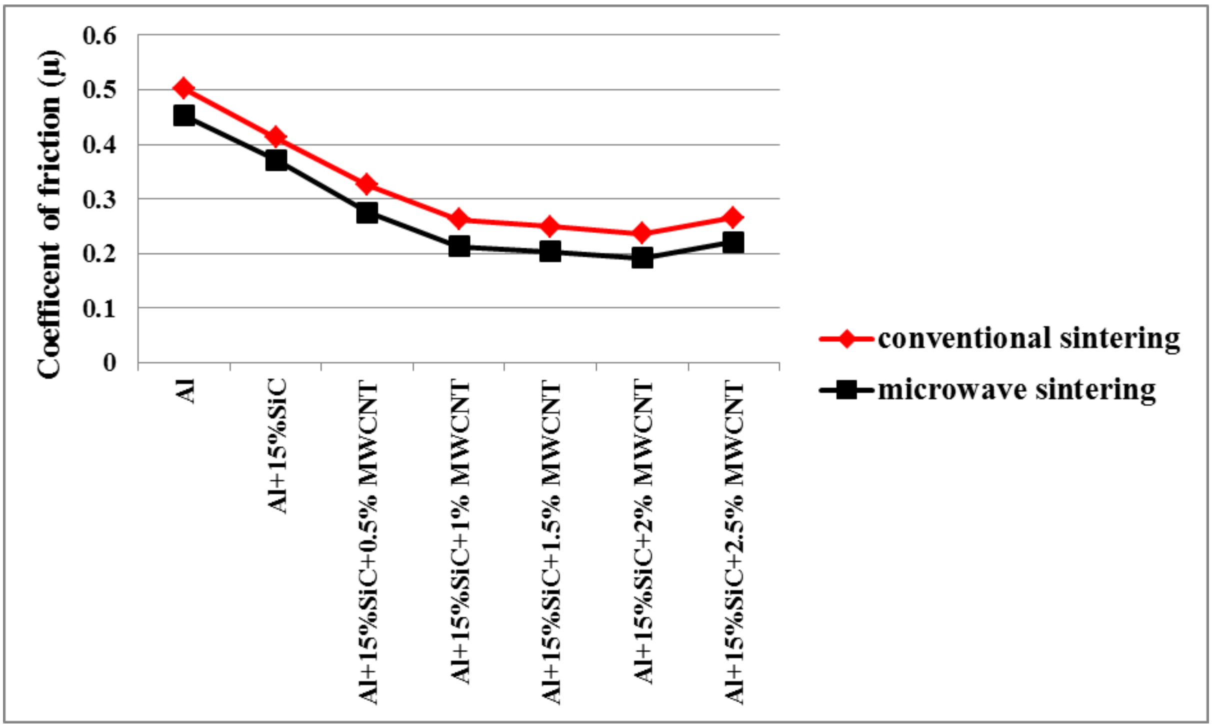


Figure 68 Coefficient of friction of h-AMMC with varying % of MWCNT

The coefficent of friction decreased by the addition of SiC in alumnium composite for about 27% from 0.442 for Al-alloy to 0.322 for Al+SiC, in the case of microwave sintering. In case of h-composite with 1%MWCNT this decrease in the coefficent of friction is about 47.87% from 0.442 to 0.232. Further addtion of MWCNT in Al+SiC composite also decreases the coefficent of friction, but at lower rate than its former. There is an overall decrease of 50.76% in the case of 2%MWCNT in h-composite. The result reveal that only 3% of decrement has been found when MWCNT wt.% fraction increases from 1% to 2% in h-composite. The possible reason for this decrease rate in coeefficient of friction could be due to starting of agglomeration of MWCNT particles when added 2% in both conventional and microwave sintering. The study of wear rate and hardness has been followed the same trends.

In this study, the coefficient of friction is reduces with the addition MWCNTs in h-composite. This might be possible due to the good fine grain structure of the aluminum matrix along with the self-lubricating effects of the MWCNTs. It was believed that with the increase % of MWCNT content in matrix, the element of the MWCNT increases on the sample surface, and therefore the direct contact between the h-composite and the disk decreases, As a result of the reduction in the coefficient of friction has been found [82]. The another possible reason of reduction in coefficient of friction was that, by increasing the amount of MWCNT, a thin film of carbon sheltered the wear surface of h-composite which act as solid lubricant which help in decreasing the coefficient of friction[110].

### 5.3.2 Friction Characteristics under different loads

To explore the friction mechanism of microwave sintered composites at higher load, the pins were slided against the cast iron at 1m/sec sliding speed, under 30N load and for a sliding distance of 2000 m. The comparison of coefficient of friction at different load is shown in Figure **69**.

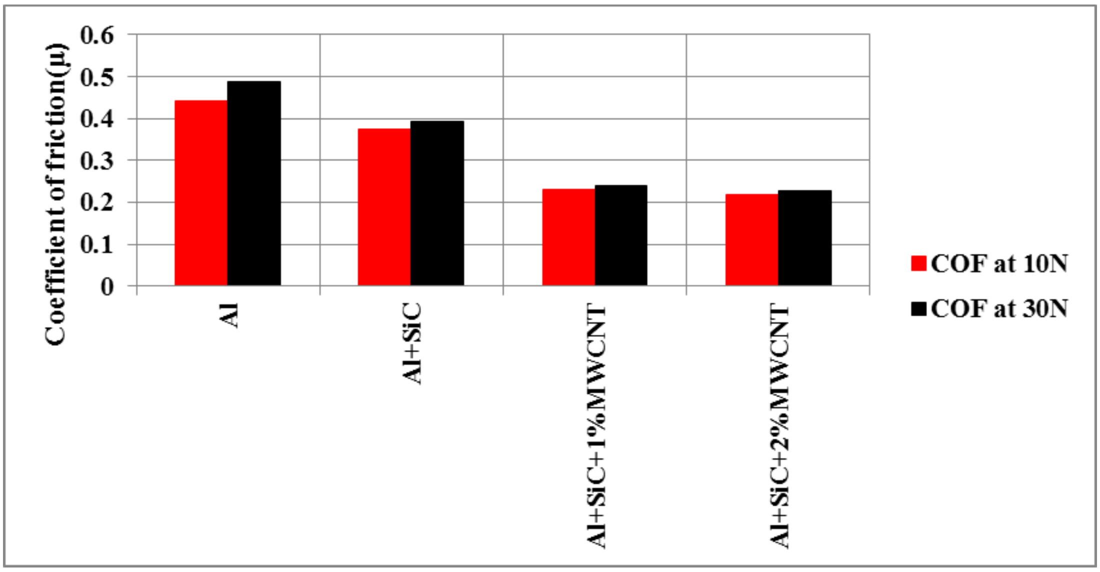


Figure 69 Comparison of wear rate of h-composite at 10N and 30N load with 1m/sec sliding speed

The coefficient of friction is increased as load increase in all the cases. But in case of Al+SiC +1% MWCNT the coefficient of friction is found to be least, as obtained in the earlier case. This might be due to the fact that at higher load the ploughing force is increased and in turn greater penetration inside the sample, which in turn increases the amount of MWCNT pulled out of the matrix, or crushed, and thus increases the efficiency of lubrication [82].

### 5.3.3 Graphical Analysis of coefficient of friction vs. sliding distance

The sliding distance plays an important role in determining the coefficient of friction in long run. Therefore, variation of coefficient of friction against sliding distance is compared both types of sintered materials.

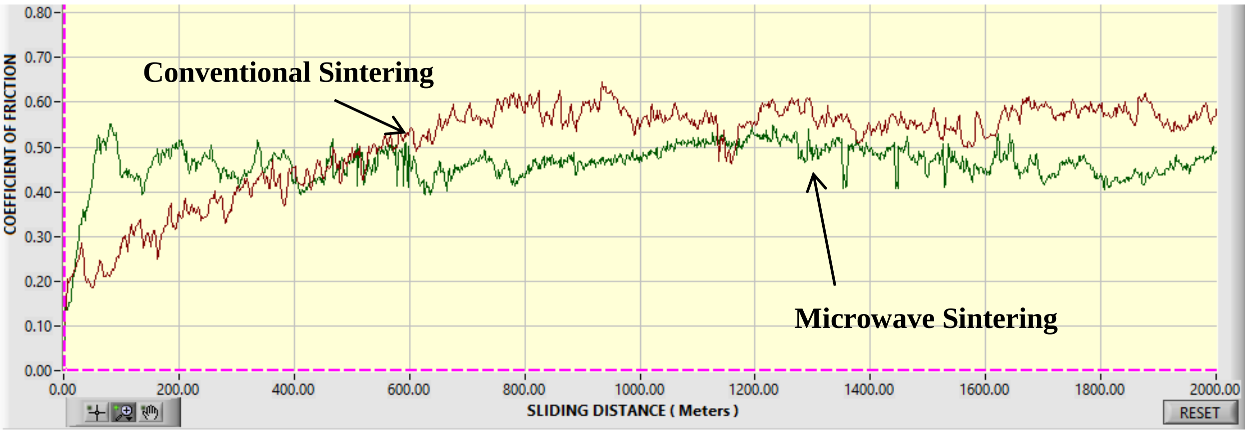


Figure 70 Graph of Coefficient of friction vs. sliding distance of conventional and microwave sintered Alumnium

Figure **70** shows the coefficient of friction behavior of aluminium with respect to sliding distance at 10N applied load. It has been clearly seen that from 0 to 400 m of sliding distance, microwave sintered aluminum show high coefficient of friction as compared to conventional sintered aluminium. This might happen due to initial run-in condition of tribo-contact between pin and disc. But after the sliding distance of 400 m, and upto to 2000 m the microwave sintered aluminium shows less coefficient of friction as compared to conventional sintered aluminium. However, microwave sintered Al-alloy shows the better stability in friction response as compared to its conventional counterpart.

Figure **71** shows the friction response of Al+ SiC composite for both microwave and conventional sintered samples. It has been clearly visible that microwave sintered sample of composite shows better behavior of coefficient of friction and show stability in friction behavior as compared to aluminum.

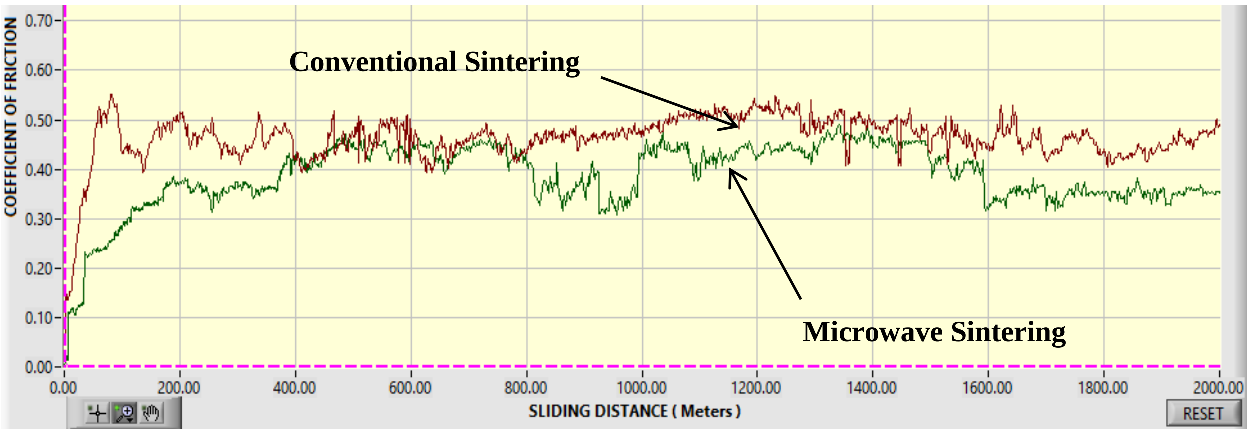


Figure 71 Graph of Coefficient of friction vs. sliding distance of conventional and microwave sintered Al+SiC

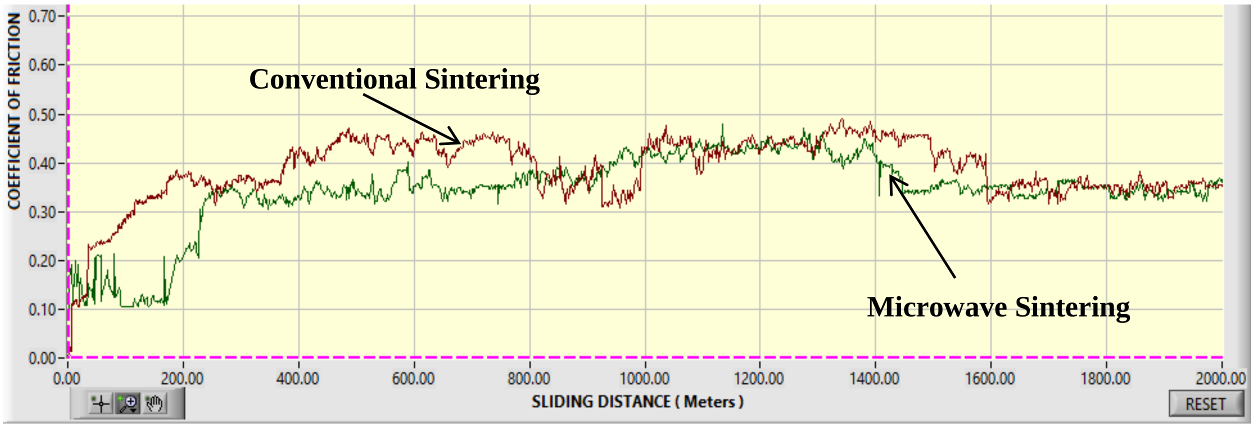


Figure 72 Graph of Coefficient of friction vs. sliding distance of conventional and microwave sintered Al+SiC+0.5% MWCNT

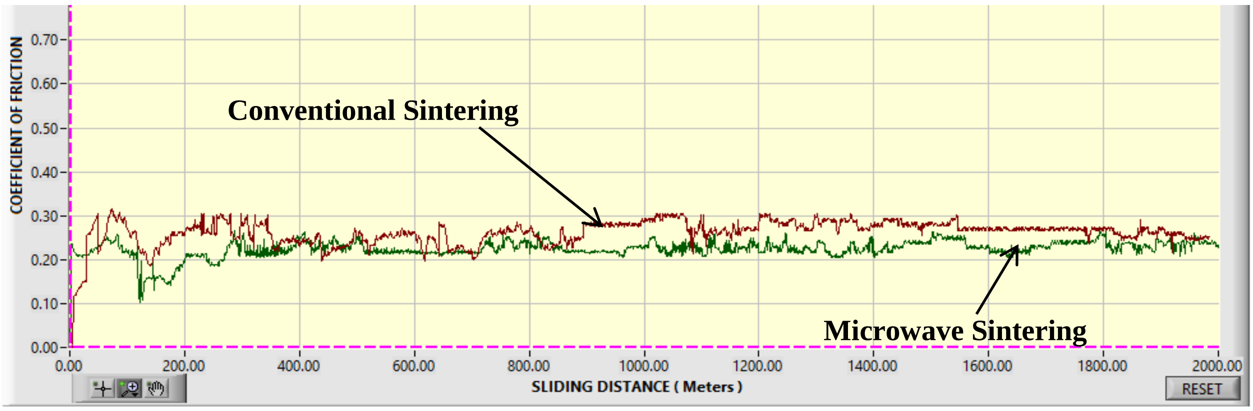


Figure 73 Graph of Coefficient of friction vs. sliding distance of conventional and microwave sintered Al+SiC+1% MWCNT

Figure 72 shows the response of coefficient of friction of h-composite with 0.5% MWCNT against sliding distance. With the addition of MWCNT there is a decrease in the coefficient of friction. Also, stability in behavior of coefficient of friction is improved to an insignificant extent. It has been clearly seen from the graph that after 1600 m sliding distance, the coefficient of friction became more stable and straight line. This change in behavior of coefficient of friction might be due to the fact that MWCNT particle with its self-lubricating properties help in the formation of carbonaceous layer. Microwave sintered h-composite shows better result as compared to the conventional sintered h-composite. This improvement becomes more prominent when CNT reinforcement in increased to 1-2%, as shown in Figure 73, Figure 74 and Figure 75. It has been clearly seen from graph that the graph was almost became a straight line or more stable for some sliding distance in both conventional and microwave sintered samples.

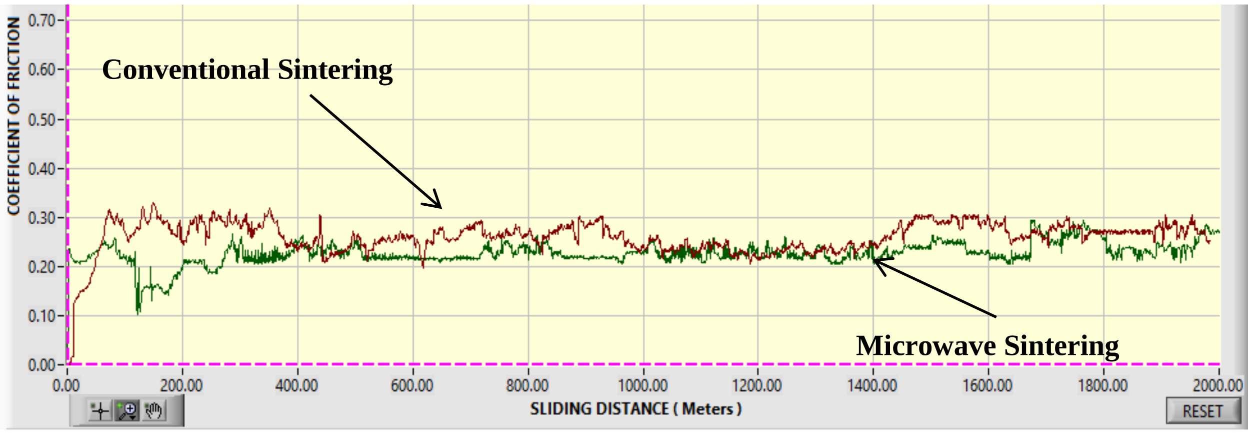


Figure 74 Graph of Coefficient of friction vs. sliding distance of conventional and microwave sintered Al+SiC+1.5% MWCNT

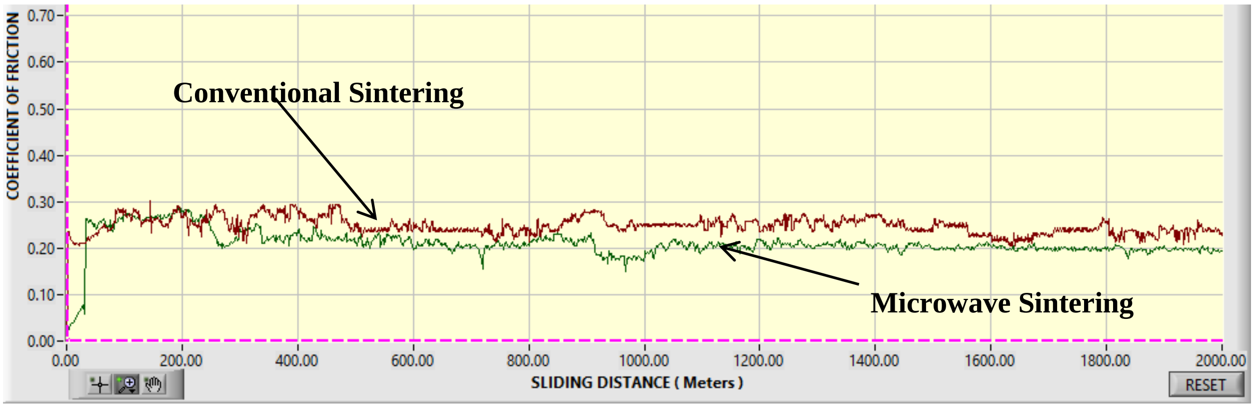


Figure 75 Graph of Coefficient of friction vs. sliding distance of conventional and microwave sintered Al+SiC+2% MWCNT

Thus, from all the above analysis of friction responses with the sliding distance it is observed that the addition of CNT upto 2% in the h-composite helps in achieving the stable friction which is attributed to the tribofilm formation in the presence of MWCNT. It is also observed that microwave sintered h-composite shows superior friction response as compared to their conventional counterpart.

# Chapter 6

## Statistical Analysis on the Functional behavior of Microwave sintered CNT reinforced h-AMMC

### 6.1 Introduction

Design of experiment is most versatile tool to perform statistical analysis as well as to find the effect of several variables simultaneously. There are several steps in it that have a particular sequence which has to be followed during arranging DOE which further helps to modify the understanding the performance. A certain number of combinations of levels and probable significant factors have to be tested to find out the response under those test conditions. In Taguchi approach those test combinations have determined by allocation of factors in a particular orthogonal arrays. The DOE process comprises three main phases: planning, conduction and analysis. The determination of combination of levels and factors to get the desired information in the DOE process is of major concern. The design of manufacturing processes improvement is focused by these methods. This method provides the series of various parameters with the interaction of factors and significance level of a factor on a particular output response.

Three parameters have been selected to perform dry sliding wear test: applied load, sliding speed and composition at constant sliding distance. The applied load, sliding speed and composition has been tested using three levels. In the current study, two orthogonal arrays has been used in order to perform the experiments and perform statistical analysis by Taguchi method. A L9 array for various compositions and another L9 array is built at selected constant composition of CNT to perform the statistical analysis.

The details of the parameters, levels and corresponding orthogonal arrays (L9) used for this study with the help of Mini Tab are shown in **Table 10-**

Table **13.**

Table 10: Details of experimental parameters with various compositions of CNT

| **Factor** | **Levels** | | |
|---|---|---|---|
| Composition | Al+SiC +0.5% MWCNT | Al+SiC +1% MWCNT | Al+SiC+1.5% MWCNT |
| Load | 10 N | 30 N | 50 N |
| Speed | 0.25 m/s | 1 m/s | 2.5 m/s |

Table 11 Design of Experiment L9 with different compositions

| **Experiment No.** | **Composition** | **Load (N)** | **Speed(m/sec)** |
|---|---|---|---|
| 1 | Al + SiC + 0.5% MWCNT | 10 | 0.25 |
| 2 | Al + SiC + 0.5% MWCNT | 30 | 1 |
| 3 | Al + SiC + 0.5% MWCNT | 50 | 2.5 |
| 4 | Al + SiC + 1% MWCNT | 10 | 1 |
| 5 | Al + SiC + 1% MWCNT | 30 | 2.5 |
| 6 | Al + SiC + 1% MWCNT | 50 | 0.25 |
| 7 | Al + SiC + 1.5% MWCNT | 10 | 2.5 |
| 8 | Al + SiC + 1.5% MWCNT | 30 | 2.5 |
| 9 | Al + SiC + 1.5% MWCNT | 50 | 1 |

Table 12 Details of experimental paraemetrs for h-composite with 1%MWCNT

| Factor | Levels | | |
|---|---|---|---|
| Load | 10N | 30N | 50N |

| Speed | 0.25m/s | 1m/s | 2.5m/s |
|---|---|---|---|

Table 13 Details of design of experiment L9 for h-composite with 1%MWCNT

| Experiment No. | Composition | Load (N) | Speed(m/sec) |
|---|---|---|---|
| 1 | Al + SiC + 1% MWCNT | 10 | 0.25 |
| 2 | Al + SiC + 1% MWCNT | 30 | 1 |
| 3 | Al + SiC + 1% MWCNT | 50 | 2.5 |
| 4 | Al + SiC + 1% MWCNT | 10 | 0.25 |
| 5 | Al + SiC + 1% MWCNT | 30 | 1 |
| 6 | Al + SiC + 1% MWCNT | 50 | 2.5 |
| 7 | Al + SiC + 1% MWCNT | 10 | 0.25 |
| 8 | Al + SiC + 1% MWCNT | 30 | 1 |
| 9 | Al + SiC + 1% MWCNT | 50 | 2.5 |

The coefficient of friction and wear rate are the output responses for these DoEs. The analysis is done at $\alpha$ =0.05, which means that confident level for analysis is 95%. So the p-value of factors which is considered significant for the experimental results in this study should be less than 0.05. If, the value is not less than 0.05 then the corresponding factor is deemed as insignificant parameter.

## 6.2 Statistical Analysis of the Experimental Results

### 6.2.1 Friction and Wear Behavior of h-Composites with various CNT reinforcements

With the help of MINITAB software the measured results are analyzed. The values of coefficient of friction and wear rates for different runs are shown in **Table 14**.

Table 14 L9 Orthogonal array for h-composite with different compositions

| S.No | Composition | Load | Sliding speed | Coefficient of friction (μ) | Wear rate ($mm^3/m$) × $10^{-4}$ |
|---|---|---|---|---|---|
| 1 | Al+SiC+0.5%MWCNT | 10 | 0.25 | 0.252 | 9.514 |
| 2 | Al+SiC+0.5%MWCNT | 30 | 1.00 | 0.268 | 14.817 |
| 3 | Al+SiC+0.5%MWCNT | 50 | 2.50 | 0.272 | 18.588 |
| 4 | Al+SiC+1%MWCNT | 10 | 1.00 | 0.232 | 3.848 |
| 5 | Al+SiC+1%MWCNT | 30 | 2.50 | 0.245 | 10.92 |
| 6 | Al+SiC+1%MWCNT | 50 | 0.25 | 0.262 | 16.016 |
| 7 | Al+SiC+1.5%MWCNT | 10 | 2.50 | 0.225 | 3.180 |
| 8 | Al+SiC+1.5%MWCNT | 30 | 0.25 | 0.238 | 10.209 |
| 9 | Al+SiC+1.5%MWCNT | 50 | 1.00 | 0.258 | 14.178 |

*6.2.1.1 Analysis of wear rate*

The experimental results of wears are analyzed with the help of ANOVA. The ANOVA table is shown in **Table 15.** The composition and load show the significant effect on wear rate. From the table it is observed that the composition and load play significant effect on wear rate while sliding speed is an insignificant factor in this study.

Table 15 Analysis of Variance for Means for coefficient of friction

| Source | DF | Seq SS | Adj SS | Adj MS | F value | P value | Pr(%) |
|---|---|---|---|---|---|---|---|
| **Composition** | 2 | 50.029 | 50.029 | 25.0141 | 33.98 | 0.029* | 23.15% |
| **Load** | 2 | 164.390 | 164.390 | 82.1951 | 111.64 | 0.009* | 77.14% |
| **Speed** | 2 | 0.215 | 0.215 | 0.1075 | 0.15 | 0.873 | 0.09% |
| **Residual** | 2 | 1.473 | 1.473 | 0.7363 | | | 0.68% |

| | | | | | | | |
|---|---|---|---|---|---|---|---|
| **error** | | | | | | | |
| **Total** | 8 | 216.101 | | | | | |
| | *Significant | | | | | | |
| | S= 0.4653 R-sq. = 98.3% R-sq. (adj) = 97.2% | | | | | | |

It is also observed from the above **Table 15** that the composition and load has 23.15% and 77.14% contribution, respectively. The R-sq. and R-sq.(adj) values shows the validity of model.

For better understanding the mean plot graph of wear rate is shown in Figure **76**. The wear rate decreases significantly with the increase of the percentage of MWCNT in h-composite. An increase in load increases the wear rate significantly. An increase in sliding speed decreases the wear rate till the sliding speed reaches upto 1m/sec, after that there is almost no effect shown in the wear rate as shown in the mean plot when speed changes from 1m/s to 2.5m/s.

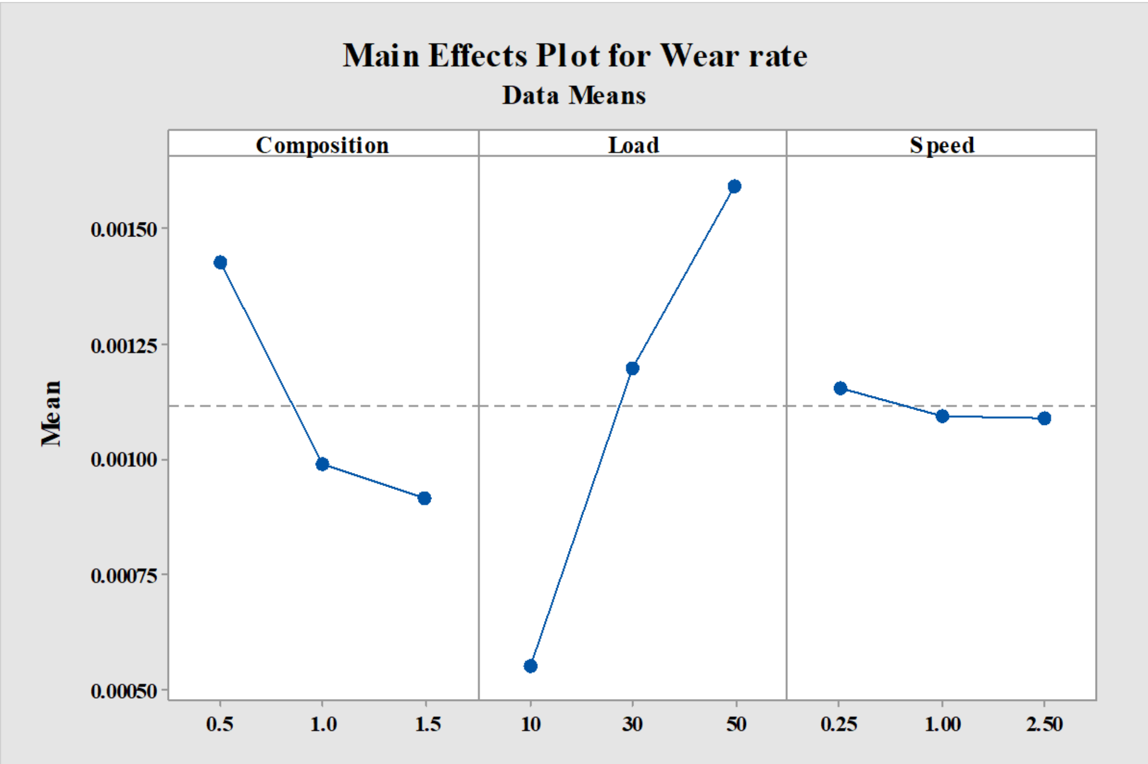


Figure 76 Main effects plot for Means – Wear rate

### *6.2.1.2 Analysis of Coefficient of friction*

The coefficient of friction is decreases as the wt. % of MWCNT increases. As load increases the coefficient of friction also increases. For better understanding the mean plot of coefficient of friction is shown in Figure 77.

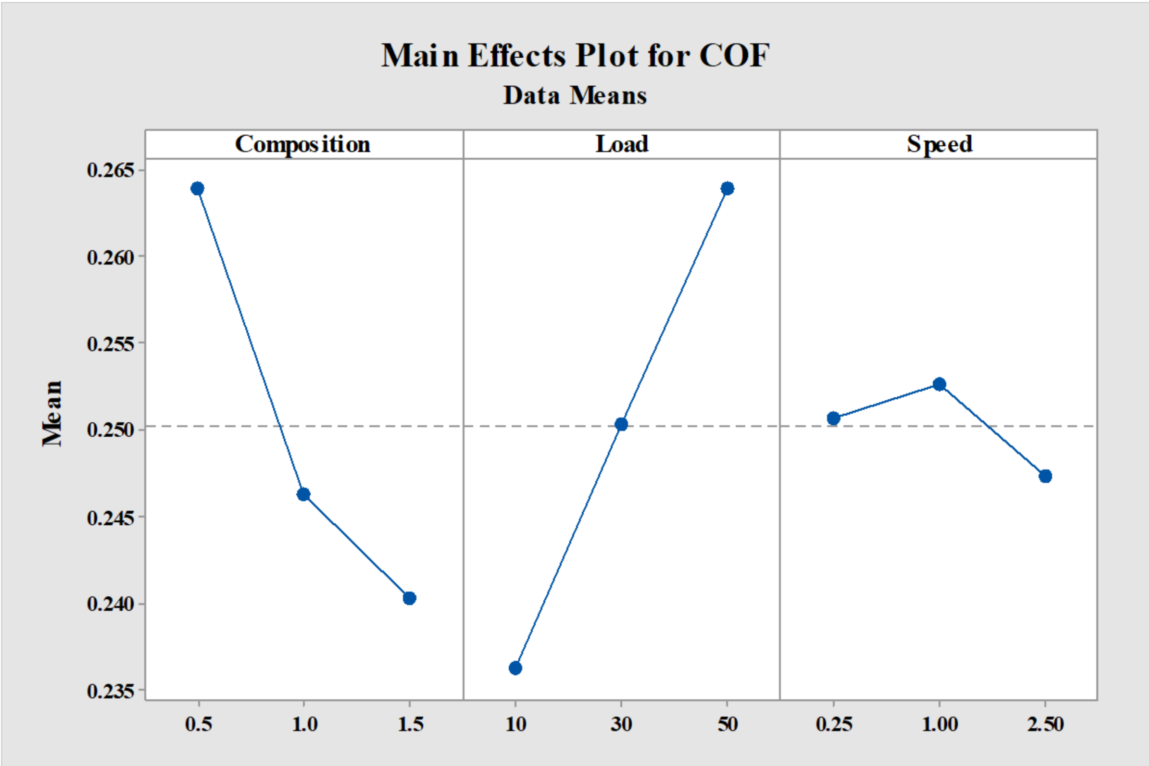


Figure 77 Main effects plot for Means – Coefficient of friction

The ANOVA **Table 16** shows that the composition and load show the significant effect on coefficient of friction while sliding speed is an insignificant factor. It is observed that composition and load has 42.46% and 53.69% influence on the coefficient of friction. The value of R-sq shows the validity of orthogonal array.

Table 16 Analysis of Variance for Means for coefficient of friction

| **Source** | **DF** | **Seq SS** | **Adj SS** | **Adj MS** | **F value** | **P value** | **Pr(%)** |
|---|---|---|---|---|---|---|---|
| **Composition** | 2 | 0.000908 | 0.000908 | 0.000454 | 24.18 | 0.040* | 42.46% |
| **Load** | 2 | 0.001148 | 0.001148 | 0.000574 | 30.57 | 0.032* | 53.69% |
| **Speed** | 2 | 0.000044 | 0.000044 | 0.000022 | 1.16 | 0.463 | 2.05% |
| **Residual error** | 2 | 0.000038 | 0.000038 | 0.000019 | | | 1.77% |
| **Total** | 8 | 0.002138 | | | | | |

| | |
|---|---|
| | *Significant |
| | S= 0.003756 R-sq. = 98.3% R-sq. (adj) = 93.2% |

*6.2.1.3 Multiple Linear Regression Model to predict the friction and wear behavior*

With the help of statistical software "MINITAB" the multiple linear regression models are developed to predict the friction and wear rate. From the observed data a linear equation is fitted which gives the relationship between independent variables & a response parameter. By establishing a correlation between the significant factors which are obtained from ANOVA analysis namely composition, load and speed, a regression equation is generated. The regression equation of wear rate and coefficient of friction for different composition, load and speed is given below. The R-sq value of regression models shows the validity of equations.

$W_r = 0.000618 + 0.000052\, L - 0.000027\, S - 0.000512\, C$ ……………………………*Equation 1*

R-sq. = 94.91%

$C_f = 0.24844 + 0.001383\, L - 0.00178\, S - 0.02367\, C$

R-sq. = 94.18% …………………………… *Equation 2*

Where L is load, S is speed and C represents composition

The R-sq. values of regression models are 94.91% and 94.18 %, respectively which indicates adequacy of the predictive models for wear rate and coefficient of friction. The negative sign in the equations indicates that with the wt. % of MWCNT and speed, both wear rate and coefficient of friction decrease. The positive associated with load implies that as load increases both wear rate and coefficient of friction increases.

**6.2.2 Friction and Wear Behavior of 1% MWCNT reinforced h-Composites with various loads and speeds**

To find more conclusive model for the specific case of CNT reinforced h-composite at different speed and load, a second L9 orthogonal array (

Table **13**) is used to perform the experiments and performed the statistical analysis of tribological behavior. The experimental parameters used are load and sliding speed with 3 levels. All experiments were performed for constant time of 30min. The

Table **17** shows the result of wear rate and coefficient of friction of h-composite with 1%MWCNT.

Table 17: L9 Orthogonal for h-composite with 1%MWCNT

| S.No. | Load | Speed | COF (μ) | Wear rate $(mm^3/m)\times10^{-4}$ |
|---|---|---|---|---|
| 1 | 10 | 0.25 | 0.239 | 5.913302 |
| 2 | 10 | 1.00 | 0.232 | 3.847563 |
| 3 | 10 | 2.50 | 0.228 | 2.517636 |
| 4 | 30 | 0.25 | 0.248 | 12.83851 |
| 5 | 30 | 1.00 | 0.247 | 11.95947 |
| 6 | 30 | 2.50 | 0.245 | 10.01156 |
| 7 | 50 | 0.25 | 0.258 | 15.01686 |
| 8 | 50 | 1.00 | 0.252 | 14.52034 |
| 9 | 50 | 2.50 | 0.250 | 13.12312 |

*6.2.2.1 Analysis of wear rate*

The **Figure 78** shows the mean effect plot of wear rate of h-composite with 1%MWCNT which indicates that as load increases the wear rate also increases whereas increase in the sliding distance decreases the wear rate. The decrease in the observed wear rate with sliding speed indicates the presence of MWCNT under the contact which contributes to the reduction of frictional heat and shear sliding, which is playing a more predominant role while defining the coefficient of friction between the contact surfaces. It is also suggested that as the sliding speed increases the centrifugal force also increases which in turn throws out the loose wear debris away from the wear track while rubbing action is undergoing [82].

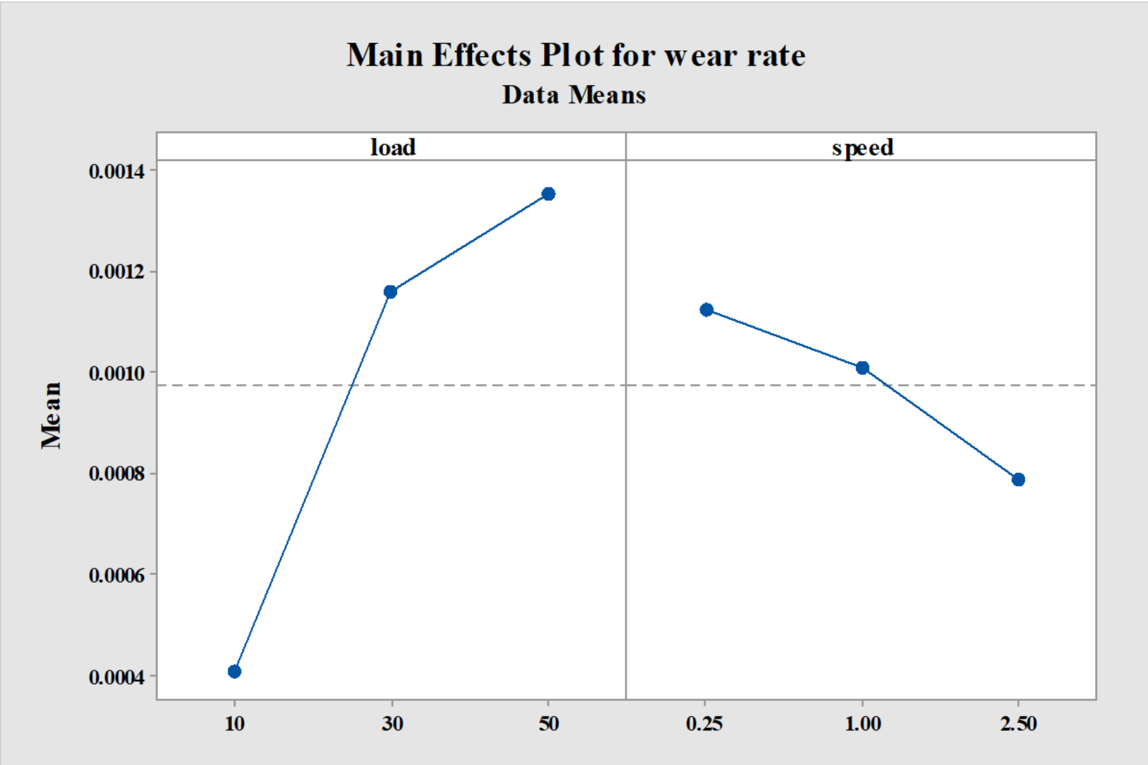


Figure 78 Main effects plot for Means – Wear rate

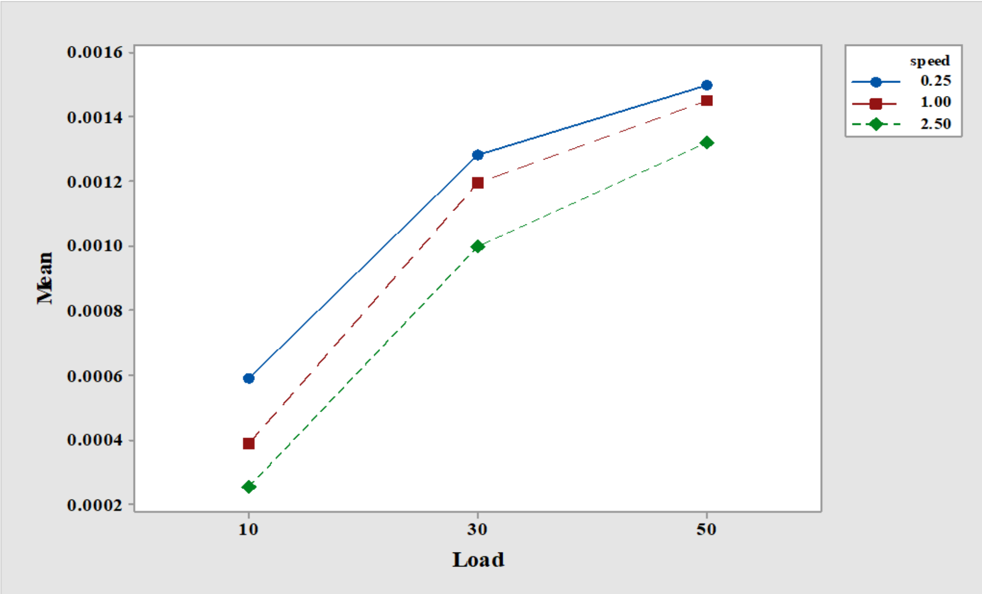


Figure 79 Graph of Wear rate vs. load for different speed

The ANOVA **Table 18** shows the analysis of variance for means for wear rate which reveals that that load and speed are significant factor for wear rate. The **Error! Not a valid bookmark self-reference.** indicates that the speed and load show the significant effect on wear rate and show the contribution of factor, where load has 80.72% contribution and speed has 10.45% influence on the wear rate.

.

Table 18: Analysis of Variance for Means for wear rate

| Source | DF | Seq SS | Adj SS | Adj MS | F value | P value | Pr(%) |
|---|---|---|---|---|---|---|---|
| **Load** | 2 | 149.712 | 149.712 | 74.8559 | 212.89 | 0.002* | 88.72% |
| **Speed** | 2 | 17.638 | 17.638 | 8.8189 | 25.34 | 0.005* | 10.45% |
| **Residual error** | 4 | 1.378 | 1.378 | 0.3468 | | | 0.81% |
| **Total** | 8 | 168.737 | | | | | |
| | *Significant | | | | | | |
| | S = 1.088 R-Sq. = 98.5% R-Sq.(adj) = 97.1% | | | | | | |

*6.2.2.2 Analysis of coefficient of friction*

The ANOVA **Table 19** indicates that the load and speed also a significant factor for coefficient of friction. But load play a dominant role in changing the coefficient of friction as contribute 86.46% effect on coefficient of friction and speed contribute only 11.12%.

Table 19**:** Analysis of Variance for Means for coefficient of friction

| **Source** | **DF** | **Seq SS** | **Adj SS** | **Adj MS** | **F value** | **P value** | **Pr(%)** |
|---|---|---|---|---|---|---|---|
| **Load** | 2 | 0.000645 | 0.000645 | 0.000322 | 69.07 | 0.001* | 86.46% |
| **Speed** | 2 | 0.000083 | 0.000083 | 0.000041 | 8.86 | 0.034* | 11.12% |
| **Residual error** | 4 | 0.000019 | 0.000019 | 0.000005 | | | 2.54% |
| **Total** | 8 | 0.000746 | | | | | |
| | *Significant | | | | | | |
| | S = 0.002160 R-Sq. = 97.5% R-Sq. (adj) = 95.0% | | | | | | |

The **Figure 80** shows the mean of coefficient of friction with respect to load and speed. It is observed that as load increases the coefficient of friction also increases but as sliding speed is increased the coefficient of friction decreases. The similar trend also reported by Choi.et al. [78]and Mina et al. [82]. The **Figure 81** shows the effect of sliding speed on coefficient of friction at different loading condition.

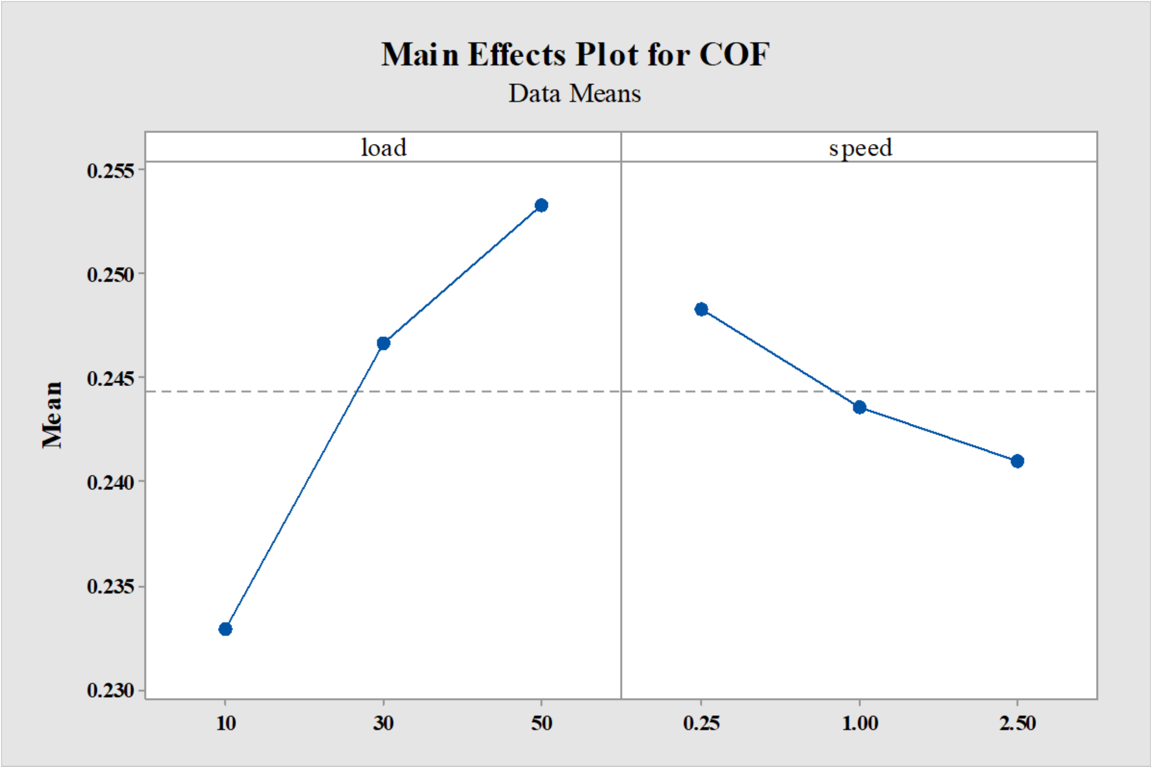


Figure 80Main effects plot for Means – Coefficient of friction

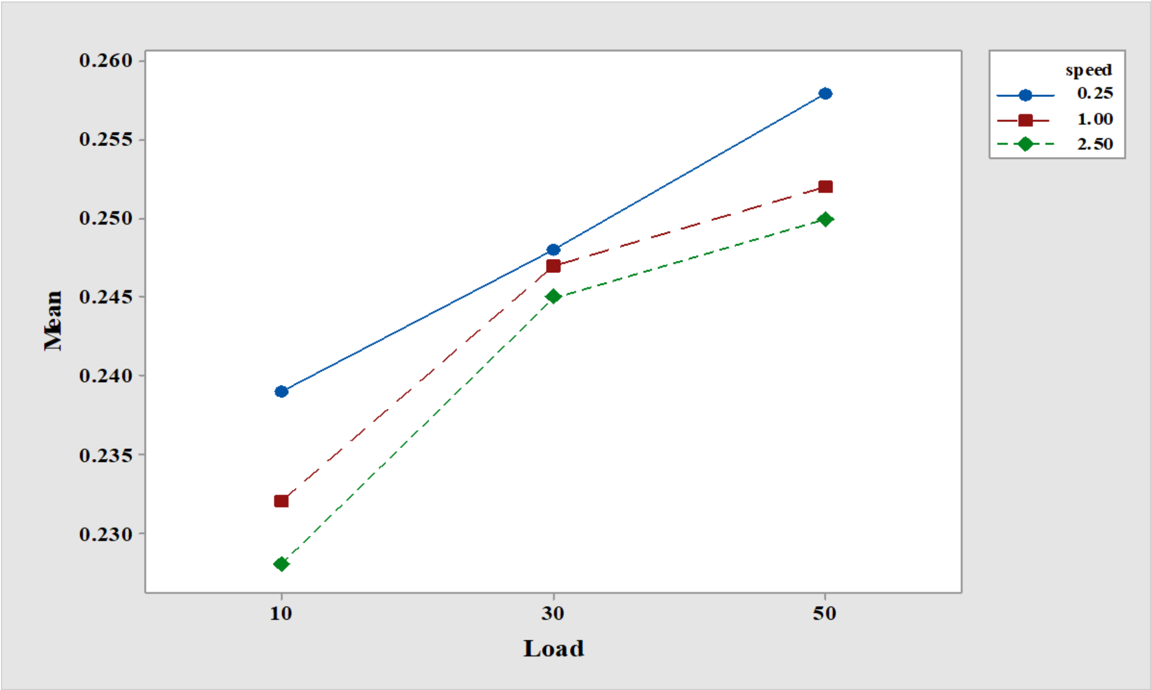


Figure 81 Graph of coefficient of friction vs. load for different speed

*6.2.2.3 Multiple Linear Regression Model to predict the friction and wear behavior*

The regression model is developed for h-composite with 1%MWCNT in similar manner, with help of statistical software MINITAB. The regression equations of wear rate and coefficient of friction for h-composite with 1%MWCNT, with different load and sliding speed conditions are given below. The R-sq value of regression model is show the validity of equation

WR = 0.000381 + 0.000025 L- 0.000116 S ……………*Equation 3*

R-sq. = 95.55%

COF = 0.23289 + 0.000508 L - 0.00305 S ………………*Equation 4*

R-sq. = 92.94%

The R-sq. values of regression models are 95.55% and 92.94 % , respectively, which indicates that the data of wear rate and coefficient of friction is not scattered. As discussed earlier, the negative sign in both equations indicates that as speed increases the wear rate and coefficient of friction decreases. On the other hand, and positive sign of load indicates that as load increase the wear rate and coefficient of friction also increases. Some confirmatory experiments at other loads and speeds for h-composite with 1%MWCNT also reasonably validates these predicted models.

# Chapter 7

# Conclusions and Future Scopes

## 7.1 Conclusions

For the present research Al-alloy, AMMC and MWCNT reinforced hybrid AMMCs have been fabricated successfully with help of Microwave hybrid heating as well following conventional route of powder metallurgy. This was followed by detailed investigations on the microstructural, physical, mechanical and functional behavior. Following conclusions are made based on the study.

### 7.1.1 Mechanical, Microstructural and Phase Analysis

- CNT reinforced h-AMMCs with high hardness, low porosity and more compact can be developed by using microwave hybrid heating route over the conventional sintering method. Higher heating rate with uniform thermal gradient reduces the processing time in microwave hybrid heating and better mechanical, physical
- The presence of MWCNT phase and structure with a moderately uniform distribution in the matrix is found in the microwave sintered h-AMMC composites as compared to the conventional sintering process.
- From the porosity analysis it is found that porosities of fabricated h-AMMC with 1%MWCNT and 2%MWCNT are 1.35% and 1.45% in case of conventional sintered samples, whereas for microwave sintered samples these are 1.04%, 1.07%, respectively.
- Hybrid composite exhibits a higher hardness than Al matrix and Al+SiC composite. The addition of 1% MWCNT in Al-SiC composite increases the hardness by 29.75% in case of conventional sintering and 24.5 % in case of microwave sintering. However, after exceeding a certain CNTs % (in the present case it is 2%), due to the cluster formation of CNT this beneficial affect has been found to be nullified.
- The intensities of different oxide phases such as $Al_2O_3$, $Cr_2O_3$, $MnO_2$ and CuO in conventional sintering process is significantly higher as compared to microwave sintering process.

- It has been found that there is more crack in case of conventional sintered composite as compared to microwave sintered composites.

### 7.1.2 Friction and Wear Study

- Wear and friction properties of h-composite are found better than Al matrix and Al+ SiC composite. However, the nature of distribution as well as % of MWCNT is found to have significant affect on the tribological characteristics.
- It is observed that around 80% weight loss is decreased by the addition of 1% MWCNT in h-AMMC as compared to Al-alloy. The wear rate is decreased by the addition of 1% MWCNT by 81.5% (from $2.0596 \times 10^{-3}$ to $3.8021 \times 10^{-4}$), in the case of microwave sintering. In case of conventional sintering, the decrease in wear rate by the addition of 1% MWCNT is in the range of 78.7% (from $2.5155 \times 10^{-3}$ to $5.3506 \times 10^{-4}$) and for 2% MWCNT this enhacement is about 84.5% (from $2.5155 \times 10^{-3}$ to $3.8803 \times 10^{-4}$).
- Beyond 2 wt% of MWCNT in h- AMMC, the wear loss and wear rate starts to increase again very rapidly for both the caseses of sintering.
- When applied load is increased from 10 N to 30 N it is seen that in case of aluminum and Al+ SiC composite the wear rate increases approximately by 70.2%, whereas in the case of h-composite with 1% MWCNT the wear rate increases at lower rate (62.5%).
- The h-composite with 1%MWCNT shows less number of voids, pits and grooves as compared to alumninium and Al+ SiC composites. Both the adhesive and abrasive components of wear are found to be less in h-composite as compared to aluminium and Al+ SiC. This is attributed to the formation of tribofilm of carbonaceous layer under the contact in the presence of MWCNT, which is verified through EDS,XRD and FESEM.
- Friction study reveals that increasing the wt. % of MWCNT in h-composite decrease the coefficient of friction up to 2%MWCNT, further increment of MWCNT increase the coefficient of friction. In case of h-composite with 1%MWCNT this decrease in the coefficent of friction is about 47.87% from 0.442 to 0.232.
- At higher load the average coefficient of friction decreases, this might be due to more MWCNT is pulled out of the h-composite.
- The sliding distance or the sliding speed has been found an insignificant factor for tribological performance, in our domain of our study.

- Finally, from the detailed investigation which is carried out in this research, it is found that h-composite with a composition (Al+15%SiC+1%MWCNT) significantly enhances the tribological performance in different operating conditions.

## 7.2 Future Scopes

The present work can be extended and following scopes of research can be recommended for future works.

- Behavior of MWCNT reinforced hybrid AMMC can be investigated with different types of hard reinforcements.
- For some specific applications such as automobile piston, cylinder liners or brake discs, etc, CNT-reinforced AMMC can be explored extensively in the corrosive and high temperature environment.
- Further, to control the cost and processing time microwave hybrid heating route can be adopted to develop high performance functionally graded hybrid AMMCs with different reinforcing agents.
- Simulation studies can be carried out to predict the mechanical and functional behavior of such types of composites.

# References


[1] K. Holmberg and A. Erdemir, “Influence of tribology on global energy consumption , costs and emissions,” vol. 5, no. 3, pp. 263–284, 2017.

[2] K. Holmberg, P. Andersson, N. Nylund, K. Mäkelä, and A. Erdemir, “Tribology International Global energy consumption due to friction in trucks and buses,” *Tribiology Int.*, vol. 78, pp. 94–114, 2014.

[3] N. Li, “Automotive Tribology Tribology Basics,” *Bruker Tech. Rep.*, pp. 1–29, 2014.

[4] T. Chaudhari and B. Sutaria, “Investigation of friction characteristics in segmented piston ring liner assembly of IC engine ☆,” *Perspect. Sci.*, vol. 8, pp. 599–602, 2016.

[5] G. Fenske, “Friction/Wear-Parasitic Energy Losses,” *US Department of Energy*, pp. 1–6, 2008.

[6] E. Estupinan and I. Santos, “Active lubrication applied to internal combustion engines - Evaluation of control strategies,” in *16th International Congress on Sound and Vibration 2009, ICSV 2009*, 2009, vol. 4, no. July, pp. 2146–2153.

[7] P. Nagendramma and S. Kaul, “Development of ecofriendly / biodegradable lubricants : An overview Development of ecofriendly / biodegradable lubricants : An overview,” *Renew. Sustain. Energy Rev.*, vol. 16, no. 1, pp. 764–774, 2018.

[8] M. Shoeab and N. Mishra, “Study of Tribology Application and its Impact on Indian Industries,” *Int. J. Sci. Eng. Technol.*, vol. 1312, no. 3, pp. 1310–1312, 2014.

[9] S. C. Tung and M. L. McMillan, “Automotive tribology overview of current advances and challenges for the future,” *Tribol. Int.*, vol. 37, no. 7, pp. 517–536, 2004.

[10] G. Pantazopoulos, A. Tsolakis, P. Psyllaki, and A. Vazdirvanidis, “Wear and degradation modes in selected vehicle tribosystems,” *Tribol. Ind.*, vol. 37, no. 1, pp. 72–80, 2015.

[11] Koji Kato and Koshi Adachi, *Wear Mechanisms. In Modern tribology handbook*. 2001.

[12] J. Singh and A. Chauhan, "Overview of wear performance of aluminium matrix composites reinforced with ceramic materials under the influence of controllable variables," *Ceramics International*, vol. 42, no. 1. Elsevier, pp. 56–81, 2016.

[13] P. L. Menezes, M. Nosonovsky, S. V. Kailas, and M. R. Lovell, "Friction and wear," in *Tribology for Scientists and Engineers: From Basics to Advanced Concepts*, vol. 9781461419, Woodhead Publishing Limited, 2013, pp. 43–91.

[14] J. Dutta Majumdar and I. Manna, "Laser surface engineering of titanium and its alloys for improved wear, corrosion and high-temperature oxidation resistance," in *Laser Surface Engineering: Processes and Applications*, Elsevier Ltd., 2014, pp. 483–521.

[15] C. Zhang, "Understanding the wear and tribological properties of ceramic matrix composites," in *Advances in Ceramic Matrix Composites: Second Edition*, Woodhead Publishing Limited, 2018, pp. 401–428.

[16] H. Dong, "Tribological properties of titanium-based alloys," in *Surface Engineering of Light Alloys: Aluminium, Magnesium and Titanium Alloys*, Woodhead Publishing Limited, 2010, pp. 58–80.

[17] K. H. Z. Gahr, "Wear by hard particles," *Tribol. Int.*, vol. 31, no. 10, pp. 587–596, 1998.

[18] M. A. Moore, "The relationship between the abrasive wear resistance, hardness and microstructure of ferritic materials," vol. 28, pp. 59–68, 1974.

[19] H. M. Alojali and K. Y. Benyounis, "Advances in Tool wear in Turning Process," in *Reference Module in Materials Science and Materials Engineering*, Elsevier Ltd., 2016, pp. 1–15.

[20] R. K. Upadhyay and L. A. Kumaraswamidhas, "Bearing failure issues and corrective measures through surface engineering," in *Handbook of Materials Failure Analysis*, Elsevier Ltd, 2018, pp. 209–233.

[21] P. E. Rossouw, "Friction: An overview," *Semin. Orthod.*, vol. 9, no. 4, pp. 218–222, 2003.

[22] A. Ruina and R. Pratap, *Introduction to Statics and Dynamics*, no. January. 2002.

[23] S. M. M. Amir *et al.*, "Nondestructive testing method for Kevlar and natural fiber and their hybrid composites," in *Durability and Life Prediction in Biocomposites, Fibre-Reinforced Composites and Hybrid Composites*, 2019, pp. 367–388.

[24] I. D. Ibrahim, T. Jamiru, R. E. Sadiku, W. K. Kupolati, S. C. Agwuncha, and G. Ekundayo, "The use of polypropylene in bamboo fibre composites and their mechanical properties - A review," *J. Reinf. Plast. Compos.*, vol. 34, no. 16, pp. 1347–1356, 2015.

[25] V. Arumugaprabu, T. J. Ko, M. Uthayakumar, and R. D. Joel Johnson, "Failure analysis in hybrid composites prepared using industrial wastes," in *Failure Analysis in Biocomposites, Fibre-Reinforced Composites and Hybrid Composites*, Elsevier Ltd, 2019, pp. 229–244.

[26] A. Krishnan, E. Dujardin, and T. Ebbesen, "Young's modulus of single-walled nanotubes," *Phys. Rev. B - Condens. Matter Mater. Phys.*, vol. 58, no. 20, pp. 14013–14019, 1998.

[27] P. Song, Z. Cao, Y. Cai, L. Zhao, Z. Fang, and S. Fu, "Fabrication of exfoliated graphene-based polypropylene nanocomposites with enhanced mechanical and thermal properties," *Polymer (Guildf).*, vol. 52, no. 18, pp. 4001–4010, 2011.

[28] D. H. Robertson, D. W. Brenner, and C. T. White, "On the way to fullerenes: molecular dynamics study of the curling and closure of graphitic ribbons," *J. Phys. Chem.*, vol. 96, no. 15, pp. 6133–6135, Jul. 1992.

[29] J. Cumings and A. Zettl, "Low-friction nanoscale linear bearing realized from multiwall carbon nanotubes," *Science (80-. ).*, vol. 289, no. 5479, pp. 602–604, 2000.

[30] L. Bokobza and J. Zhang, "Raman spectroscopic characterization of multiwall carbon nanotubes and of composites," *Express Polym. Lett.*, vol. 6, no. 7, pp. 601–608, 2012.

[31] A. S. Biris, E. I. Galanzha, Z. Li, M. Mahmood, Y. Xu, and V. P. Zharov, "In vivo Raman flow cytometry for real-time detection of carbon nanotube kinetics in lymph, blood, and tissues," *J. Biomed. Opt.*, vol. 14, no. 2, p. 021006, 2009.

[32] R. L. Schulz, G. G. Wicks, D. C. Folz, and D. E. Clark, "Overview of Hybrid Microwave Technology," *J. South Carolina Acad. Sci.*, vol. 9, no. 1, pp. 25–29, 2011.

[33] M. T. Sijo and K. R. Jayadevan, "Analysis of stir cast aluminium silicon carbide metal matrix composite : A comprehensive review," *Procedia Technol.*, vol. 24, pp. 379–385, 2016.

[34] S. Kayal, "Solidification behavior of stir - cast Al alloy metal matrix composites," *Int. J. Appl. Eng. Res.*, vol. 2, no. 2, pp. 350–359, 2011.

[35] V. V. Vani and S. K. Chak, "The effect of process parameters in Aluminum Metal Matrix Composites with Powder Metallurgy," *Manufacturing Review*, vol. 5. pp. 1–13, 2018.

[36] A. Al-reashed, S. Holecek, M. Prazak, and M. Procio, "Powder metallurgy route in production of aluminum alloy matrix particulate composites," *J. Phys.*, vol. 3, no. 7 pt 3, pp. 1821–1823, 1993.

[37] I. Zohourkari, S. Assarzadeh, and M. Zohoor, "Modeling and analysis of hot extrusion metal forming process using artificial neural network and ANOVA," in *ASME 2010 10th Biennial Conference on Engineering Systems Design and Analysis, ESDA2010*, 2010, vol. 4, no. November 2017, pp. 831–839.

[38] M. Nygren and Z. Shen, "Spark Plasma Sintering : Possibilities and Limitations," *Key Eng. Mater.*, vol. 268, pp. 719–724, 2004.

[39] G. Maizza, S. Grasso, Y. Sakka, T. Noda, and O. Ohashi, "Relation between microstructure, properties and spark plasma sintering (SPS) parameters of pure ultrafine WC powder," *Sci. Technol. Adv. Mater.*, vol. 8, no. 7–8, pp. 644–654, 2007.

[40] J. Liao and M. Tan, "A simple approach to prepare Al / CNT composite : Spread – Dispersion ( SD ) method," *Mater. Lett.*, vol. 65, no. 17–18, pp. 2742–2744, 2011.

[41] A. D. LaLonde, T. Ikeda, and G. J. Snyder, "Rapid consolidation of powdered materials by induction hot pressing," *Rev. Sci. Instrum.*, vol. 82, no. 2, 2011.

[42] P. Vitanov, A. Harizanova, T. Ivanova, C. Trapalis, and N. Todorova, "Sol-gel ZrO2 and ZrO2-Al2O3 nanocrystalline thin films on Si as high-k dielectrics," *Mater. Sci. Eng. B Solid-State Mater. Adv. Technol.*, vol. 165, no. 3, pp. 178–181, 2009.

[43] M. Oghbaei and O. Mirzaee, "Microwave versus conventional sintering : A review of fundamentals , advantages and applications," *J. Alloys Compd.*, vol. 494, no. 1–2, pp.

175–189, 2010.

[44] D. E. Clark, D. C. Folz, and J. K. West, "Processing materials with microwave energy," *Mater. Sci. Eng. A*, vol. 287, no. 2, pp. 153–158, 2000.

[45] D. Demirskyi, D. Agrawal, and A. Ragulya, "Tough ceramics by microwave sintering of nanocrystalline titanium diboride ceramics," *Ceram. Int.*, vol. 40, no. 1, pp. 1303–1310, 2014.

[46] R. R. Mishra and A. K. Sharma, "Microwave-material interaction phenomena: Heating mechanisms, challenges and opportunities in material processing," *Composites Part A: Applied Science and Manufacturing*, vol. 81. Elsevier Ltd, pp. 78–97, 2016.

[47] D. Gupta and A. K. Sharma, "Surface & Coatings Technology Development and microstructural characterization of microwave cladding on austenitic stainless steel," *Surf. Coat. Technol.*, vol. 205, no. 21–22, pp. 5147–5155, 2011.

[48] R. R. Mishra and A. K. Sharma, "A Review of Research Trends in Microwave Processing of Metal-Based Materials and Opportunities in Microwave Metal Casting," *Crit. Rev. Solid State Mater. Sci.*, vol. 41, no. 3, pp. 217–255, 2016.

[49] P. Matli, R. Shakoor, A. Amer Mohamed, and M. Gupta, "Microwave Rapid Sintering of Al-Metal Matrix Composites: A Review on the Effect of Reinforcements, Microstructure and Mechanical Properties," *Metals (Basel).*, vol. 6, no. 7, p. 143, 2016.

[50] V. M. Kevorkijan, "Metal matrix composites in the automotive industry," *Metalurgija*, vol. 38, no. 4, pp. 245–249, 1999.

[51] N. Chawla and K. K. Chawla, "Metal-matrix composites in ground transportation," *JOM*, vol. 58, no. 11. pp. 67–70, 2006.

[52] T. Donomoto, K. Funatani, N. Miura, and N. Miyake, "Ceramic fiber reinforced piston for high performance diesel engines," in *SAE Technical Papers*, 1983, p. DOI: 10.4271/830252.

[53] Hunt.WH *et al.*, "Composites," in *ASM Handbook*, vol. 21, 2001, p. 3470.

[54] A. Dolata-Grosz, M. Dyzia, J. Śleziona, J. Wieczorek, J. Sleziona, and J. Wieczorek, "Composites applied for pistons," *Arch. Foundry Eng.*, vol. 7, no. 1/2007, pp. 37–40,

2007.

[55] J. Goñi, P. Egizabal, J. Coleto, I. Mitxelena, I. Leunda, and J. R. Guridi, “High performance automotive and railway components made from novel competitive aluminium composites,” *Materials Science and Technology*, vol. 19, no. 7. pp. 931–934, 2003.

[56] S. V Prasad and R. Asthana, “Aluminum metal-matrix composites for automotive applications: Tribological considerations,” *Tribol. Lett.*, vol. 17, no. 3, pp. 445–453, 2004.

[57] N. Panwar and A. Chauhan, “Fabrication methods of particulate reinforced Aluminium metal matrix composite-A review,” *Mater. Today Proc.*, vol. 5, no. 2, pp. 5933–5939, 2018.

[58] G. Moona, R. S. Walia, V. Rastogi, and R. Sharma, “Aluminium metal matrix composites: A retrospective investigation,” *Indian J. Pure Appl. Phys.*, vol. 56, no. 2, pp. 164–175, 2018.

[59] V. Suresh, “Future in Metal Matrix Composites for Automotive Industry : A Review,” *Int. Res. J. Automot. T ECHNOLOGY*, vol. 1, no. November, pp. 88–100, 2018.

[60] B. P. Krishnan, N. Raman, K. Narayanaswamy, and P. K. Rohatgi, “Elsevier Sequoia S.A., Lausanne -Printed 205 in the Netherlands,” 1980, vol. 60, no. April 1979, pp. 205–215.

[61] M. Karthe and S. Prasanna, “Performance of Al-si-glass fiber composite piston in an IC Engine,” *J o u r n a l o f A d v a n c e s i n c h e m i s t r y*, vol. 12, no. October, pp. 4650–4654, 2016.

[62] A. John, “Design and Analysis of Piston by SiC Composite Material,” *Int. J. Innov. Res. Sci. Technol.*, vol. 1, no. 12, pp. 578–590, 2015.

[63] M. Singh and M. Bhargava, “Analysis and Comparison of Different Materials for a Single Cylinder Four Stroke 225cc Piston using FEA,” *Int. J. Therm. Technol.*, vol. 6, no. 4, pp. 355–358, 2016.

[64] A. Umma, M. A. Maleque, I. Y. Iskandar, and Y. A. Mohammed, “Carbon nano tube reinforced aluminium matrix nano-composite: A critical review,” *Aust. J. Basic Appl.*

*Sci.*, vol. 6, no. 12, pp. 69–75, 2012.

[65] B. Sadeghi *et al.*, “Hot rolling of MWCNTs reinforced Al matrix composites produced via spark plasma sintering,” *Adv. Compos. Hybrid Mater.*, vol. https://do, 2019.

[66] T. Kuzumaki, K. Miyazawa, H. Ichinose, and K. Ito, “Processing of carbon nanotube reinforced aluminum composite,” *J. Mater. Res.*, vol. 13, no. 9, pp. 2445–2449, 1998.

[67] A. M. K. Esawi, K. Morsi, A. Sayed, M. Taher, and S. Lanka, “Effect of carbon nanotube ( CNT ) content on the mechanical properties of CNT-reinforced aluminium composites,” *Compos. Sci. Technol.*, vol. 70, no. 16, pp. 2237–2241, 2010.

[68] D. Marini, V. Genova, F. Marra, G. Pulci, and M. Valente, “Mechanical behaviour with temperatures of aluminum matrix composites with CNTs,” *Chem. Eng. Trans.*, vol. 60, pp. 25–30, 2017.

[69] M. Mansoor and M. Shahid, “Carbon nanotube-reinforced aluminum composite produced by induction melting,” *Rev. Mex. Trastor. Aliment.*, vol. 14, no. 4, pp. 215–224, 2016.

[70] J. Liao, M. J. Tan, R. V Ramanujan, and S. Shukla, “Carbon nanotube evolution in aluminum matrix during composite fabrication process,” in *Materials Science Forum,* 2011, vol. 690, pp. 294–297.

[71] H. Kurita, H. Kwon, M. Estili, and A. Kawasaki, “Multi-walled carbon nanotube-aluminum matrix composites prepared by combination of hetero-agglomeration method, spark plasma sintering and hot extrusion,” *Mater. Trans.*, vol. 52, no. 10, pp. 1960–1965, 2011.

[72] A. B. Elshalakany, T. A. Osman, A. Khattab, B. Azzam, and M. Zaki, “Microstructure and mechanical properties of MWCNTs reinforced A356 aluminum alloys cast nanocomposites fabricated by using a combination of rheocasting and squeeze casting techniques,” *J. Nanomater.*, vol. 2014, 2014.

[73] M. Majid, G. H. Majzoobi, G. A. Noozad, A. Reihani, S. Z. Mortazavi, and M. S. Gorji, “Fabrication and mechanical properties of MWCNTs-reinforced aluminum composites by hot extrusion,” *Rare Met.*, vol. 31, no. 4, pp. 372–378, 2012.

[74] M. Jagannatham, M. S. S. Saravanan, K. Sivaprasad, and S. P. K. Babu, “Mechanical

and Tribological Behavior of Multiwalled Carbon Nanotubes-Reinforced AA7075 Composites Prepared by Powder Metallurgy and Hot Extrusion," *J. Mater. Eng. Perform.*, vol. 27, no. 11, pp. 5675–5688, 2018.

[75] C. Berger *et al.*, "Ultrathin epitaxial graphite: 2D electron gas properties and a route toward graphene-based nanoelectronics," *J. Phys. Chem. B*, vol. 108, no. 52, pp. 19912–19916, 2004.

[76] P. J. F. Harris, "Carbon nanotube composites," *International Materials Reviews*, vol. 49, no. 1. pp. 31–43, 2004.

[77] S. R. Bakshi, D. Lahiri, and A. Agarwal, "Carbon nanotube reinforced metal matrix composites - A review," *International Materials Reviews*, vol. 55, no. 1. pp. 41–64, 2010.

[78] H. J. Choi, S. M. Lee, and D. H. Bae, "Wear characteristic of aluminum-based composites containing multi-walled carbon nanotubes," *Wear*, vol. 270, no. 1–2, pp. 12–18, 2010.

[79] A. M. Al-qutub, A. Khalil, N. Saheb, and A. S. Hakeem, "Wear and friction behavior of Al6061 alloy reinforced with carbon nanotubes," *Wear*, vol. 297, no. 1–2, pp. 752–761, 2013.

[80] M. L. H. P. Dinesh, "Fabrication , Microstructure, Hardness and Wear properties of Extruded MWCNT- Reinforced with 6061Al Metal Matrix Composites," *Int. J. Sci. Eng. Res.*, vol. 4, no. 4, pp. 974–990, 2013.

[81] R. Pérez-Bustamante *et al.*, "Wear behavior in Al 2024-CNTs composites synthesized by mechanical alloying," *Wear*, vol. 292–293, pp. 169–175, 2012.

[82] M. M. H. Bastwros, A. M. K. Esawi, and A. Wifi, "Friction and wear behavior of Al-CNT composites," *Wear*, vol. 307, no. 1–2, pp. 164–173, 2013.

[83] K. R. Padmavathi and R. Ramakrishnan, "Tribological behaviour of Aluminium Hybrid Metal Matrix Composite," *Procedia Eng.*, vol. 97, pp. 660–667, 2014.

[84] O. Carvalho, M. Buciumeanu, S. Madeira, D. Soares, F. S. Silva, and G. Miranda, "Tribology International Dry sliding wear behaviour of AlSi – CNTs – SiCp hybrid composites," *Tribiology Int.*, vol. 90, pp. 148–156, 2015.

[85] B. Hekner, J. Myalski, N. Valle, A. Botor-Probierz, M. Sopicka-Lizer, and J. Wieczorek, “Friction and wear behavior of Al-SiC(n) hybrid composites with carbon addition,” *Compos. Part B Eng.*, vol. 108, pp. 291–300, 2017.

[86] R. N and R. V S, “Tribological Characterization of Al7075/Al203/Sic Reinforced Hybrid Particulate Metal Matrix Composite Developed by Stir Casting Process,” *Int. J. Recent Adv. Mech. Eng.*, vol. 4, no. 3, pp. 113–127, 2015.

[87] M. Zakaulla, R. Arjun, M. Ahmed Khan, I. Hussein Khan, and N. Pasha, “Tribological characteristics of multiwalled carbon nanotubes and boron carbide particles reinforced Al2024 matrix composites,” in *Materials Today: Proceedings*, 2018, vol. 5, no. 2, pp. 5762–5767.

[88] A. Alizadeh, A. Abdollahi, and H. Biukani, “Creep behavior and wear resistance of Al 5083 based hybrid composites reinforced with carbon nanotubes ( CNTs ) and boron carbide ( B 4 C ),” *J. Alloys Compd.*, vol. 650, pp. 783–793, 2015.

[89] B. Hekner, J. Myalski, T. Pawlik, and M. Sopicka-Lizer, “Effect of carbon in fabrication Al-SiC nanocomposites for tribological application,” *Materials (Basel).*, vol. 10, no. 6, 2017.

[90] M. Karthik, C. Honnaiah, S. L. Ajit Prasad, and M. S. Srinath, “A Study on Fatigue Characteristics of Al-SiC Metal Matrix Composites Processed Through Microwave Energy,” in *IOP Conference Series: Materials Science and Engineering*, 2018, vol. 376, no. 1.

[91] S. Singh, D. Gupta, V. Jain, and A. K. Sharma, “Microwave processing of materials and applications in manufacturing industries: A Review,” *Materials and Manufacturing Processes*, vol. 30, no. 1. pp. 1–29, 2015.

[92] S. Kaushal, D. Gupta, and H. Bhowmick, “On Microstructure and Wear Behavior of Microwave Processed Composite Clad,” *J. Tribol.*, vol. 139, no. 6, p. 061602, 2017.

[93] E. Ghasali, A. Fazili, M. Alizadeh, K. Shirvanimoghaddam, and T. Ebadzadeh, “Evaluation of microstructure and mechanical properties of Al-TiC metal matrix composite prepared by conventional, microwave and spark plasma sintering methods,” *Materials (Basel).*, vol. 10, no. 11, 2017.

[94] E. Ghasali, P. Sangpour, A. Jam, H. Rajaei, K. Shirvanimoghaddam, and T. Ebadzadeh, "Microwave and spark plasma sintering of carbon nanotube and graphene reinforced aluminum matrix composite," *Arch. Civ. Mech. Eng.*, vol. 18, no. 4, pp. 1042–1054, 2018.

[95] M. Madhan and G. Prabhakaran, "Microwave versus conventional sintering: Microstructure and mechanical properties of Al 2 O 3 -SiC ceramic composites," *Bol. la Soc. Esp. Ceram. y Vidr.*, vol. 58, no. 1, pp. 14–22, 2019.

[96] S. Singh, D. Gupta, and V. Jain, "Microwave melting and processing of metal–ceramic composite castings," *Proc. Inst. Mech. Eng. Part B J. Eng. Manuf.*, vol. 232, no. 7, pp. 1235–1243, 2018.

[97] M. P. Reddy, F. Ubaid, R. A. Shakoor, A. M. A. Mohamed, and W. Madhuri, "Structural and mechanical properties of microwave sintered Al–Ni50Ti50 composites," *J. Sci. Adv. Mater. Devices*, vol. 1, no. 3, pp. 362–366, 2016.

[98] P. Matli *et al.*, *Microwave rapid sintering of al-metal matrix composites: A review on the effect of reinforcements, microstructure and mechanical properties*, vol. 6, no. 7. 2016, p. 143.

[99] R. Zhong, H. Cong, and P. Hou, "Fabrication of nano-Al based composites reinforced by single-walled carbon nanotubes," *Carbon*, vol. 41, no. 4. pp. 848–851, 2003.

[100] B. J. Rael, Y. Fu, T. A. Khraishi, and Y. B. Jiang, "Optimizing powder metallurgy methods: Effects of carbon nanotube dispersal mechanisms on mechanical properties of aluminium/carbon nanotube composites," *J. Compos. Mater.*, vol. 50, no. 17, pp. 2375–2388, 2016.

[101] D. Agrawal, "Microwave sintering of ceramics, composites and metallic materials, and melting of glasses," *Trans. Indian Ceram. Soc.*, vol. 65, no. 3, pp. 129–144, 2006.

[102] M. G. Ananda Kumar, S. Seetharamu, P. Sampath Kumaran, and J. Nayak, "The influence of microwave sintering on the tribological performance of powder metallurgy based aluminum cenospheres composites," in *Materials Science Forum*, 2015, vol. 830–831, pp. 71–74.

[103] C. Padmavathi, A. Upadhyaya, and D. Agrawal, "Effect of microwave and

conventional heating on sintering behavior and properties of Al – Mg – Si – Cu alloy," *Mater. Chem. Phys.*, vol. 130, no. 1–2, pp. 449–457, 2011.

[104] M. R. Akbarpour and A. Pouresmaeil, "The influence of CNTs on the microstructure and strength of Al-CNT composites produced by flake powder metallurgy and hot pressing method," *Diam. Relat. Mater.*, vol. 88, no. April, pp. 6–11, 2018.

[105] R. Das, S. Hamid, M. Ali, S. Ramakrishna, and W. Yongzhi, "Carbon Nanotubes Characterization by X-ray Powder Diffraction – A Review," *Curr. Nanosci.*, vol. 11, no. 1, pp. 23–35, 2014.

[106] X. Zhang, S. Li, B. Pan, D. Pan, S. Zhou, and S. Yang, "A novel strengthening effect of in-situ nano Al 2 O 3 w on CNTs reinforced aluminum matrix nanocomposites and the matched strengthening mechanisms," *J. Alloys Compd.*, vol. 764, pp. 279–288, 2018.

[107] T. Koyanagi, Y. Katoh, and M. J. Lance, "Raman spectroscopy of neutron irradiated silicon carbide: Correlation among Raman spectra, swelling, and irradiation temperature," *J. Raman Spectrosc.*, vol. 49, no. 10, pp. 1686–1692, 2018.

[108] J. Wasyluk, T. S. Perova, S. A. Kukushkin, A. V Osipov, N. A. Feoktistov, and S. A. Grudinkin, "Raman investigation of different polytypes in SiC thin films grown by solid-gas phase epitaxy on Si (111) and 6H-SiC substrates," in *Materials Science Forum*, 2010, vol. 645–648, pp. 359–362.

[109] T. Thongchai, S. Larpkiattaworn, D. Atong, and M. Kitiwan, "COMPARISON OF MICROWAVE AND CONVENTIONAL SINTERING OF Al2O3-ZrO2 COMPOSITES," in *18TH INTERNATIONAL CONFERENCE ON COMPOSITE MATERIALS*, 2011, pp. 1–5.

[110] I. Y. Kim, J. H. Lee, G. S. Lee, S. H. Baik, Y. J. Kim, and Y. Z. Lee, "Friction and wear characteristics of the carbon nanotube-aluminum composites with different manufacturing conditions," *Wear*, vol. 267, no. 1–4, pp. 593–598, 2009.

# A Comparative Investigation on the Tribology and Microstructure of MWCNT Reinforced h-AMMC Sintered by Conventional and Microwave Heating Route

ORIGINALITY REPORT

| 9% | 1% | 5% | 7% |
|---|---|---|---|
| SIMILARITY INDEX | INTERNET SOURCES | PUBLICATIONS | STUDENT PAPERS |

PRIMARY SOURCES

| | | |
|---|---|---|
| 1 | Tribology for Scientists and Engineers, 2013.<br>Publication | 1% |
| 2 | Submitted to Indian Institute of Technology, Madras<br>Student Paper | 1% |
| 3 | digital.library.yale.edu<br>Internet Source | <1% |
| 4 | Submitted to VIT University<br>Student Paper | <1% |
| 5 | Submitted to National University of Singapore<br>Student Paper | <1% |
| 6 | S Dhanalakshmi, N Mohanasundararaju, P G Venkatakrishnan, V Karthik. " Optimization of friction and wear behaviour of Al7075-Al O -B C metal matrix composites using Taguchi method ", IOP Conference Series: Materials Science and Engineering, 2018<br>Publication | <1% |